

申 报	系列：教师系列教学 科研并重型
	专业：生物学
	职称：副教授

业绩成果材料

（申报人的业绩成果材料包括论文、科研项目、获奖以及其他成果等）

单 位（二级单位） 生命科学学院

姓 名 周峰

材料核对人：

单位盖章：

核对时间：

华南农业大学制

目 录

一、教学研究业绩

1. 编写教材：普通高等教育农业农村部“十三五”规划教材《基因工程原理与实验》 4
2. 编写教材：普通高等教育农业农村部“十四五”规划教材、普通高等教育“十四五”规划教材生物科学类专业系列教材《基因工程原理与实验》 12

二、科研项目

1. 主持：转基因生物新品种培育重大专项课题“转基因生物安全监测技术”专题“华南地区 Bt 水稻环境影响监测”任务合同书 21
2. 主持：农业农村部科技发展中心“农业转基因生物安全科普进校园”任务（合同）书 33
3. 主持：广州市基础与应用基础研究项目“OsSSD1 调控水稻植株形态的分子机理研究”项目合同书 39
4. 主参：国家自然科学基金面上项目“亚洲稻自私遗传座位 ARSL1 的克隆和功能分析”项目计划书 50
5. 主参：农业产品质量安全监管专项经费项目“农业转基因生物安全检测”任务委托书 62
6. 主参：国家自然科学基金面上项目“火炬松叶绿体基因组遗传多样性及育种群体亲缘关系调控”项目计划书 76
7. 主参：国家自然科学基金面上项目“与生长素相关的水稻卷叶突变基因克隆及功能分析”项目计划书及申报书 87
8. 主参：广东省自然科学基金项目“水稻 mTERF 基因 v14 调控叶绿体发育的分子机理研究”项目合同书 116

三、论文、著作等

1. 检索证明.....	127
2. 以第一作者发表本专业论文情况	
2.1. Multiscale simulation of elastic modulus of rice.....	130
2.2. The ties of brotherhood between japonica and indica rice for regional adaptation.....	148
2.3. A rice mTERF protein V14 sustains photosynthesis establishment and temperature acclimation in early seedling leaves.	159

四、科研成果

五、其他业绩

1.个人荣誉	
1.1. 2017 年度华南农业大学“优秀共产党员”荣誉证书.....	170
1.2. 2016 年度华南农业大学生命科学学院“优秀班主任”奖状.....	171
1.3. 2019 年度华南农业大学生命科学学院“管理先进个人”奖状.....	172
1.4. 2011 年度华南农业大学年度考核结果“优秀等次”通知书	173
1.5. 2014 年度华南农业大学年度考核结果“优秀等次”通知书	174
1.6. 2017 年度华南农业大学年度考核结果“优秀等次”通知书	175

【佐证材料切记与目录页所列页码对应，不要用图片格式的材料进行打印。】



普通高等教育农业农村部“十三五”规划教材

基因工程原理与实验

Principles and Experiments of Genetic Engineering

易继财 主编



中国农业大学出版社
China Agricultural University Press



普通高等教育农业农村部“十三五”规划教材

基因工程原理与实验

易继财 主编

http://hp2:

中国农业大学出版社

• 北京 •

内 容 简 介

本书包括基因工程原理篇和基因工程实验篇两部分内容。基因工程原理篇阐述了基因工程原理与技术,其内容包括绪论、基因工程的工具酶和基因工程载体、DNA 的连接、转化和重组子筛选等基因工程相关的基本原理和新发展以及基因工程技术与方法、基因工程在农业作物上的应用。同时,基因工程也是一门实践性很强的学科,为了增强本书的实操性,在基因工程实验篇,编者结合自身的科研实践经验以及农林生物类研究人员的实际需要,整理并收录了编者所在教研室历年来为本校师生及相关研究人员开出的各种基因工程实用性实验。

期望读者既能从本书的原理中获得基因工程的相关理论和技术知识,又能从本书的实验中获得指导和参考依据,并能将相关的理论和技术直接应用到科研中,以此为迅速开展研究奠定牢固的理论和实践基础。

图书在版编目(CIP)数据

基因工程原理与实验/易继财主编. —北京:中国农业大学出版社,2020.9

ISBN 978-7-5655-2428-8

I. ①基… II. ①易… III. ①基因工程-高等学校-教材 IV. ①Q78

中国版本图书馆 CIP 数据核字(2020)第 179371 号

书 名 基因工程原理与实验

作 者 易继财 主编

策划编辑 司建新

责任编辑 司建新

封面设计 郑 川

出版发行 中国农业大学出版社

社 址 北京市海淀区圆明园西路 2 号

邮政编码 100193

电 话 发行部 010-62818525,8625

读者服务部 010-62732336

编辑部 010-62732617,2618

出 版 部 010-62733440

网 址 <http://www.caupress.cn>

E-mail cbsszs@cau.edu.cn

经 销 新华书店

印 刷 涿州市星河印刷有限公司

版 次 2020 年 9 月第 1 版 2020 年 9 月第 1 次印刷

规 格 787×1092 16 开本 16.75 印张 410 千字

定 价 56.00 元

图书如有质量问题本社发行部负责调换

编写人员

- 主 编 易继财 (华南农业大学)
- 副 主 编 刘振兰 (华南农业大学)
赵均良 (广东省农业科学院)
- 编写人员 (按姓氏笔画排序)
- 刘振兰 (华南农业大学)
- 李 静 (华南农业大学)
- 余红兵 (广东医科大学)
- 张群宇 (华南农业大学)
- 陈 亮 (华南农业大学)
- 易继财 (华南农业大学)
- 周 峰 (华南农业大学)
- 周 海 (华南农业大学)
- 周玲艳 (仲恺农业工程学院)
- 赵均良 (广东省农业科学院)
- 谢先荣 (华南农业大学)
- 穆 虹 (华南农业大学)
- 顾 问 庄楚雄 (华南农业大学)

目 录

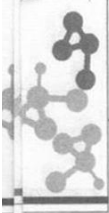
第一部分 基因工程原理篇

第 1 章 绪论	2
1.1 基因学说与基因的现代概念	2
1.1.1 经典遗传学阶段的基因学说	3
1.1.2 分子遗传学阶段的基因学说	3
1.1.3 现代的基因学说	4
1.2 基因工程的诞生与发展	5
1.3 基因工程的研究内容	8
1.4 基因工程应用概况	9
1.4.1 基因工程在工业上的应用	10
1.4.2 基因工程在农业上的应用	10
1.4.3 基因工程在医学上的应用	10
1.4.4 基因工程在军事和国防上的应用	11
第 2 章 基因工程的工具酶	12
2.1 核酸酶	12
2.1.1 限制性核酸内切酶	12
2.1.2 非限制性核酸酶	18
2.2 聚合酶	19
2.2.1 DNA 聚合酶	19
2.2.2 RNA 聚合酶	22
2.2.3 末端转移酶	22
2.3 DNA 连接酶	22
2.4 修饰酶	28
第 3 章 基因工程载体	29
3.1 质粒载体	30

3.1.1 质粒载体的生物学特性·····	30
3.1.2 质粒载体的发展·····	33
3.1.3 常见的质粒载体·····	34
3.2 噬菌体载体·····	39
3.2.1 噬菌体的生物学特性·····	39
3.2.2 常见噬菌体载体·····	40
3.2.3 噬菌粒和柯斯质粒·····	44
3.3 人工染色体载体·····	45
3.4 其他载体·····	48
第4章 DNA的连接、转化和重组子筛选 ·····	49
4.1 DNA的连接·····	49
4.2 DNA分子导入受体细胞·····	51
4.3 重组子的筛选与鉴定·····	55
4.3.1 重组子的初步筛选·····	55
4.3.2 重组子的进一步筛选·····	56
第5章 基因工程技术与方法 ·····	58
5.1 核酸的分离纯化·····	58
5.1.1 DNA的分离纯化·····	58
5.1.2 RNA的分离纯化·····	60
5.2 凝胶电泳技术·····	61
5.2.1 琼脂糖凝胶电泳·····	61
5.2.2 聚丙烯酰胺凝胶电泳·····	64
5.2.3 脉冲电场凝胶电泳·····	64
5.3 PCR技术·····	65
5.3.1 PCR的基本原理·····	66
5.3.2 未知序列DNA片段的PCR·····	70
5.3.3 反转录PCR·····	73
5.3.4 差异显示PCR·····	73
5.3.5 实时定量PCR·····	75
5.4 探针标记技术·····	78
5.4.1 放射性探针标记·····	78
5.4.2 非放射性标记·····	80
5.5 分子杂交技术·····	81
5.6 DNA测序技术·····	86
5.6.1 第一代测序技术·····	87
5.6.2 新一代测序技术·····	90
5.7 DNA定点突变与基因编辑技术·····	92
5.7.1 基因编辑技术概述·····	93



5.7.2	CRISPR/Cas9 基因编辑技术	94
5.7.3	基因编辑突变的检测	96
5.8	抑制缩减杂交技术	97
5.9	基因芯片技术	99
5.10	分子标记技术	103
5.10.1	遗传标记的类型	103
5.10.2	RFLP 标记	106
5.10.3	RAPD 标记	108
5.10.4	AFLP 标记	109
5.10.5	SSR 标记	111
5.10.6	SNP 标记	113
5.10.7	其他类型分子标记	115
5.10.8	分子标记在植物分子育种中的应用	117
5.11	目的基因的分离技术	120
5.11.1	化学合成法	121
5.11.2	基因文库法	124
5.11.3	PCR 法	130
5.11.4	图位克隆法	131
5.11.5	DNA 标签法	133
5.11.6	基于 RNA 差异表达的分离方法	134
5.12	外源基因表达技术	137
5.12.1	基因表达的分子生物学基础	137
5.12.2	外源基因在大肠杆菌中的表达	138
5.12.3	外源基因在酵母中的表达	147
5.12.4	外源基因在哺乳动物细胞中的表达	150
5.12.5	外源基因在植物细胞中的表达	154
5.12.6	外源基因表达产物的检测与纯化	157
第 6 章	基因工程在农业作物上的应用	161
6.1	基因工程技术在农业上的应用	161
6.1.1	培育转基因作物	161
6.1.2	改进常规育种	161
6.1.3	分子育种	162
6.2	基因工程技术在育种上的应用	162
6.2.1	提高光合作用效率	162
6.2.2	固氮基因的利用	163
6.2.3	作物品质改良	163
6.2.4	增加次生代谢物的产率	163
6.2.5	增强作物抗病虫害的能力	164
6.2.6	增强作物的抗除草剂的能力	164



6.3 植物基因工程产品的安全性问题	164
--------------------------	-----

第二部分 基因工程实验篇

实验一 碱裂解法抽提质粒 DNA	170
实验二 琼脂糖凝胶电泳	175
实验三 DNA 浓度测定与酶切反应	178
实验四 目的片段的回收	181
实验五 DNA 的体外连接	184
实验六 重组 DNA 的转化	188
实验七 重组转化子的快速鉴定	192
实验八 聚合酶链式反应(PCR)	194
实验九 植物基因组 DNA 提取	197
实验十 Southern 杂交	202
实验十一 植物总 RNA 提取	207
实验十二 RNA 质量的检测	210
实验十三 Northern 杂交	212
实验十四 反转录 PCR(RT-PCR)	215
实验十五 外源基因在原核生物细菌中的表达	218
实验十六 外源基因在真核生物毕赤酵母中的表达	224
实验十七 外源基因在无细胞表达系统麦胚提取物中的表达	228
实验十八 Western 杂交	231
实验十九 微卫星(SSR)标记分析	235
综合性设计性实验一 重组子鉴定方法探索	239
综合性设计性实验二 大肠杆菌 DNA 转化方法探索	241
综合性设计性实验三 大豆转基因成分检测	243
综合性设计性实验四 大米转基因成分检测	246
附录 I 溶液配方	248
附录 II 常用器皿的清洗	251
附录 III 实验所用引物	252
附录 IV 移液器使用与维护	254
附录 V 实验守则	255
参考文献	256



普通高等教育农业农村部“十四五”规划教材



普通高等教育“十四五”规划教材
生物科学类专业系列教材



基因工程 原理与实验

第2版

Principles and Experiments of
Genetic Engineering

易继财◎主编



中國農業大學出版社
China Agricultural University Press



普通高等教育农业农村部“十四五”规划教材



普通高等教育“十四五”规划教材
生物科学类专业系列教材

基因工程原理与实验

第2版

易继财 主编

中国农业大学出版社

· 北京 ·

内 容 简 介

本书由基因工程原理篇和基因工程实验篇两大部分组成,全面而系统地介绍了基因工程领域的理论和实践知识。在基因工程原理篇中,详细探讨了基因工程的基本原理与技术,涵盖绪论、工具酶、载体、基因连接、转化、筛选等核心内容,并关注了其最新发展动态。此外,深入剖析了基因工程在农业作物、园艺植物、林木及植物性食品等领域中的实际应用,同时对转基因作物的研究现状及未来发展趋势进行了重点探讨。本篇旨在帮助读者全面把握基因工程领域的前沿动态,并深化对其科学原理的理解。基因工程实验篇则充分展现了基因工程作为高度实践性学科的特点。编者依托自身的科研实践经验,紧密结合农林生物类研究人员的实际需求,精心整理并收录了教研室多年来为本校师生及相关研究人员开设的一系列具有代表性的基因工程实验。通过本篇的实际操作指导,旨在帮助读者更加直观且深入地理解和掌握基因工程的实验原理与操作方法,从而提升本书的实用性和指导意义。

图书在版编目(CIP)数据

基因工程原理与实验 / 易继财主编. --2 版. --北京:中国农业大学出版社,2024.5
ISBN 978-7-5655-3201-6

I. ①基… II. ①易… III. ①基因工程—高等学校—教材 IV. ①Q78

中国国家版本馆 CIP 数据核字(2024)第 065338 号

农业农村部教材办公室审定编号:NY-1-0087

书 名 基因工程原理与实验 第2版

Jiyin Gongcheng Yuanli yu Shiyao

作 者 易继财 主编

策划编辑 赵 艳

责任编辑 赵 艳

封面设计 李尘工作室

出版发行 中国农业大学出版社

社 址 北京市海淀区圆明园西路2号

邮政编码 100193

电 话 发行部 010-62733489,1190

读者服务部 010-62732336

编辑部 010-62732617,2618

出 版 部 010-62733440

网 址 <http://www.caupress.cn>

E-mail cbsszs@cau.edu.cn

经 销 新华书店

印 刷 河北虎彩印刷有限公司

版 次 2024年5月第2版 2024年5月第1次印刷

规 格 185 mm×260 mm 16开本 21印张 524千字

定 价 66.00元

图书如有质量问题本社发行部负责调换

第2版编审人员

主 编 易继财 (华南农业大学)

副主编 周 海 (华南农业大学)

赵均良 (广东省农业科学院水稻研究所)

刘振兰 (华南农业大学)

陈乐天 (华南农业大学)

编 者 (按姓氏笔画排序)

刘祖培 (华南农业大学)

刘振兰 (华南农业大学)

阮小蕾 (华南农业大学)

李 静 (华南农业大学)

杨美艳 (华南农业大学)

余红兵 (广东医科大学)

张群宇 (华南农业大学)

陈 亮 (华南农业大学)

陈长明 (华南农业大学)

陈乐天 (华南农业大学)

陈忠正 (华南农业大学)

林 同 (华南农业大学)

易继财 (华南农业大学)

周 峰 (华南农业大学)

周 海 (华南农业大学)

周玲艳 (仲恺农业工程学院)

郑少燕 (华南农业大学)

赵均良 (广东省农业科学院水稻研究所)

姜大刚 (华南农业大学)

祝钦洸 (华南农业大学)

谢先荣 (华南农业大学)

谢勇尧 (华南农业大学)

主 审 庄楚雄 (华南农业大学)

目 录

第一部分 基因工程原理篇

第 1 章 绪论	2
1.1 基因学说与基因的现代概念	2
1.1.1 经典遗传学阶段的基因学说	3
1.1.2 分子遗传学阶段的基因学说	3
1.1.3 现代基因学说	4
1.2 基因工程的诞生与发展	5
1.3 基因工程的研究内容	8
1.4 基因工程应用概况	10
1.4.1 基因工程在农业上的应用	10
1.4.2 基因工程在工业上的应用	11
1.4.3 基因工程在医学上的应用	11
1.4.4 基因工程在军事和国防上的潜在应用	12
第 2 章 基因工程的工具酶	14
2.1 核酸酶	14
2.1.1 限制性核酸内切酶	14
2.1.2 非限制性核酸酶	20
2.2 聚合酶	22
2.2.1 DNA 聚合酶	22
2.2.2 RNA 聚合酶	24
2.2.3 末端转移酶	24
2.3 连接酶	25
2.4 修饰酶	30
第 3 章 基因工程载体	31
3.1 质粒载体	32
3.1.1 质粒载体的生物学特性	32
3.1.2 质粒载体的发展	35



3.1.3 常见的质粒载体.....	36
3.2 噬菌体载体.....	40
3.2.1 噬菌体概述.....	40
3.2.2 噬菌体的生物学特性.....	42
3.2.3 常见噬菌体载体.....	43
3.3 人工染色体载体.....	48
3.4 其他载体.....	51
第4章 DNA的连接、转化和重组子筛选	52
4.1 DNA的连接	52
4.1.1 传统依赖连接酶的DNA重组连接技术	52
4.1.2 现代不依赖连接酶的DNA重组连接新技术	54
4.2 DNA分子导入受体细胞	55
4.2.1 DNA分子导入细菌细胞	56
4.2.2 重组DNA分子导入真核细胞	57
4.3 重组子的筛选与鉴定.....	59
4.3.1 重组子的初步筛选.....	59
4.3.2 重组子的进一步筛选.....	61
第5章 基因工程技术与方法	63
5.1 核酸的分离纯化.....	63
5.1.1 DNA的分离纯化	64
5.1.2 RNA的分离纯化	65
5.2 凝胶电泳技术.....	66
5.2.1 琼脂糖凝胶电泳.....	67
5.2.2 聚丙烯酰胺凝胶电泳.....	69
5.2.3 脉冲电场凝胶电泳.....	70
5.3 PCR技术	71
5.3.1 PCR的基本原理	72
5.3.2 未知序列DNA片段的PCR	76
5.3.3 反转录PCR	79
5.3.4 差异显示RT-PCR	79
5.3.5 抑制热交错PCR技术	81
5.3.6 Ω -PCR技术	84
5.3.7 实时定量PCR	85
5.4 探针标记技术.....	88
5.4.1 放射性探针标记.....	88
5.4.2 非放射性标记.....	90
5.5 分子杂交技术.....	91
5.5.1 Southern杂交	92
5.5.2 Northern杂交	94



5.5.3	Western 杂交	94
5.5.4	原位杂交	95
5.5.5	斑点杂交和狭线杂交	95
5.5.6	基因芯片杂交	96
5.6	DNA 测序技术	96
5.6.1	第一代测序技术	97
5.6.2	新一代测序技术	99
5.7	DNA 定点突变与基因编辑技术	102
5.7.1	基因编辑技术概述	103
5.7.2	CRISPR/Cas9 基因编辑技术	104
5.7.3	基因编辑突变的检测	105
5.8	抑制缩减杂交技术	108
5.9	基因芯片技术	110
5.9.1	基因芯片技术简介	110
5.9.2	基因芯片的制作	111
5.9.3	杂交流程与结果检测	112
5.9.4	基因芯片技术的应用	112
5.10	分子标记技术	113
5.10.1	遗传标记的类型	114
5.10.2	RFLP 标记	117
5.10.3	RAPD 标记	118
5.10.4	AFLP 标记	120
5.10.5	SSR 标记	120
5.10.6	SNP 标记	123
5.10.7	其他类型分子标记	125
5.10.8	分子标记在植物分子育种中的应用	127
5.11	目的基因的分离技术	131
5.11.1	化学合成法	132
5.11.2	基因文库法	134
5.11.3	PCR 法	141
5.11.4	图位克隆法	141
5.11.5	DNA 标签法	143
5.11.6	基于 RNA 差异表达的分离方法	144
5.11.7	基于蛋白质互作的分离方法	147
5.12	外源基因表达技术	153
5.12.1	基因表达的分子生物学基础	153
5.12.2	外源基因在大肠杆菌中的表达	154
5.12.3	外源基因在酵母中的表达	163
5.12.4	外源基因在哺乳动物细胞中的表达	165



5.12.5 外源基因在植物细胞中的表达	170
5.12.6 外源基因表达产物的检测与纯化	173
5.13 合成生物学技术	176
5.13.1 合成生物学研究概述	176
5.13.2 合成生物学技术的原理	176
5.13.3 合成生物学研究发展与展望	179
第6章 基因工程在农业作物上的应用	182
6.1 植物转基因技术概述	182
6.2 植物转基因技术在农业作物上的关键应用	184
6.2.1 提高作物的光合作用效率	185
6.2.2 增强作物的固氮能力	187
6.2.3 改良作物的品质	189
6.2.4 增加作物的次生代谢产物含量	190
6.2.5 增强作物的抗病虫害能力	192
6.2.6 增强作物的抗除草剂能力	196
6.2.7 增强作物的抗非生物胁迫能力	198
第7章 基因工程在园艺植物上的应用	201
7.1 改善园艺植物的抗性	201
7.1.1 提高抗病能力	201
7.1.2 提高抗虫能力	202
7.1.3 提高抗逆能力	203
7.2 改良园艺产品的品质	203
7.3 改善园艺产品的耐储性	204
7.4 在园艺植物其他方面的应用	205
第8章 基因工程在林木上的应用	207
8.1 林木基因工程研究历史	207
8.2 林木遗传转化技术进展	208
8.3 林木基因工程改良的主要性状	209
8.4 林木基因工程实例:杨树抗虫基因工程	210
第9章 基因工程在植物性食品上的应用	212
9.1 改良植物食品的营养品质及风味	212
9.2 改进植物食品的加工工艺	213
9.3 提升植物食品的耐储性	214
9.4 生产功能性食品	214
第10章 转基因作物研究发展与展望	216
10.1 转基因作物的种植情况	217
10.2 转基因作物的安全性评价	220
10.3 转基因作物检测技术的发展	221
10.4 转基因作物的监管与研究展望	222



第二部分 基因工程实验篇

实验一 碱裂解法抽提质粒 DNA	228
实验二 琼脂糖凝胶电泳	232
实验三 DNA 浓度测定与酶切反应	235
实验四 目的片段的回收	238
实验五 DNA 的体外连接	241
实验六 重组 DNA 的转化	247
实验七 重组转化子的快速鉴定	251
实验八 聚合酶链式反应(PCR)	253
实验九 植物基因组 DNA 提取	256
实验十 Southern 杂交	261
实验十一 植物总 RNA 提取	266
实验十二 RNA 质量的检测	269
实验十三 Northern 杂交	271
实验十四 反转录 PCR(RT-PCR)	274
实验十五 实时荧光定量 PCR	277
实验十六 外源基因在原核生物细菌中的表达	282
实验十七 外源基因在真核生物毕赤酵母中的表达	288
实验十八 外源基因在无细胞表达系统麦胚提取物中的表达	292
实验十九 Western 杂交	295
实验二十 微卫星(SSR)标记分析	299
综合性设计性实验一 大肠杆菌 DNA 转化方法探索	303
综合性设计性实验二 重组子鉴定方法探索	305
综合性设计性实验三 大米转基因成分检测	307
综合性设计性实验四 大豆转基因成分检测	309
附录 I 溶液配方	311
附录 II 常用器皿的清洗	314
附录 III 实验所用引物	315
附录 IV 移液器使用与维护	317
附录 V 实验守则	318
参考文献	319

转基因生物新品种培育重大专项课题

“转基因生物安全监测技术”

专题任务合同书

课 题 来 源: 转基因生物新品种培育重大专项课题

课 题 名 称: 转基因生物安全监测技术

课 题 编 号: 2008ZX08012-04

课题主持单位: 中国农业科学院植物保护研究所

课题主持人: 吴孔明

专 题 名 称: 华南地区 Bt 水稻环境影响监测

专题主持单位: 华南农业大学

专题主持人: 周峰

起 止 年 限: 2008 年 7 月至 2010 年 12 月

一、研究内容与考核指标

1 研究内容

以水稻种子和稻株为材料,监测水稻主产区福建、广东、广西、安徽等地转基因水稻非法种植的总体情况;开展三化螟的人工饲料及饲养技术研究,实现继代饲养。

2 考核指标

提交上述地区转基因水稻安全监测报告 1 份;初步建立 1 种水稻主要鳞翅目害虫的继代饲养技术;培养研究生 1-2 名;发表学术论文 2-3 篇;申请专利 1 项。

3 备注

本专题隶属于课题中第六任务(Bt 水稻与转植酸酶基因玉米环境影响监测技术,中国水稻研究所傅强研究员负责)。

二、承担人员

负 责 人	姓 名	性 别	出生 年月	专业技 术职务	工 作 单 位	工作时间 (人月)	签 字
	周峰	男	1972-12	助理研究员	华南农业大学	18	周峰
参 加 人 员	罗建军	男	1971-08	讲师	华南农业大学	16	罗建军
	姜大刚	男	1977-12	助理研究员	华南农业大学	14	姜大刚
	姚涓	女	1974-04	实验师	华南农业大学	12	姚涓
	易继财	男	1971-10	副教授	华南农业大学	10	易继财
	梅曼彤	女	1942-10	教授	华南农业大学	8	梅曼彤

三、经费额度及账号

其中：2008 年国拨经费 14.0 万元

单位名称：华南农业大学

开户银行：广州工行五山支行

账 号：3602002609000310520

四、签字盖章及意见

专题负责人签字:

我将严格遵守转基因生物新品种培育重大专项经费项目和经费管理的各项规定, 根据本专题任务书, 按计划组织专题组开展研究, 完成专题研究计划和考核指标, 实现预期目标。

专题负责人(签字):

周峰

2009年4月29日

专题承担单位(部门)盖章:

我单位严格遵守转基因生物新品种培育重大专项和经费管理的各项规定, 对专题研究提供保障和支持, 对专题经费使用进行监督, 督促专题组按计划完成预期目标。

负责人(签字):

(专题承担单位或部门盖章)

2009年4月29日

课题负责人意见:

课题负责人(签字):

吴孔明

单位公章

2009年4月29日

备注: 本合同一式六份, 课题承担单位三份, 任务承担单位一份, 专题承担单位两份。

转基因生物新品种培育重大专项课题

“转基因生物安全监测技术”

专题任务合同书

课 题 来 源: 转基因生物新品种培育重大专项课题

课 题 名 称: 转基因生物安全监测技术

课 题 编 号: 2008ZX08012-04

课题主持单位: 中国农业科学院植物保护研究所

课题主持人: 吴孔明

专 题 名 称: 华南地区 Bt 水稻环境影响监测

专题主持单位: 华南农业大学

专题主持人: 周峰

起 止 年 限: 2008 年 7 月至 2010 年 12 月

一、研究内容与考核指标

1 研究内容

以水稻种子和稻株为材料,监测水稻主产区福建、广东、广西、安徽等地转基因水稻非法种植的总体情况;开展三化螟的人工饲料及饲养技术研究,实现继代饲养。

2 考核指标

提交上述地区转基因水稻安全监测报告 1 份;初步建立 1 种水稻主要鳞翅目害虫的继代饲养技术;培养研究生 1-2 名;发表学术论文 2-3 篇;申请专利 1 项。

3 备注

本专题隶属于课题中第六任务(Bt 水稻与转植酸酶基因玉米环境影响监测技术,中国水稻研究所傅强研究员负责)。

二、承担人员

负 责 人	姓 名	性 别	出生 年月	专业技 术职务	工 作 单 位	工作时间 (人月)	签 字
	周峰	男	1972-12	助理研究员	华南农业大学	18	周峰
参 加 人 员	罗建军	男	1971-08	讲师	华南农业大学	16	罗建军
	姜大刚	男	1977-12	助理研究员	华南农业大学	14	姜大刚
	姚涓	女	1974-04	实验师	华南农业大学	12	姚涓
	易继财	男	1971-10	副教授	华南农业大学	10	易继财
	梅曼彤	女	1942-10	教授	华南农业大学	8	梅曼彤

三、经费额度及账号

其中：2009 年国拨经费 52.0 万元

单位名称：华南农业大学

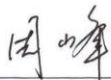
开户银行：广州工行五山支行

账 号：3602002609000310520

四、签字盖章及意见

专题负责人签字:


我将严格遵守转基因生物新品种培育重大专项经费项目和经费管理的各项规定,根据本专题任务书,按计划组织专题组开展研究,完成专题研究计划和考核指标,实现预期目标。

专题负责人(签字): 

2009年9月15日


专题承担单位(部门)盖章:

我单位严格遵守转基因生物新品种培育重大专项和经费管理的各项规定,对专题研究提供保障和支持,对专题经费使用进行监督,督促专题组按计划完成预期目标。

负责人(签字): 
(专题承担单位或部门盖章)

2009年9月16日

课题负责人意见:

课题负责人(签字): 

单位公章

2009年9月15日

备注:本合同一式六份,课题承担单位三份,任务承担单位一份,专题承担单位两份。

转基因生物新品种培育重大专项课题

“转基因生物安全监测技术”

专题任务合同书

课 题 来 源: 转基因生物新品种培育重大专项课题

课 题 名 称: 转基因生物安全监测技术

课 题 编 号: 2008ZX08012-04

课题主持单位: 中国农业科学院植物保护研究所

课题主持人: 吴孔明

专 题 名 称: 华南地区 Bt 水稻环境影响监测

专题主持单位: 华南农业大学

专题主持人: 周峰

起 止 年 限: 2008 年 7 月至 2010 年 12 月

一、研究内容与考核指标

1 研究内容

以水稻种子和稻株为材料，监测水稻主产区福建、广东、广西、安徽等地转基因水稻非法种植的总体情况；开展三化螟的人工饲料及饲养技术研究，实现继代饲养。

2 考核指标

提交上述地区转基因水稻安全监测报告 1 份；初步建立 1 种水稻主要鳞翅目害虫的继代饲养技术；培养研究生 1-2 名；发表学术论文 2-3 篇；申请专利 1 项。

3 备注

本专题隶属于课题中第六任务（Bt 水稻与转植酸酶基因玉米环境影响监测技术，中国水稻研究所傅强研究员负责）。

二、承担人员

负 责 人	姓 名	性 别	出生 年月	专业技 术职务	工 作 单 位	工作时间 (人月)	签 字
	周峰	男	1972-12	助理研究员	华南农业大学	18	周峰
参 加 人 员	罗建军	男	1971-08	讲师	华南农业大学	16	罗建军
	姜大刚	男	1977-12	助理研究员	华南农业大学	14	姜大刚
	姚涓	女	1974-04	实验师	华南农业大学	12	姚涓
	易继财	男	1971-10	副教授	华南农业大学	10	易继财
	梅曼彤	女	1942-10	教授	华南农业大学	8	梅曼彤

三、经费额度及账号

其中：2010 年国拨经费 44.0 万元

单位名称：华南农业大学

开户银行：广州工行五山支行

账 号：3602002609000310520

四、签字盖章及意见

专题负责人签字:

我将严格遵守转基因生物新品种培育重大专项经费项目和经费管理的各项规定,根据本专题任务书,按计划组织专题组开展研究,完成专题研究计划和考核指标,实现预期目标。

专题负责人(签字):

2010年5月25日

专题承担单位(部门)盖章:

我单位严格遵守转基因生物新品种培育重大专项和经费管理的各项规定,对专题研究提供保障和支持,对专题经费使用进行监督,督促专题组按计划完成预期目标。

负责人(签字):
(专题承担单位或部门盖章)

2010年5月25日

课题负责人意见:

课题负责人(签字):

单位公章

2010年 月 日

备注:本合同一式六份,课题承担单位三份,任务承担单位一份,专题承担单位两份。

农业转基因生物安全科普进校园 任务（合同）书

任务名称：转基因生物安全科普进校园

任务下达单位（甲方）：农业农村部科技发展中心

任务承担单位（乙方）：华南农业大学

起止年限：2018 年 6 月 01 日～2018 年 11 月 30 日

农业农村部科技发展中心制

2018 年 3 月 01 日

一、科普目的与意义

以转基因技术为核心的现代农业生物技术在缓解资源约束、保障粮食安全、保护生态环境、拓展农业功能等方面已显现出巨大潜力，成为世界各国农业科技竞争的焦点，在现代农业发展中发挥着先导和引领作用。当前，按照党中央、国务院的战略部署，要进一步强化战略、法律、科技、行政、舆论五大支撑，积极研究、审慎应用、严格管理、科学宣传，保持定力，把握节奏，积极稳妥推进转基因研究与应用。

转基因技术是一项新技术，也是一个新产业，具有广阔发展前景。随着转基因生物的商业化应用，转基因生物安全问题相伴而生，引起人们的普遍关注，不同人群对转基因的态度不一，考虑问题的出发点错综复杂，涉及科学、政治、经济、贸易、宗教、伦理等诸多因素。能否正确认识转基因技术和转基因生物安全，严重制约着转基因技术的应用、普及和快速发展，成为亟待解决的瓶颈问题。

为进一步提高转基因生物安全科普宣传水平，广泛深入地宣传转基因科学知识和转基因生物安全管理政策法规，提高公众认知程度，引导公众科学理性看待转基因技术及其安全性，急需提升社会民众特别是青年学生的认知水平，营造转基因研究与应用的良好舆论氛围。

二、科普目标与任务

面向在校大学生普及转基因生物安全知识，提升青年学生科学素养，增进对转基因技术的认同感，培育潜在的转基因生物安全宣传力量。

1. 编制（购置）并发放转基因生物安全科普宣传材料 1000 份以上；
2. 制作转基因科普宣传挂图或展板 10 副以上；
3. 组织广东省 2 所高校在校学生科普讲座，培训师生 800 人次以上；
4. 在农事训练课程中增设转基因科普模块，或组织 1 次大学生转基因生物安

<p>全知识有奖问卷调查；</p> <p>5. 提交转基因科普宣传进校园工作总结报告，并附相关证明材料；提交相关科普宣传素材。</p>
<p>三、科普对象与内容</p> <p>科普对象：广东省在校大学生</p> <p>科普内容：转基因技术及转基因生物安全基础知识、转基因食品安全与人体健康问题、转基因作物环境安全、转基因谣言解析等。</p>
<p>四、组织分工</p> <p>农业农村部科技发展中心负责科普宣传进校园工作的指导；</p> <p>华南农业大学负责科普宣传进校园工作的具体组织和实施。</p>
<p>五、时间进度</p> <p>2018 年 6 月，制定科普工作方案，准备宣传材料。</p> <p>2018 年 7 月～11 月，完成科普工作。</p> <p>2018 年 11 月，提交工作总结和相关科普宣传素材。</p>
<p>六、经费预算与筹措</p> <p>转基因生物安全科普宣传材料 1500 份，每份 20 元，小计 3.0 万元（包括编制费、印刷费、购置费等）；制作转基因科普宣传挂图或展板 10 副，每副 500 元，小计 0.5 万元；在校大学生科普讲座 2 场，每场 1.5 万元，小计 3.0 万元（包括场</p>

地费、讲课费、培训材料等)；组织大学生转基因生物安全知识有奖问卷调查，小计 1.4 万元（包括组织、教学用具及奖品购置等）；其它费用（包括差旅费等）2.1 万元。经费共计 10 万元，全部由农业农村部科技发展中心拨付，经费预算详见下表：

经济分类科目	预算金额（万元）	支出内容
宣传资料费	3.5	制作、购买宣传资料
会务费	3.0	科普讲座
专用材料等	1.4	有奖问卷调查
其他	2.1	差旅费等

七、参与人员与分工

科普负责人

姓 名	性别	年龄	职务 (职称)	从事专业	工作单位	承担任务与职责
周峰	男	46	助研 检测室主任	生物学	华南农业大学	项目负责人

主要参加人

王声斌	男	51	副教授 常务副主任	生物学	华南农业大学	协调沟通
何冬梅	女	42	副书记	高等教育管理	华南农业大学	讲座报告联络
姜大刚	男	41	副研究员 副主任	生物学	华南农业大学	专业技术指导
姚涓	女	44	高级实验师 办公室主任	生物学	华南农业大学	宣传材料
董皓	男	26	辅导员	生物学	华南农业大学	问卷调查
叶景欣	男	26	辅导员	设施农业	华南农业大学	问卷调查

九、共同条款与约定

甲方组织开展转基因科普进校园工作，将部分任务委托乙方实施。为保证工作的正常开展和任务的顺利完成，双方签署并严格执行本任务（合同）书的约定。

1、甲、乙双方共同遵守《农业转基因生物安全管理条例》及其配套管理办法的规定，确保本次科普工作的顺利实施。

2、甲方负责提出转基因科普进校园的内容和要求。同时，向乙方拨付科普经费 10.0 万元，工作经费拨付到乙方指定的下列帐户：

收款单位：华南农业大学

开户银行：广州工行五山支行

帐 号：3602002609000310520

乙方应在收到工作经费后 15 个工作日内向甲方开具正规税务发票。

3、乙方在甲方指导下，负责科普宣传活动的组织和联系转基因科普宣讲专家等。乙方应按照计划进度完成科普内容和任务，保证任务（合同）书中负责人及主要参加人员的工作时间，并按规定和要求及时向甲方提供工作总结报告和相关资料。同时，乙方应及时向甲方报告与科普工作有关的重大问题。

4、本任务（合同）书执行过程中产生的文章、海报、图书、视频等产权归双方共同所有，可利用上述材料开展其他工作。

5、乙方必须保证本任务（合同）书中负责人及主要参加人的稳定，如遇特殊原因需要变动，必须及时提出申请，经甲方同意方可更换。对甲方所拨工作经费的支出，必须严格按任务要求和财务规定专款专用。若经费超支，由乙方自筹解决，但不得影响本任务（合同）书的执行。

6、在任务执行过程中，如遭遇不可抗力因素和发生其它可能影响本任务（合同）书按期完成的重大事件，或本合同内容和任务需要调整、撤消时，乙方应当及时向甲方提交书面报告，经甲方确定后执行。乙方因主观原因致使本任务（合同）书无法执行，甲方有权中止执行，追回全部工作经费，若甲方无故不履行本任务（合同）书，不得追回工作经费。

7、本任务（合同）书执行过程中发生争议或纠纷时，由甲、乙双方协商解决，协商不成可以提交法院仲裁或裁决。

8、本任务（合同）书正式文本一式 4 份，分存甲方（2 份）、乙方（2 份），甲、乙双方签字、盖章后生效。

9、本合同自签订之日起生效。

十、合同双方与签章

甲 方：农业农村部科技发展中心（公章）

单位领导：（签字）

经 办 人：（签字）

通讯地址：北京市亦庄开发区荣华南路甲 18 号科技大厦 407 室

邮政编码：100122

联 系 人：李文龙


联系电话：（010）59198148

电子信箱：bj_liwenlong@163.com

签约日期：2018 年 7 月 16 日

乙 方：华南农业大学（公章）

单位领导：（签字）

经 办 人：（签字）

通讯地址：广州市天河区五山路 483 号华南农业大学科技楼 1116 室

邮政编码：510642

联 系 人：周峰

联系电话：13825042322

电子信箱：zhoufeng@scau.edu.cn

签约日期：2018 年 6 月 22 日

项目编号：202201010028

基础与应用基础研究项目 合同书

项目名称：OsSSD1调控水稻植株形态的分子机理研究

承担单位：华南农业大学

项目负责人：周峰

计划类别：基础研究计划

专题名称：基础与应用基础研究项目

支持方向：一般项目（其他类）

组织单位：华南农业大学

起止时间：2022年04月01日 至 2024年03月31日

主管处室：基础研究处

广州市科学技术局
(二〇二二年制)

填写说明

一、本合同书的项目编号由市科学技术局（以下简称市科技局）统一确定。

二、本合同书由申报书在后台自动转换生成，如有错漏之处需修正，请联系市科技局项目责任处室退回承担单位修正。

三、项目经费分为直接费用和间接费用。

基础与应用基础研究专题项目试点实施“包干制”，经费支出不设科目比例限制，由项目研究团队自主调剂使用，按照市科研项目经费“包干制”管理有关规定执行，同时应符合以下要求：

（1）经费支出应实际用于项目研究支出，使用范围限于设备费、材料费、测试化验加工费、燃料动力费、差旅/会议/国际合作与交流费、出版/文献/信息传播/知识产权事务费、劳务费、专家咨询费、依托单位管理费用、绩效支出以及其他合理支出。

（2）经费支出应按照市级财政科研项目资金开支范围和标准使用；

（3）间接费用是指项目承担单位在组织实施项目过程中发生的无法直接列支的相关费用，主要用于补偿项目承担单位为了项目研究提供的现有仪器设备及房屋，水、电、气、暖消耗，有关提高科研管理、服务能力等费用，以及绩效支出等。间接费用按照不超过项目直接费用扣除设备购置费后的一定比例核定，具体比例按《广州市财政局 广州市科学技术局 广州市审计局关于市级财政科研项目资金绩效提升和管理监督办法》规定确定。

（4）不得列支基建费；

（5）项目验收时应提交经费决算表

四、本合同书仅适用于广州市基础与应用基础研究项目

一、基本信息

项目负责人	姓名	周峰	证件类型	身份证	证件号码	340104197212273037	性别	男
	出生年月	1972年12月27日	民族	汉族	国籍	中国	学历	博士研究生
	学位	博士	学位授予国家(或地区)	中国	职务	无	职称	助理研究员
	所学专业	作物遗传育种	手机号码	13825042322	办公电话	020-38297793	电子邮箱	68529268@qq.com

项目承担单位	单位名称	华南农业大学	统一社会信用代码或组织机构代码	124400004554165634
	注册时间	1952-01-01	单位类型	高等院校
	注册地址	广东省广州市天河区五山路483号		
	办公地址	广东省广州市天河区五山路483号		
	联系人	姓名	倪慧群	
		手机号码	15920301530	
		电子邮箱	kjcgxk@scau.edu.cn	
	开户银行	广东广州工行五山支行		
	开户户名	华南农业大学		
	银行帐号	3602002609000310520		
研究平台				

项目 基本 信息	项目名称	OsSSD1调控水稻植株形态的分子机理研究		
	所属学科	生命-农学基础与作物学-作物种质资源与遗传育种学-稻类作物种质资源与遗传育种		
	申请金额	5.00万元	研究期限	2022年04月01日-2024年03月31日
项目 摘要	<p>已发现的控制水稻植株形态发育的基因多与赤霉素（GA）、油菜素内酯（BR）及独脚金内酯（SLs）等植物激素的合成或信号传导途经有关。在前期研究中我们发现了一个新的水稻矮秆突变体，该突变体在株高、穗长、分蘖数、种子大小及结实率等方面均与野生型存在极为显著的表型差异。研究表明，突变体是由于一个含DUF4378结构域的基因OsSSD1突变造成的，并已通过互补试验及CRISPR/cas9基因敲除试验加以证实。</p> <p>迄今为止，含DUF4378结构域的基因对植物植株形态发育调控的详细机理未见研究报道。本项目拟通过RNA干涉、过表达及亚细胞定位分析并结合转录组测序、iTRAQ蛋白质组分析和蛋白质互作分析，初步阐明OsSSD1基因参与细胞内的代谢途径及对水稻植株形态发育调控的分子机理。</p>			

二、项目预期成果

论文及专著情况	国家统计局刊物以上刊物发表论文（篇）		1		科技报告（篇）		1	
	其中，被SCI/EI/ISTP收录论文数（篇）		1		培养人才（人）		1	
	专著（册）		0		引进人才（人）		0	
专利情况(项)	发明专利		实用新型专利		外观设计专利		国外专利	
	申请	授权	申请	授权	申请	授权	申请	授权
	0	0	0	0	0	0	0	0
其他	无							

三、项目经费预算

本项目总投入：¥（ 5.00 ）万元，其中，市财政补助经费：¥（ 5.00 ）万元，自筹经费：¥（ 0 ）万元。

（单位：万元）

1. 经费下达计划			
资金来源	小计	市科技局经费	自筹资金
2023年	5.00	5.00	/
合计	5.00	5.00	/

注：本项目市科技局经费试点实施“包干制”，经费支出不设科目比例限制，由项目研究团队自主调剂使用，按照市科研项目经费“包干制”管理有关规定执行。

四、合同条款

第一条 甲、乙、丙方根据《中华人民共和国科学技术进步法》《广东省自主创新促进条例》《广州市科技创新条例》及《中华人民共和国民法典》等国家有关法规和规定，经协商一致，特订立本合同，作为甲、乙、丙方在合同执行中共同遵守的依据。

第二条 甲方、乙、丙三方应当严格履行《广州市科技计划项目管理办法》《广州市级财政科研项目资金绩效提升和管理监督办法》《广州市科技创新发展专项资金管理办法》《广州市科技计划项目经费“包干制”改革试点工作方案》《广州市科技计划项目全过程管理简政放权改革工作方案》的规定要求。

第三条 甲方应：

1. 根据财政经费预算安排，及时进行拨付项目经费。
2. 赋予乙方和丙方广州市科技业务管理阳光政务平台（以下简称阳光政务平台）的使用权限，保障丙方进行项目全过程管理的使用需求。
3. 根据甲方需要，在不影响乙方工作的前提下，定期或不定期对乙方项目的实施情况和经费使用情况进行检查或抽查。
4. 审核丙方提交的年度工作报告，制定下一年度的资金切块方案。
5. 对丙方进行周期绩效考核和检查评估，重新评估丙方资格。

第四条 乙方应：

1. 作为项目具体组织实施的责任主体，为本单位提供的与本项目有关的全部材料真实、合法、有效性负责，同意甲方向行业协会等第三方机构直接调取乙方与本项目相关的数据、信息、材料，包括但不限于工商登记信息、审计报告等；
2. 按照《合同书》规定的内容组织实施项目，接受并配合甲方、丙方以及各级财政、审计部门，或上述部门委托的机构进行评估、稽查、审计、检查和绩效评价，并按要求提供项目任务与预算执行情况和有关财务资料；
3. 按照市财政科技经费管理“包干制”相关要求对项目经费单独设账，专款专用；
4. 保证自筹资金按时到位和其它配套条件的落实；
5. 在项目研究开发过程中优先考虑使用“广东省科技资源共享服务平台”的仪器设备，项目购置的设备仪器若符合入网条件应及时办理入网手续对社会共用共享，提高设备仪器的使用率。按照《中华人民共和国采购法》要求，对符合政府采购范围的设备仪器，执行政府采购；
6. 项目合同执行期内需进行变更的，按照《广州市科技计划项目管理办法》《广州市级财政科研项目资金绩效提升和管理监督办法》《广州市科技创新发展专项资金管理办法》《广州市科技计划项目全过程管理简政放权改革工作方案》相关程序办理；
7. 项目合同执行期满后3个月内向丙方提出验收申请，并出具在广州注册会计市协会备案的验收专项审计报告，提前完成合同规定任务的可提前申请验收；
8. 按照相关规定，在项目验收时提交科技报告，办理《验收证书》和科技成果登记手续；

9. 在项目实施期间和项目结题验收后3年内，配合甲方开展对财政资金年度绩效跟踪，按照甲方要求提供相关信息和数据，完成年度报告填报任务；

第五条 丙方应：

1. 明确项目管理依据的管理办法或管理规程，承担项目全过程管理职责；
2. 自主安排立项评审和结题验收工作，充分利用阳光政务平台，推进项目全过程管理的网络化电子化，主动配合推行合同电子签章；
3. 严格落实信息公开制度，公示遴选和结题验收结果，并及时处理异议；
4. 及时报送相关材料，按广州市科学技术局要求，每年按时提交拟立项项目清单，报送年度工作总结；
5. 按广州市科学技术局要求配合开展绩效评价和监督检查工作；
6. 主动追回终止项目未使用和不合规支出的市财政科技经费；
7. 按照本单位相关项目管理办法组织项目验收工作，并按相关规定做好存档工作；
8. 协助甲方对项目的实施过程进行跟踪、检查和提供相关信息，并对所提供信息的客观真实性负责；
9. 负责监管乙方严格遵守本合同规定的任务；

第六条 甲方同意给予乙方人民币（5.00万）的资助，立项后一次性拨付。

第七条 合同终止：

1. 项目因故无法继续进行的，按照相关规定实施合同终止。
2. 发现存在以下情况之一的，立即启动终止程序：
 - ①因不可抗力因素导致项目无法继续进行、没有必要继续进行或无法完成合同预期目标任务的；
 - ②不接受项目监督检查、检查不合格限期整改后仍未通过的或拒不配合项目验收工作的；
 - ③无正当理由项目合同执行期满后3个月以后仍未提交验收申请的；
 - ④项目承担单位已迁出本市，或已停止经营活动，或已注销的；
 - ⑤发现在项目申报、实施过程中有违法、欺骗等事实的；
 - ⑥存在其他导致项目不能正常实施的原因。
3. 合同终止由乙方提出申请，丙方审定，也可由丙方强制实施。具体由丙方按照《广州市科技创新发展专项项目全过程管理简政放权改革试点工作方案》的规定要求进行办理。
4. 合同终止后，乙方或承接乙方法定义务的责任人应停止使用该项目财政经费；上缴尚未使用和使用不符合规定的财政经费。

第八条 对合同正常执行期及项目整改期之外的经费开支，不属于财政项目经费列支范围。

第九条 在履行本合同的过程中，乙方发现可能导致项目失败或部分失败的情形时，应及时通知甲方，并采取适当措施减少损失，没有及时通知并采取适当措施，致使损失扩大的，应当就扩大的损失承担责任。

第十条 在履行本合同的过程中，如遇到市财政计划改变等不可抗力情况，甲方对所核拨经费的数量和时间可进行相应变更。

第十一条 成果转化：

1. 本项目技术成果及知识产权的归属、转让和实施技术成果所产生的经济利益的分享，除另有约定外，按国家和省、市有关规定执行；正式发表的论文、论著应标注“广州市科技计划项目资助”字样及项目编号；项目所取得的技术成果和知识产权应优先广州产业化或推广转让。

第十二条 属技术保密的项目，经协商订立如下技术保密条款：

1. 本合同书保密内容范围为：本合同及其补充协议和附件、乙方因履行本合同所接触或知晓的甲方工作秘密（包括但不限于甲方的任何技术性资料、以及甲方为完成本合同提供的任何其他信息资料并且在提供时未说明是公开信息的）、在合同履行过程中，乙方接触到的，或履行合同产生的任何国家、商业、工作信息（包括但不限于计算机系统数据信息、审计工作资料、技术文档及相关敏感资料等）。

2. 本合同书保密期限为：\

3. 乙方及乙方人员（包括但不限于项目组人员、乙方雇员、代理人、顾问等工作人员，下同）采取有效的保密措施以避免泄露给任何第三方；乙方增强对项目组人员的保密教育，每年至少开展一次保密自查，并与可能知悉保密内容的人员签订技术保密保护协议，确保项目组人员遵守保密协议，乙方应保密义务不得低于本合同书的约定；甲乙双方应建立技术保密制度。

4. 乙方在合同履行的过程中，对接触到的相关信息，乙方及项目组人员承担保密责任；乙方应将项目组人员的身份证复印件、劳动合同、学历职称证明、项目经验等资料提供给甲方，更换项目负责人时需事先征得甲方书面同意并提交上述资料。

5. 在本合同有效存续期间及合同终止后，未经甲方事先的书面同意，不得以任何方式记录、复制、拍摄、摘抄、收藏、公布、发表、公开、披露、散播本合同项下保密信息的任何部分，或对其加以任何形式的利用或使用；乙方及乙方人员未经甲方书面同意不得私自下载、拷贝计算机内项目相关数据信息，不得擅自携带记载项目内容的载体（例如移动硬盘、U盘等）和打印资料外出，严禁将工作系统的程序、口令等泄露给他人。

6. 属技术保密的项目必须经相关负责技术保密部门审查、批准后，方可发表或用于境外合作与交流。

7. 乙方应当制定泄密应急预案，一旦发现本单位持有的国家科学技术秘密可能泄露或者已经泄露，应当在24小时内向甲方报告，同时启动应急预案，并协助有关部门查处泄密事件。

8. 乙方应严格遵守国家、省市规定的其他技术保密相关法律、法规和政策。
在项目实施过程中，乙方或项目合作单位及其相关人员违反科学技术保密管理相关规定，给国家安全和利益造成损害的，应当依法追究单位和相关人员的法律责任。

第十三条 廉洁责任

甲方、丙方、评审机构及其工作人员不得索取、收受利益相关方财物或其他不正当利益，严格遵守中央八项规定精神及其实施细则。

乙方应严格遵守国家、省、市关于科技专项经费使用的有关法律、法规，相关政策以及廉洁建设的各项规定，积极开展人员廉洁从业教育，防范科技项目组成员在科研活动中出现“法律、行政法规、部门规章或规范性文件规定的其他相关违规行为”。

第十四条 科研诚信和科技伦理要求

乙方应建立健全促进科研诚信和科技伦理的规章制度，落实以下职责：

1. 建立健全本单位学术论文发表诚信承诺制度、科研过程可追溯制度、科研成果检查和报告制度等成果管理制度。对本项目形成的科研成果的署名、研究数据真实性、实验可重复性等进行诚信审核和学术把关。防范科技项目组成员在项目申报、研发过程中出现提供虚假信息或材料，抄袭、剽窃他人科研成果，捏造、变造或篡改科研数据等违反科研诚信和科技伦理要求的情形。

2. 加强对科技项目参加人员的科研诚信和科技伦理教育，督促科技项目组成员恪守科学道德准则，遵守科研活动规范。对在科研诚信和科技伦理方面存在问题情节较严重的，应及时调整出项目团队并及时以书面形式报告甲方；

3. 加强对项目合作单位的科研诚信管理，正确履行管理、指导、监督职责，全面落实科研诚信和科技伦理要求；

4. 乙方或项目合作单位及其相关人员被记入科研严重失信行为数据库或相关社会领域信用“黑名单”，乙方应及时以书面形式报告甲方；

5. 乙方应严格遵守国家、省市规定的其他科研诚信管理和科技伦理相关法律、法规和政策。

6. 其他：在项目实施过程中，对乙方或项目合作单位及其相关人员有严重违背科研诚信和科技伦理要求的行为，甲方和相关部门可依照相关法律、法规规定对乙方采取责令改正、终止或撤销项目并追回财政性资金、记入科研诚信严重失信行为数据库等处理处罚措施。

第十五条 争议解决

因本合同书所产生的争议，各方应友好协商解决；协商不成的，各方同意由本合同签订地人民法院管辖。

第十六条 书面通知与送达

甲方在本合同履行过程中向乙方或丙方发出或者提供的所有书面通知、文件、文书、资料等，均以本合同所列明的乙方或丙方地址送达。乙方或丙方如果迁址，应当书面通知甲方；未履行书面通知义务的，甲方按原地址邮寄相关材料即视为已履行送达义务。

第十七条 鼓励开展科普工作

鼓励项目承担单位和人员结合科研任务对适合进行科学普及的项目内容加强科普工作。

本合同一式四份，各份具有同等效力。甲方和丙方各存一份，乙方存二份。本合同签订各方均负有相应的法律责任，不受机构、人事变动而影响。

说明：本《合同书》中，凡是三方约定无需填写的条款，在该条款的空白处划（\）。

附件：项目承担单位（乙方）及项目负责人承诺书

承诺书

本单位/本人作为广州市科技计划项目承担单位/项目负责人，将严格遵守广州市科技计划管理相关规定，严格履行自身责任，加强对项目组人员及合作单位的管理，在此郑重承诺：

（一）确保与本项目有关的全部材料真实、合法、有效，未侵犯其他方知识产权等权利；

（二）严格遵守《广州市科技计划项目管理办法》《广州市级财政科研项目资金绩效提升和管理监督办法》《广州市科技创新发展专项资金管理办法》《广州市科技计划项目全过程管理简政放权改革工作方案》等相关规定，实施项目和经费管理。

（三）严格遵守国家、省、市关于科研诚信和科技伦理的有关法律、法规，相关政策以及各项规定，加强项目实施过程中的科研诚信及科技伦理管理，恪守科研道德准则。

（四）_____

如有违反，本单位/本人愿意接受相关部门做出的各项处理决定，包括但不限于终止项目，停拨或核减经费，追回项目经费，取消一定期限广州市科技计划项目申报资格，记入科研诚信严重失信行为数据库，将不良行为向社会公开以及主要责任人接受相应党纪政纪处理等。

项目承担单位签章：

日期：2022.6.7

项目负责人签章：

日期：2022.6.9



合同书各方签章

广州市科学技术局（甲方）：广州市科学技术局

项目经办人：李磊

联系电话：020-83124052

责任处室负责人：莫雪华



项目承担单位（乙方）：华南农业大学

二级部门：华南农业大学生命科学学院

项目负责人：周峰

项目经费汇入账号

帐户名：华南农业大学

帐号：3602002609000310520

开户银行：广东广州工行五山支行

财务负责人：肖斐

财务负责人联系电话：020-5286032



组织单位（丙方）：华南农业大学

项目经办人：倪慧群





项目批准号	32270671
申请代码	C0606
归口管理部门	
依托单位代码	51064208A0499-0932



32270671 1006988

国家自然科学基金 资助项目计划书 (预算制项目)

资助类别: 面上项目

亚类说明:

附注说明:

项目名称: 亚洲稻自私遗传座位ARSL1的克隆和功能分析

直接费用: 54万元 执行年限: 2023.01-2026.12

负责人: 谢勇尧

通讯地址: 广东省广州市天河区五山路483号华南农业大学科技楼505

邮政编码: 510642 电 话: 020-38297231

电子邮件: yyxie@scau.edu.cn

依托单位: 华南农业大学

联系人: 唐家林 电 话: 020-85280070

填表日期: 2022年09月12日

国家自然科学基金委员会制

Version: 1.006.988



国家自然科学基金资助项目计划书填报说明 (预算制项目)

- 一、项目负责人收到《国家自然科学基金资助项目批准通知》（以下简称《批准通知》）后，请认真阅读本填报说明，参照国家自然科学基金相关项目管理办​​法和新修订的《国家自然科学基金资助项目资金管理办法》（以下简称《资金管理办法》，请查阅国家自然科学基金委员会官方网站首页“政策法规”栏目），按《批准通知》的要求认真填写和提交《国家自然科学基金资助项目计划书》（以下简称《计划书》）。
- 二、填写《计划书》时要科学严谨、实事求是、表述清晰、准确。《计划书》经国家自然科学基金委员会相关项目管理部门审核批准后，将作为项目研究计划执行、检查和验收的依据。
- 三、《计划书》各部分填写要求如下：
 - （一）简表：由系统自动生成。
 - （二）摘要及关键词：各类获资助项目都应当填写中、英文摘要及关键词。
 - （三）项目组主要成员：计划书中列出姓名的项目组主要成员由系统自动生成，与申请书原成员保持一致，不可随意调整。如果《批准通知》所附“项目评审意见及修改意见表”中“修改意见”栏目有调整项目组成员相关要求的，待项目开始执行后，按照项目成员变更程序另行办理。
 - （四）资金预算表：根据批准的项目资助额度，按规定调整项目预算，并按照《国家自然科学基金项目计划书预算表编制说明》填报资金预算表和预算说明书。
 - （五）正文：
 1. 面上项目、地区科学基金项目：如果《批准通知》所附“项目评审意见及修改意见表”中“修改意见”栏目没有修改要求的，只需选择“研究内容和研究目标按照申请书执行”即可；如果《批准通知》中上述栏目明确要求调整研究期限或研究内容等的，须选择“根据研究方案修改意见更改”并填报相关修改内容。
 2. 重点项目、重点国际（地区）合作研究项目、重大项目、国家重大科研仪器研制项目、原创探索计划项目：须选择“根据研究方案修改意见更改”，根据《批准通知》的要求填写研究（研制）内容，不得自行降低、更改研究目标（或仪器研制的技术性能与主要技术指标、验收技术指标等）或缩减研究（研制）内容。此外，还要突出以下几点：
 - （1）研究的难点和在实施过程中可能遇到的问题（或仪器研制风险），拟采用的研究（研制）方案和技术路线；
 - （2）项目主要参与者分工，合作研究单位（如有）之间的关系与分工，重大项目还需说明课题之间的关联；
 - （3）详细的年度研究（研制）计划。
 3. 创新研究群体项目：须选择“根据研究方案修改意见更改”，按下列提纲撰写：
 - （1）研究方向；



- (2) 结合国内外研究现状，说明研究工作的学术思想和科学意义（限两个页面）；
 - (3) 研究内容、研究方案及预期目标（限两个页面）；
 - (4) 年度研究计划；
 - (5) 研究队伍的组成情况。
4. 基础科学中心项目：须选择“根据研究方案修改意见更改”，根据《批准通知》的要求和现场考察专家组的意见和建议，进一步完善并细化研究计划，按下列提纲撰写：
 - (1) 五年拟开展的研究工作（包括主要研究方向、关键科学问题与研究内容）；
 - (2) 研究方案（包括骨干成员之间的分工及合作方式、学科交叉融合研究计划等）；
 - (3) 年度研究计划；
 - (4) 五年预期目标和可能取得的重大突破等；
 - (5) 研究队伍的组成情况。
5. 对于其他类型项目，参照面上项目的方式进行选择和填写。



简表

项目负责人信息	姓 名	谢勇尧	性 别	男	出生年月	1985年01月	民 族	汉族
	学 位	博士			职 称	副教授		
	是否在站博士后	否			电子邮件	yyxie@scau.edu.cn		
	电 话	020-38297231			个人网页	无		
	工 作 单 位	华南农业大学						
	所 在 院 系 所	生命科学学院						
依托单位信息	名 称	华南农业大学					代码	51064208A0499
	联 系 人	唐家林			电子邮件	kycjhl@scau.edu.cn		
	电 话	020-85280070			网站地址	http://kjc.scau.edu.cn/		
合作单位信息	单 位 名 称							
项目基本信息	项 目 名 称	亚洲稻自私遗传座位ARSL1的克隆和功能分析						
	资 助 类 别	面上项目				亚 类 说 明		
	附 注 说 明							
	申 请 代 码	C0606:群体遗传与数量遗传						
	基 地 类 别	亚热带农业生物资源保护与利用国家重点实验室						
	执 行 年 限	2023.01-2026.12						
	直 接 费 用	54万元						



项目摘要

中文摘要:

亚洲栽培稻和非洲栽培稻（简称亚非稻）种间存在严重的杂种不育，阻碍了远缘杂交稻杂种优势利用。已发现多个非稻自私遗传座位参与亚非稻杂种不育这一复杂数量性状，但鲜有报道亚稻自私遗传座位参与亚非稻杂种不育。在本项目，申请人发现亚稻自私遗传座位也参与亚非稻杂种不育。通过遗传分析，本项目鉴定到一个亚稻自私遗传座位ARSL1，发现亚非杂种中携带亚稻ARSL1基因座位的花粉能自私遗传。通过图位克隆，将ARSL1基因定位在亚稻114-kb范围。序列分析发现，该区域仅含一个亚非稻功能分化基因ORF5。利用基因编辑，功能敲除ORF5能消除杂种不育。在此基础上，本项目拟利用功能互补，验证其产生亚稻型配子自私遗传的遗传基础；拟通过表达分析，亚细胞定位，分子互作和组学分析等分子技术，解析其分子功能；拟利用生物信息学和PCR验证，追溯其进化起源。本项目的实施将能全面解析ARSL1产生亚稻型配子自私遗传的分子调控网络。

Abstract:

The hybrids between Asian-African cultivated rice display serious hybrid sterility, which hinders the utilization of heterosis in distant hybrid rice. It was shown that several African rice selfish genetic loci are involved in the interspecific hybrid sterility of Asian-African genetic rice which is a complex quantitative trait. However, it is rarely reported that the Asian rice selfish genetic locus confers the hybrid sterility of Asian-African rice. In this study, the applicant found that Asian rice selfish genetic loci are also involved in the interspecific hybrid sterility of Asian-African rice. In this project, an Asian rice selfish genetic locus ARSL1 has been identified through genetic analysis, showing that ARSL1 causes the selfish transmission of the pollen carrying Asian rice ARSL1. The ARSL1 was fine-mapped within a 114-kb region by map-based cloning. Sequencing analysis showed that only one gene ORF5 exist functional divergence between Asian and African rice. Knocking-out ORF5 can eliminate hybrid sterility by gene editing. Based on these observations, we intend to verify the genetic basis of ORF5 causing selfish transmission of gamete carrying Asian rice ORF5 by functional complementarity. Furthermore, we intend to clarify the molecular function of ORF5 by expression analysis, subcellular localization, molecular interaction and omics analysis. In addition, bioinformatics and PCR validation will be used to trace its evolutionary origin. This project will elaborate the molecular regulatory network of ARSL1 for causing the transmission advantage of the pollen carrying Asian rice ARSL1.

关键词(用分号分开): 水稻; 等基因系; 自私遗传座位; 图位克隆; 功能分析

Keywords (用分号分开): rice; isogenic lines; selfish genetic locus; map-based cloning; functional analysis



项目组主要成员

编号	姓名	出生年月	性别	职称	学位	单位名称	电话	证件号码	项目分工	每年工作 时间 (月)
1	谢勇亮	1985.01	男	副教授	博士	华南农业大学	020-38297231	44142119850107 6410	项目负责人	10
2	赵秀彩	1982.11	女	实验师	硕士	华南农业大学	020-85288395	44018319821123 3803	遗传转化	10
3	周峰	1972.12	男	助理研究员	博士	华南农业大学	020-38297793-1 7	34010419721227 3037	互作基因克隆	6
总人数			高级		中级	初级	博士后		博士生	硕士生
8			1		2	0	0		2	3



国家自然科学基金预算制项目预算表

项目批准号：32270671

项目负责人：谢勇亮

金额单位：万元

序号	科目名称	金额
1	一、基金资助项目直接费用合计	54.0000
2	1、设备费	0.0000
3	其中：设备购置费	0.0000
4	2、业务费	37.6000
5	3、劳务费	16.4000
6	二、其他来源资金	0.0000
7	三、合计	54.0000

注：请按照项目研究实际需要合理填写各科目预算金额。



预算说明书

（请按照《国家自然科学基金项目计划书预算编制说明》等的有关要求，按照预算相关性、目标相关性和经济合理性原则，实事求是编制项目预算。填报时，直接费用应按设备费、业务费、劳务费三个类别填报，每个类别结合科研任务按支出用途进行说明。填报时，对单价≥50万元的设备费详细说明，对单价<50万元的设备费用分类说明，劳务费填写单位经费及资金来源使用情况，自筹资金填写必要说明。）

本课题获批经费54.00万元，详细经费预算说明如下：

一、设备费（0万元，占总经费0%）：项目依托单位具有良好的科研条件，基本可保障课题科研工作的顺利实施，暂不购买仪器设备。

二、业务费（37.6万元，占总经费69.63%）

材料费（16.80万元）：用于课题研究过程中需使用各种生化试剂、辅助材料等消耗品的采购及运输。

1. 分子生物学实验使用的各种酶类试剂预算3.60万元。

KOD酶 1400元×10支=1.40万元

Taq酶 30元×200支=0.60万元

M-MLV逆转录酶 200元×20支=0.40万元

限制性内切酶 300元×20支=0.60万元

连接酶 200元×30支=0.60万元

2. 各类生物试剂盒预算6.40万元，如质粒提取、RNA提取、DNA纯化、反转录试剂盒、实时荧光定量PCR试剂盒等。

质粒提取试剂盒 100元×50盒=0.50万元

DNA纯化试剂盒 100元×50盒=0.50万元

RNA提取试剂盒 600元×20盒=1.20万元

荧光定量PCR试剂盒 1200元×10盒=1.20万元

反转录试剂盒 1000元×20盒=2.00万元

T-载体试剂盒 500元×20盒=1.00万元

3. 各类常规生化和分子生物学试剂预算2.80万元。

X-Gal 200元×10支=0.20万元

IPTG 300元×10瓶=0.30万元

Trizol 1500元×5瓶=0.75万元

工业酒精 150元×50桶=0.75万元

三氯甲烷 20元×100瓶=0.20万元



无水乙醇、甲醇、异丙醇、盐酸 10元×300瓶=0.30万元

异戊醇、丙酮、硫酸 20元×100瓶=0.20万元

氯化钠、氢氧化钠 10元×100瓶=0.10万元

4. 生物实验使用的一次性耗材以及其他辅助材料预算4.00万元，如移液器枪头、离心管、PCR板、培养皿、电转杯、三角瓶、烧杯、一次性手套、乳胶手套、一次性口罩等，合计4.00万元。

测试化验加工费（18.60万元）：实验过程中需委托专业公司和实验室进行DNA测序、引物合成、水稻基因组、转录组的高通量测序和遗传转化等工作，具体测算如下：

1. 常规PCR、测序所需的引物合成费用预算6.00万元：每年预计合成300对引物，每对引物平均单价25元×2条=50元，4年合计6.00万元。
2. 常规DNA片段测序费用预算4.80万元，平均每年需要测1000个反应（12元/反应），4年合计4.80万元。
3. 转录组预算4.80万元：预计对24份不同条件处理的水稻材料进行转录组测序，每份材料测序费用2000元，合计4.80万元。
4. 水稻转基因与基因编辑费用预算3.00万元，预计送公司完成相关遗传转化10次，每个遗传转化费用3000元，合计3.00万元。

出版/文献/信息传播/知识产权事务费（2.20万元）：用于文章出版、专利申请、文献检索费、课题组联络邮寄通信、打印复印等费用。

1. 发表1-2篇SCI论文，以2篇为测算依据，平均每篇版面费8000元，合计1.60万元。
2. 申请专利1-2项，平均每项专利申请费3000元，专利申请费0.60万元。

三、劳务费（16.40万元，占总经费30.37%）：用于参与课题研究的研究生和临时用工人员的劳务费用。

1. 研究生劳务费14.40万元，参加课题研究工作的博士研究生2人，硕士研究生3人，博士生每人每月补助900元，硕士生每月补助600元，每人每年工作10个月，研究生劳务费合计14.40万元。
2. 临时工劳务费2.00万元，水稻取花药等需聘请临时工，每年平均用工20人天，临时工每天250元，4年临时工费用合计2.00万元。



报告正文

研究内容和研究目标按照申请书执行。



国家自然科学基金项目负责人、依托单位承诺书

国家自然科学基金项目负责人承诺书

本人郑重承诺：我接受国家自然科学基金的资助，严格遵守中共中央办公厅、国务院办公厅《关于进一步加强科研诚信建设的若干意见》《关于进一步弘扬科学家精神加强作风和学风建设的意见》《关于加强科技伦理治理的意见》等规定，及国家自然科学基金委员会关于资助项目管理、项目资金管理等各项规章，在《计划书》填写及项目执行过程中：

（一）按照《批准通知》《国家自然科学基金资助项目计划书填报说明》的要求填写《计划书》，未自行降低、更改目标任务或约定要求，或缩减研究（研制）内容；

（二）树立“红线”意识，严格履行科研合同义务，按照《计划书》负责实施本项目（批准号：32270671），切实保证研究工作时间，按时报送有关材料，及时报告重大情况变动，不违规将科研任务转包、分包他人，不以项目实施周期外或不相关成果充抵交差；

（三）遵守科研诚信、科技伦理规范和学术道德，认真开展研究工作，对资助项目发表的论著和取得的研究成果按规定进行标注，不在非本项目资助的成果或其他无关成果上标注本项目批准号，反对无实质学术贡献者“挂名”，不在成果署名、知识产权归属等方面侵占他人合法权益，并如实报告本人及项目组成员发生的违背科研诚信要求的任何行为；

（四）尊重科研规律，弘扬科学家精神，严谨求实，追求卓越，反对浮夸浮躁、投机取巧，不人为夸大学术或技术价值，不传播未经科学验证的现象和观点；

（五）将项目资金全部用于与本项目研究工作相关的支出，并结合科研活动需要，科学合理安排项目资金支出进度；

（六）做好项目组成员的教育和管理，确保遵守以上相关要求。

如违背上述承诺，本人愿接受国家自然科学基金委员会和相关部门做出的各项处理决定。

项目负责人（签字）：

年 月 日

依托单位科研管理部门：

负责人（签章）：

年 月 日

依托单位财务管理部门：

负责人（签章）：

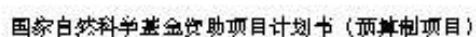
年 月 日

国家自然科学基金项目依托单位承诺书

我单位同意承担上述国家自然科学基金项目，将保证项目负责人及其研究队伍的稳定和研究项目实施所需的条件，严格遵守国家自然科学基金委员会有关资助项目管理、项目资金管理、科研诚信管理和科技伦理管理各项规定，并督促实施。

依托单位（公章）

年 月 日



科学处审查意见:

负责人(签章):

年 月 日

科学部审查意见:

负责人(签章):

年 月 日

本栏目由自然科学基金委填写

编号: 091821301092362057

农业产品质量安全监管专项经费项目 任务委托书

项目名称: 农业转基因生物安全检测

委托单位: 农业农村部科技教育司 (甲方)

承担单位: 华南农业大学 (乙方)

签订时间: 2018 年

农业农村部科技教育司印制

一、委托理由

根据《国务院关于第三批清理规范国务院部门行政审批中介服务事项的决定》(国发〔2017〕8号)以及新修订的《农业转基因生物安全管理条例》(以下简称《条例》)(国务院令第687号),研发人申请“境外研发商首次申请农业转基因生物安全证书(进口)”,以及“农业转基因生物安全证书(生产应用)”,原应由申请人开展的转基因生物安全检测,改由农业农村部委托有关机构开展。

为贯彻落实《条例》和《农业转基因生物安全评价管理办法》等的规定,保障农业转基因生物行政审批有序开展,委托相关具备检测条件和能力的技术检测机构进行检测。

二、任务内容

(一) 项目任务

现委托华南农业大学承担2种转基因作物分子特征及环境安全检测。

(二) 项目内容

1、分子特征检测

2个转化体分子特征检测项目包括:

(1) 外源基因筛查与纯度鉴定:根据统计学原理,在合理置信度水平下,采用已有标准或提交方法进行基因筛查与纯度鉴定,每个转化体测定参数10个。

(2) 定性PCR方法循环验证:验证方案认证;验证样品制备;8家实验室循环验证,验证内容为特异性、灵敏度、重复性及重演性;数据统计及验证报告认证。

(3) 定量PCR方法循环验证:验证方案认证;标准曲线与验证样品制

备；8家实验室循环验证，验证内容为特异性、准确性、精确性、检测极限、定量极限、重复性及重演性；数据统计、不确定性分析及验证报告认证。

(4) 外源插入序列及拷贝数分析：克隆测序，10个参数；数字PCR方法6个参数；DNA提取与纯化酶切，共5份；Southern方法，10个探针。

2、环境安全检测

2个转化体环境安全检测项目包括：

(1) 生存竞争性：荒地、栽培地生存竞争力试验4批次；发芽力与休眠性；再生苗；自生苗调查及其分子检测；自然延续力；数据分析与报告编制。

(2) 花粉活力测定：试验测定，数据分析与报告编制。

(3) 目标性状功能效率测定：3种抗虫或抗病性状测定；3种除草剂耐受性测定，调查与数据分析、报告编制。其中每个转化体抗虫分别进行室内测定和田间测定。

(4) 非靶标生物测定：测定6种非靶标生物，数据分析与报告编制。

(5) 生物多样性测定：2个试验点检测，数据分析与报告编制。

(三) 项目单位情况

1、单位性质、隶属关系、相关职能业务范围。

农业农村部植物及植物用微生物生态环境安全监督检验测试中心（广州）依托华南农业大学建设，业务上受农业农村部、广东省农业厅指导。

为加强对农业转基因生物及其产品的监管，提高农业转基因生物及其产品检测和监测能力，根据国家农业部农办科[2002]15号文《关于开展第一批农业部转基因生物技术检测机构认定工作的通知》，2002年4月华南农业大学以遗传工程研究室的设备、技术和人员为基础，向农业部申请成立农业转

基因生物(产品)检验机构,并获批为第一批农业转基因生物技术检测机构筹建单位(农科教发[2003]6号文)。2004年,农业部(农计函[2004]518号文)批准在我校建设“国家农业转基因作物检测与监测中心(南方)”,并下达项目经费350万元,单位自筹35万元。2005年,根据农业部农市发[2005]14号文“关于下达农业部第五批部级质检中心筹建计划的通知”的决定,华南农业大学在上述项目建设的基础上开始筹建农业部转基因植物及植物用微生物环境安全监督检验测试中心(广州)。中心的建设于2008年完成,于2008年11月初次通过了国家计量认证和农业部质量安全检测机构考核、机构审查认可的现场评审。2009年2月正式获得了国家计量认证证书,2009年4月获得了农业部审查认可证书和农产品质量安全检测机构考核合格证书,并分别于2011年12月、2014年11月和2018年3月连续3次通过了“三认证”现场复审,2018年5月根据“中华人民共和国农业农村部公告【第25号】”更名为农业农村部植物及植物用微生物生态环境安全监督检验测试中心(广州)。

2、现有工作基础。

本中心已具备转基因植物及其产品成分的检测,以及转基因植物环境安全检测的业务能力。先后承担了转基因大豆、油菜、水稻、玉米、木瓜等成分检测任务,同时还承担了转基因生物新品种培育重大专项“土壤磷素高效利用转基因大豆新品系环境安全评价技术体系的建立”和“华南地区 Bt 水稻环境影响监测”、广东省重大科技专项“转基因农产品安全检测技术的研究”等研究项目,并于2017年承担了深圳市作物分子设计育种研究院委托的转基因水稻环境安全检测任务。

3、技术和设备条件、财务收支和资产状况、内部管理制度建设情况。

中心现有人员 12 名，其中博士 4 人，高级职称人员 5 人、中级职称人员 4 名、初级职称 3 名；学科专业涵盖了分子生物学、植物学、遗传学、植物病理学、昆虫学、杂草科学等相关的领域。组成了一支多学科的科技队伍，人员结构良好，并已积累了多年的科研和检测工作经验，具备了承担转基因质检工作的能力。

本中心现有实验室及办公用房总面积 775 平方米，建有转基因植物成分检测室（试剂配制室、样品前处理室、核酸提取纯化室、前 PCR 室、PCR 室、电泳检测室、蛋白质分析室）、环境安全检测室（环境生态学检测室、昆虫室、分子生物学检测室、植物生物学检测室等）以及接样室、样品库、生物灭活间、洗涤间以及田间实验室等。各实验室已安装了相应的控温、通风及安全管理系统。中心另在华南农业大学增城教学科研基地建成转基因生物环境安全试验基地，包括农田面积约 80 亩，并建有配套的 600 m² 网室、30m² 日光温室、60m² 智能温室及 500 m² 晒场等。试验基地严格按照相关要求隔离，专门用于转基因生物环境安全试验。

中心现有相应的主要仪器设备 213 台（件），价值 365 万元。其中价值五万元以上 10 余台件，如定量 PCR 仪、PCR 仪、凝胶成像系统、紫外可见分光光度计、核酸浓度测定仪、酶标仪、高速冷冻离心机等，其中用于检测的主要仪器设备 64 台。这些设备已满足了开展转基因植物（产品）成分检测和环境安全检测工作的需要。

本中心不设独立财务，财务上受华南农业大学财务处指导。学校实行党委领导下的校长负责制，实行“统一领导，集中核算”的财务管理体制，校长

对学校财务工作统一领导。

华南农业大学依据国家的相关法律法规，结合学校及科技经费财务管理实际情况，制定了完整的内部控制制度，主要包括：《华南农业大学经济责任制》、《华南农业大学经费审批管理办法（试行）》、《华南农业大学科研经费审计实施办法（试行）》、《华南农业大学财务管理实施细则》、《华南农业大学关于进一步加强财务管理工作的意见》、《华南农业大学自然科学类纵向科研项目与资金管理办法（试行）》、《华南农业大学差旅费管理办法》、《华南农业大学招标投标管理办法》、《华南农业大学国有资产管理办 法》等。在执行过程中，能够按制度规定和标准控制经费支出，按规定的审批程序保证专项经费的使用。

本中心还制定了《转基因生物安全管理制度》、《检测室安全管理制度》、《农业转基因安全突发事件报告及处理制度》等转基因生物安全管理制度，确保对转基因生物的安全管理。

4、有无不良记录（财政部门及审计机关处理处罚决定、行业通报批评、媒体曝光等）。

无。

5、人员项目分工。

姓 名	性别	年龄	工作单位	职务/职称	项目分工
王声斌	男	51	农业农村部植物及植物用微生物生态环境安全监督检验检测中心（广州）	常务副主任	项目整体协调
周峰	男	46	同上	环境安全检测室主任	负责环境安全检测
姜大刚	男	41	同上	成分检测室主任	负责分子特征检测
姚涓	女	44	同上	业务办公室主任	负责数据分析及报告编制
罗建军	男	47	同上	检测员	目标性状功能效率测定、非靶标生物测定、生物多样性测定
李敏慧	女	45	同上	检测员	目标性状功能效率测定、生物多样性测定
张荣京	男	39	同上	检测员	生存竞争检测、花粉活力测定
陈伟庭	男	34	同上	检测员	外源基因筛查与纯度鉴定、外源插入序列及拷贝数分析
潘志文	男	32	同上	检测员	定性 PCR 方法循环验证、定量 PCR 方法循环验证
高洁儿	女	30	同上	业务员	数据统计及分析、各类报告的编制

三、实施步骤

第一步：项目启动，样品接收；

第二步：分子特征检测进行外源基因筛查与纯度鉴定和外源插入序列及拷贝数分析；环境安全评价，进行生存竞争性评价和花粉活力测定；

第三步：分子特征检测进行定性 PCR 方法循环验证；环境安全评价进行目标性状功能效率和生物多样性测定。

第四步：分子特征检测进行定量 PCR 方法循环验证；环境安全评价进行非靶标生物测定。

第五步：撰写报告，结题。

四、经费预算

分子特征检测经费预算

单位：(万元)

类型	检测项目	价格	测算依据
分子特征 合计 110.0万元	外源基因筛查 与纯度鉴定	6.0	测定参数 10 个，0.3 万元/参数，2 个转化体共计 6.0 万元。
	定性 PCR 方法 循环验证	20.0	验证方案认证 0.2 万元；验证样品制备 3 万元；8 家实验室循环验证，0.8 万元/家，计 6.4 万元；数据统计及验证报告认证 0.4 万元。2 个转化体共计 20.0 万元。
	定量 PCR 方法 循环验证	48.0	验证方案认证 0.2 万元；标准曲线与验证样品制备 10.0 万元；8 家实验室循环验证，1.6 万元/家，计 12.8 万元；数据统计、不确定性分析及验证报告认证 1.0 万元。2 个转化体共计 48.0 万元。
	外源插入序列 及拷贝数分析	36.0	克隆测序，0.2 万元/参数，10 个参数计 2.0 万元；数字 PCR 方法，1.0 万元/参数，6 个参数计 6.0 万元；Southern 方法，0.8 万元/探针，10 个探针计 8.0 万元；DNA 提取与纯化酶切，0.2 万元/份，5 份计 1.0 万元；杂交膜、显色试剂盒等 1.0 万元。2 个转化体共计 36.0 万元。

环境安全检测经费预算

单位：(万元)

类型	检测项目	价格	测算依据
环境安全 合计 215.2 万元	生存竞争性	32.0	荒地、栽培地生存竞争力试验 4 批次，每次 1.5 万元，计 6.0 万元；发芽力与休眠性 1.5 万元；再生苗 0.5 万元；自生苗调查及其分子检测 5.5 万元；自然延续力 1.5 万元；数据分析与报告编制费 1.0 万元。2 个转化体共计 32.0 万元。
	花粉活力测定	2.0	试验测定费 0.8 万元，数据分析与报告编制费 0.2 万元。2 个转化体共计 2.0 万元。
	目标性状功能效率测定	57.6	3 种抗虫或抗病性状测定，每种 6.6 万元，小计 19.8 万元；3 种除草剂耐受性，每种 3.0 万元，小计 9.0 万元。其中每个转化体抗虫室内测定 1.5 万元，田间测定每种虫 5.1 万元（试虫饲养或购置费 2.8 万元，用地费 0.3 万元，管理费 0.8 万元，调查与数据分析、报告编制费 1.2 万元）。每个转化体除草剂耐受性：每种除草剂 3.0 万元，包括用地费 0.6 万元，管理费 1.2 万元，调查与数据分析、报告编制费 1.2 万元。2 个转化体共计 57.6 万元。
	非靶标生物测定	57.6	每种生物 4.8 万元，6 种生物合计 28.8 万元。（每种用地 0.4 万元，管理费 1.0 万元，试虫饲养或购置费 1.2 万元，测定费 1.9 万元，数据分析与报告编制费 0.3 万元。）2 个转化体共计 57.6 万元。
	生物多样性测定	66.0	每个试验点 16.5 万元，2 点合计 33.0 万元。（测算依据：用地费 2.2 万元，管理费 1.8 万元，田间调查费 5.0 万元，分类鉴定费 5.5 万元，数据分析与报告编制费 2.0 万元。）2 个转化体共计 66.0 万元。

(三) 申请资金经济分类明细表

项目内容	合计	商品和服务支出有关科目												
		小计	印刷费	咨询费	水费	电费	邮电费	差旅费	维修(护)费	租赁费	培训费	专用材料费	劳务费	委托业务费
分子特征	110.0		2.8	2.4			0.4	3.8				32.0	27.2	41.4
环境安全	215.2		5.4	5.4			1.2	9.6				112.4	63.2	18
合 计	325.2		8.2	7.8			1.6	13.4				144.4	90.4	59.4

五、双方权利义务





- (一)项目承担单位和农业农村部严格执行本项目委托任务。
- (二)项目承担单位自觉接受农业农村部的监督、检查和指导。
- (三)项目承担单位应按项目委托任务规定的内容对项目委托经费专款专用。
- (四)项目委托任务执行过程中，项目承担单位不得随意调整项目委托任务内容。确需调整的，必须报农业部批准。
- (五)项目涉及保密的有关内容，按照国家有关保密工作法律法规执行。未经农业农村部项目主管司局批准，项目承担单位不得将项目研究成果上传到网上、对外泄露或发表文章。
- (六)项目承担单位在项目结束后将项目执行情况和资金使用情况总结报农业农村部项目主管司局。

六、违约责任

(一) 农业农村部按照批复的项目委托任务对项目承担单位的项目执行和资金使用情况进行检查，实行项目执行和资金使用情况与下年度项目资金安排挂钩。未完成项目内容和经费支出不合理的，下年度酌情减少项目资金或不予考虑资金支持，情节严重的将终止项目并视情况予以相应处罚。

(二) 项目承担单位因主观原因致使项目委托任务无法执行，农业农村部有权终止项目委托任务，追回全部项目经费。项目承担单位因故要求终止项目委托任务，农业农村部可视情况追回全部或部分项目经费。

七、双方签章

委托单位 (甲方)	项目委托单位	单位领导签字： 单位公章： 		
	业务负责处室	负责人签字： 		
	联系人	张宪法 王 东	联系电话	010-59193009
	通讯地址	北京市朝阳区农展南里 11 号	邮政编码	100125
承担单位 (乙方)	项目承担单位	项目承担单位领导签章： 项目承担单位公章： 		
	业务负责部门	负责人签章： 		
	项目联系人	王声斌	联系电话	13168831229
	通讯地址	广州市天河区五山路 483 号华南农业大学科技楼 1116 室	邮政编码	510642
	收款单位账户名称	华南农业大学		
	开户银行名称	广州工行五山支行	账号	3602002609000310520



项目批准号	31570654
申请代码	C161001
归口管理部门	
依托单位代码	51064208A0499-0932



3 1570654 1004610

国家自然科学基金委员会 资助项目计划书

资助类别: 面上项目

亚类说明:

附注说明: 常规面上项目

项目名称: 火炬松叶绿体基因组遗传多样性及育种群体亲缘关系调控

直接费用: 64万元 间接费用: 12.4万元

项目资金: 76.4万元 执行年限: 2016.01-2019.12

负责人: 黄少伟

通讯地址: 广州市天河区五山路483号

邮政编码: 510642 电 话: 020-85280259

电子邮件: shwhuang@scau.edu.cn

依托单位: 华南农业大学

联系人: 全锋 电 话: 020-85280070

填表日期: 2015年09月06日

国家自然科学基金委员会制

Version: 1.004.610



国家自然科学基金委员会资助项目计划书填报说明

- 一、项目负责人收到《关于国家自然科学基金资助项目批准及有关事项的通知》（以下简称《批准通知》）后，请认真阅读本填报说明，参照国家自然科学基金相关项目管理办法及《国家自然科学基金资助项目资金管理办法》（请查阅国家自然科学基金委员会官方网站首页“政策法规”-“管理办法”栏目），按《批准通知》的要求认真填写并提交《国家自然科学基金委员会资助项目计划书》（以下简称《计划书》）。
- 二、填写《计划书》时要求科学严谨、实事求是、表述清晰、准确。《计划书》经国家自然科学基金委员会相关项目管理部门审核批准后，将作为项目研究计划执行和检查、验收的依据。
- 三、《计划书》各部分填写要求如下：
 - （一）简表：由系统自动生成。
 - （二）摘要及关键词：各类获资助项目都必须填写中、英文摘要及关键词。
 - （三）项目组主要成员：计划书中列出姓名的项目组主要成员由系统自动生成，与申请书原成员保持一致，不可随意调整。如果批准通知中“项目评审意见及修改意见表”中“对研究方案的修改意见”栏目有调整项目组成员相关要求的，待项目开始执行后，按照项目成员变更程序另行办理。
 - （四）资金预算表：按批准资助的直接费用填报资金预算表和预算说明书，其中的劳务费、专家咨询费金额不应高于申请书中相应金额；间接费用及项目总经费由系统自动生成。国家重大科研仪器研制项目还应按照预算评审后批复的直接费用各科目金额填报资金预算表、预算说明书及相应的预算明细表。
 - （五）正文：
 1. 面上项目、青年科学基金项目、地区科学基金项目：如果《批准通知》中没有修改要求的，只需选择“研究内容和研究目标按照申请书执行”即可；如果《批准通知》中“项目评审意见及修改意见表”中“对研究方案的修改意见”栏目明确要求调整研究期限和研究内容等的，须选择“根据研究方案修改意见更改”并填报相关修改内容。
 2. 重点项目、重点国际（地区）合作研究项目、重大项目、国家重大科研仪器研制项目：须选择“根据研究方案修改意见更改”，根据《批准通知》的要求填写研究（研制）内容，不得自行降低、更改研究目标（或仪器研制的技术性能与主要技术指标以及验收技术指标）或缩减研究（研制）内容。此外，还要突出以下几点：
 - （1）研究的难点和在实施过程中可能遇到的问题（或仪器研制风险），拟采用的研究（研制）方案和技术路线；
 - （2）项目主要参与者分工，合作研究单位之间的关系与分工，重大项目还需说明课题之间的关联；
 - （3）详细的年度研究（研制）计划。



3. 国家杰出青年科学基金、优秀青年科学基金和海外及港澳学者合作研究基金项目：须选择“根据研究方案修改意见更改”，按下列提纲撰写：
 - (1) 研究方向；
 - (2) 结合国内外研究现状，说明研究工作的学术思想和科学意义（限两个页面）；
 - (3) 研究内容、研究方案及预期目标（限两个页面）；
 - (4) 年度研究计划；
 - (5) 研究队伍的组成情况。
4. 对于其他类型项目，参照面上项目的方式进行选择和填写。



简表

申请者信息	姓 名	黄少伟	性 别	男	出生年月	1964年01月	民 族	汉族
	学 位	博士			职 称	教授		
	电 话	020-85280259		电子邮件	shwhuang@scau.edu.cn			
	传 真			个人网页				
	工 作 单 位	华南农业大学						
	所 在 院 系 所	林学与风景园林学院						
依托单位信息	名 称	华南农业大学					代 码	51064208A0499
	联 系 人	全锋		电子邮件	kycjhl@scau.edu.cn			
	电 话	020-85280070		网站地址	http://web.scau.edu.cn/kjc/			
合作单位信息	单 位 名 称							代 码
项目基本信息	项 目 名 称	火炬松叶绿体基因组遗传多样性及育种群体亲缘关系调控						
	资 助 类 别	面上项目				亚 类 说 明		
	附 注 说 明	常规面上项目						
	申 请 代 码	C161001: 林木种质资源				C161003: 林木育种理论与方法		
	基 地 类 别							
	执 行 年 限	2016.01-2019.12						
	直 接 费 用	64万元				间 接 费 用	12.4万元	
	项 目 资 金	76.4万元						



项目摘要

中文摘要(500字以内):

以课题组将测序并提交到NCBI数据库的一个火炬松叶绿体基因组序列为参考序列,采用高通量测序技术测定火炬松第一代核心育种群体混合样品的叶绿体基因组序列,经过比对分析,绘制火炬松叶绿体基因组个体水平突变图谱,筛选多态性位点,开发基于特异引物PCR的SNP标记,用于检测火炬松第二代核心群体的亲缘关系,验证多态性位点在完全谱系交配设计条件下世代传递的遗传稳定性,经验证的标记用于检测火炬松两个世代主群体的亲缘关系,建立育种群体亲缘关系图谱,确立亲缘关系在不完全谱系交配设计条件下在不同世代间的传递模式,作为群体亲缘关系调控的依据。本项目将全面阐明火炬松叶绿体基因组序列多态性以及个体水平的变异模式,建立新型的松树育种群体亲缘关系调控技术体系,创新松树多世代轮回选择育种模式,对提高火炬松遗传改良水平具有重要意义。

关键词: 火炬松; 叶绿体基因组; 遗传多样性; 育种群体; 亲缘关系

Abstract(Limited to 4000 words):

Based on the previously accomplished sequence of loblolly pine (*Pinus taeda*) chloroplast genome, which has been submitted to NCBI database and been released, in this project, mixed sample from the first-generation nucleus breeding population will be sequenced by using high-throughput sequencing technology, with the above mentioned submission as the reference sequence. After comparison, genetic diversity and variation in the chloroplast genome of loblolly pine will be profiled, and diversity loci will be screened. Featured primer PCR based single nucleotide polymorphism (SNP) markers will be developed with the high frequent mutation loci. The new developed SNP markers will be used to detect the second-generation nucleus population, in order to test the stability of the polymorphic loci among different generations under complete pedigree mating design. The tested SNP markers will be used to detect and profile the genetic relationship in the main populations of two generations and then, inheritance model of genetic relationship among different generations under incomplete pedigree mating design will be established. This will be the basis of regulation for the genetic relationship in the breeding population. The project will systematically explain the polymorphism and variation in the chloroplast genome sequence of loblolly pine, establish a new technology system to regulate the genetic relationship in the breeding populations of loblolly pine, innovate the model of multi-generation recurrent selection. This is significantly important to increase the level of genetic improvement in loblolly pine.

Keywords: *Pinus taeda*; chloroplast genome; genetic diversity; breeding population; genetic relationship



项目组主要成员

编号	姓名	出生年月	性别	职称	学位	单位名称	电话	证件号码	项目分工	每年工作 时间 (月)
1	黄少伟	1964.01	男	教授	博士	华南农业大学	020-85280259	440106196401271913	项目负责人	6
2	刘天顺	1976.09	女	副教授	博士	华南农业大学	020-85280259	440102197609230625	叶绿体基因组测序	6
3	周峰	1972.12	男	助理研究员	博士	华南农业大学	020-38297793-19	340104197212273037	叶绿体基因组序列分析	4
4	杨会肖	1981.11	女	博士后	博士	华南农业大学	020-85280259	132337198111110701	叶绿体基因组序列分析, 育种群体茶缘关系分析	8
5	刘纯鑫	1966.08	男	高级实验师	硕士	华南农业大学	020-85280259	440106196608020310	育种群体评价与选种	5
6	祝文娟	1991.03	女	博士生	学士	华南农业大学	020-85280259	341222199103053084	叶绿体基因组序列多态性检测, 育种群体茶缘关系分析	8
7	谢莹	1989.07	女	硕士生	学士	华南农业大学	020-85280259	411323198907140103	育种群体茶缘关系分析	6
8	毛积鹏	1990.12	男	硕士生	学士	华南农业大学	020-85280259	362321199012052712	育种群体茶缘关系分析	8
总人数				高级	中级	初级	博士后	博士生	硕士生	
8				3	1		1	1	2	



国家自然科学基金项目资金预算表（定额补助）

项目名称：火炬松叶蝉体基因组遗传多样性及育种亲缘关系调控

项目负责人：黄少伟

金额单位：万元

序号	科目名称	金额	备注
	(1)	(2)	(3)
1	一、项目资金支出	76.4000	/
2	(一) 直接费用	64.0000	共有9项支出
3	1、设备费	3.0000	小型设备购置及设备改造
4	(1) 设备购置费	2.0000	购置小型仪器，如涡旋振荡器、小型离心机等
5	(2) 设备试制费	0.0000	无
6	(3) 设备改造与租赁费	1.0000	磨样仪的改装等
7	2、材料费	20.0000	原材料、试剂、药品、小工具、衣液等
8	3、测试化验加工费	8.0000	合成引物及DNA测序等
9	4、燃料动力费	0.0000	无
10	5、差旅费	6.0000	取样、调查、参加国内学术会议等
11	6、会议费	3.2000	举办专家咨询会及学术研讨会
12	7、国际合作与交流费	8.0000	人员出国交流及国外专家来华交流
13	8、出版/文献/信息传播/知识产权事务费	6.0000	版面、信息检索、参考资料、印刷、复印费等
14	9、劳务费	9.0000	研究生补助，临时工工资
15	10、专家咨询费	0.8000	聘请咨询专家
16	11、其他支出	0.0000	无
17	(二) 间接费用	12.4000	按统一规定执行
18	其中：绩效支出	3.1000	按统一规定执行
19	二、自筹资金	0.0000	无



预算说明书

(请对各项支出的主要用途和测算理由及合作研究外拨资金等内容进行详细说明,可根据需要另加附页。)

1. 设备费 3万元, 其中:

(1) 设备购置费: 2万元, 用于购置小型仪器, 如涡旋振荡器、小型离心机。

(2) 设备试制费: 无。

(3) 设备改造费: 1万元, 用于磨样仪的改装等。

2. 材料费 20万元, 其中:

(1) 原材料、试剂、药品购置费18万元, 高质量叶绿体DNA提取费用为100元/样, 提取680个样品需要100元/样 \times 680样=6.8万元; HRM-PCR费用为3元/反应, 共有680个样品, 每样品50个位点, 3元/反应 \times 680样 \times 50位点=10.2万元; 普通PCR费用为2.2元/反应, 用于前期引物筛选等, 约需1万元, 6.8+10.2+1=18万元。

(2) 其他费用2.0万元, 购置野外作业用的工具、农资等。

3. 测试化验加工费 8万元, 其中:

(1) 引物合成3.2万元, 合成一对200引物费用约为64元, 对680个样品50个位点进行扩增, 每对引物约需200D, 引物合成费用为64元/200 \times 50位点 \times 200D/20D=3.2万元。

(2) DNA测序4.8万元, DNA测序费用为16元/反应, 每一PCR产物需分别进行正反双向各1次测序, 对50个位点PCR产物进行测序, 用30个体进行位点筛选, 约需16元/反应 \times 2反应 \times 50位点 \times 30个体=4.8万元。

4. 燃料动力费 无。

5. 差旅费 6万元, 其中:

(1) 种质资源调查及采样的往返差旅费4万元, 头三年采样, 每年2次, 共6次, 种质资源调查2次, 合计8次, 每次每人往返路费220元, 住宿费300元/人/天, 伙食费及公杂费180元/人/天, 平均每次3天, 则每次每人费用=220+(300+180) \times 3=1660元, 平均每次3人, 则1660元/次 \times 人 \times 8次 \times 3人=3.984万元 \approx 4万元。

(2) 参加国内学术会议往返差旅费2万元, 参加国内学术会议2次, 每次3天, 共6人次, 其中往返路费2000元/人, 住宿费300元/人, 伙食费及公杂费180元/人, 则[2000元+(300+180)元/天 \times 3天]/人 \times 6人/次=2.064万元 \approx 2万元。

6. 会议费 3.2万元

举办专家咨询会1次, 邀请专家5名, 会期2天; 举办“桉树叶体基因组序列多态性及种群群体亲缘关系调控”学术研讨会, 参会代表30人, 会期2天, 两次会议共35人 \times 2天 \times 450/天/人=3.15万元 \approx 3.2万元。

7. 国际合作与交流费 8万元, 其中:

(1) 项目组成员出国合作交流5.5万元, 项目组派出2人次赴美国北卡罗来纳州立大学合作交流或参加国际学术会议, 为期5天。

① 广州经樟杉机往返罗利(北卡罗来纳州立大学)国际旅费: 1.7万元/人/次 \times 2人/次=3.4万元;

② 国外生活费(住宿费: 160美元/天/人; 伙食费: 55美元/天/人; 公杂费: 45美元/天/人): [(160+55+45)元/天/人] \times 汇率 \times 5天 \times 2人=260 \times 6.1 \times 5 \times 2=1.586万元;

③ 会费每人500美元, 500美元/人次 \times 2人次 \times 汇率=500 \times 2 \times 6.1=0.61万元;
3.4+1.586+0.61=5.596万元。



(2) 聘请美国北卡罗来纳州立大学从事火炬松分子生物学研究的专家1人来华开展学术交流, 为其5天。

① 国际旅费1.7万元。

② 专家在华交通、住宿、伙食费每天1500元, $1500\text{元}/\text{天} \times 5\text{天} = 0.75\text{万元}$ 。

$1.7 + 0.75 = 2.45\text{万元}$ 。

$5.596 + 2.45 = 8.046 \approx 8\text{万元}$ 。

8. 出版/文献/信息/传播/知识产权事务费 6万元

预计课题研究成果在国际学术期刊发表论文3篇, 版面费10000元/篇, 合计3万元; 在国内核心期刊发表学术论文2篇, 版面费5000元/篇, 合计1万元; 信息检索及相关参考资料费2500元/年, 4年合计1万元; 课题总结报告印刷、复印费等共1万元。

$3 + 1 + 1 = 6\text{万元}$ 。

9. 劳务费 9万元, 其中:

(1) 研究生补助6万元。参加本课题的研究生3名, 其中博士研究生1名, 每年工作8个月, 每月补助1000元, 每年8000元; 硕士研究生2名, 合计每年工作14个月(8个月+6个月), 每月补助500元, 每年14月 $\times 500\text{元}/\text{月} = 7000\text{元}$, 4年合计需要支出劳务费 $=(8000+7000) \times 4 = 6\text{万元}$ 。

(2) 临时工劳务费3万元。聘请临时工协助进行野外调查、样品采集、实验室清洁等工作, 工资每人150元/天, 每年约50天/人, 4年共计200天/人, 合计费用 $=150\text{元}/\text{天} \cdot \text{人} \times 200\text{天} \cdot \text{人} = 3\text{万元}$ 。

10. 专家咨询费 0.8万元

举办专家咨询会, 聘请5名专家, 会期2天, $(5 \times 2)\text{天} \cdot \text{人} \times 800/\text{天} \cdot \text{人} = 0.8\text{万元}$ 。

11. 其他支出 无。

项目负责人签字:

科研部门公章:

财务部门公章:



报告正文

研究内容和研究目标按照申请书执行。



国家自然科学基金资助项目签批审核表

<p>我接受国家自然科学基金的资助，将按照申请书、项目批准意见和计划书负责实施本项目（批准号：51570654），严格遵守国家自然科学基金委员会有关资助项目管理、财务等各项规定，切实保证研究工作时间，认真开展研究工作，按时报送有关材料，及时报告重大情况变动，对资助项目发表的论著和取得的研究成果按规定进行标注。</p> <p>项目负责人（签署）： 年 月 日</p>	<p>我单位同意承担上述国家自然科学基金项目，将保证项目负责人及其研究队伍的稳定和研究项目实施所需的条件，严格遵守国家自然科学基金委员会有关资助项目管理、财务等各项规定，并督促实施。</p> <p>依托单位（公章） 年 月 日</p>														
<p>本栏目由基金委填写</p>	<p>科学处审查意见：</p> <p>建议年度拨款计划（本栏目为自动生成，单位：万元）：</p> <table border="1"> <thead> <tr> <th>年度</th> <th>总额</th> <th>第一年</th> <th>第二年</th> <th>第三年</th> <th>第四年</th> <th>第五年</th> </tr> </thead> <tbody> <tr> <td>金额</td> <td></td> <td></td> <td></td> <td></td> <td></td> <td></td> </tr> </tbody> </table> <p>负责人（签署）： 年 月 日</p>	年度	总额	第一年	第二年	第三年	第四年	第五年	金额						
	年度	总额	第一年	第二年	第三年	第四年	第五年								
	金额														
<p>科学部审查意见：</p> <p>负责人（签署）： 年 月 日</p>															
<p>本栏目主要用于重大项目等</p>	<p>相关处室审查意见：</p> <p>负责人（签署）： 年 月 日</p>														
	<p>委领导审批意见：</p> <p>委领导（签署）： 年 月 日</p>														



项目批准号	30671279
归口管理部门	
申请代码	C02020501
收件日期	

国家自然科学基金委员会 资助项目计划书

资助类别：面上项目

亚类说明：自由申请项目

附注说明：

项目名称：与生长素相关的水稻卷叶突变基因克隆及功能分析

资助经费：24.00 万元 执行年限：2007.01-2009.12

负责人：易继财

通讯地址：广州天河五山华南农业大学生命科学学院

邮政编码：510642 电话：020-85288399

电子邮件：jicai@scau.edu.cn

依托单位：华南农业大学

联系人：陈奕 电话：020-85280070

填表日期：2006年10月9日

国家自然科学基金委员会



国家自然科学基金委员会资助项目计划书填报说明

- 一、收到《国家自然科学基金委员会资助项目批准通知》（以下简称《批准通知》）后，请认真阅读本填报说明和自然科学基金相关项目及财务管理办法（查阅[Http://www.nsf.gov.cn/](http://www.nsf.gov.cn/)），按《批准通知》的要求认真填写《国家自然科学基金委员会资助项目计划书》（以下简称《计划书》）。
- 二、填写《计划书》时要求科学严谨、实事求是、表述清晰、准确。《计划书》经主管科学部审核批准后，将作为项目研究计划执行和检查、验收的依据。
- 三、《计划书》为个性化表格，简表部分自动生成，不同类别的项目按不同要求撰写。请按以下提纲撰写《计划书》：
 - 1、各类资助项目都必须撰写中、英文摘要及主题词，填报经费预算表。
 - 2、对于基金面上项目，项目组成员和研究内容按申请书执行，一般不得修改。如果《批准通知》中明确要求调整研究内容，须在《计划书》报告正文中对修改的内容作详细说明。没有要求修改的内容时，只需在报告正文中填写“研究内容和研究目标按照申请书执行”即可。
 - 3、重点、重大项目的项目组成员和研究内容根据批准项目的实际情况填报，不能自行降低、更改研究目标，或缩减关键的研究内容。此外，还要突出以下几点：
 - （1）研究的难点和在实施过程中可能碰到的问题，拟采用的研究方案和技术路线；
 - （2）项目组主要成员分工，并请说明课题及合作单位之间的关系与分工；
- 4、国家杰出青年科学基金和海外青年学者合作研究基金的计划书正文按下列提纲撰写：
 - 1) 研究方向
 - 2) 结合国内外研究现状，说明研究工作的学术思想和科学意义（限两个页面）
 - 3) 研究内容、研究方案及预期目标（限两个页面）
 - 4) 分年度进度安排
 - 5) 研究队伍的组成情况



简表

申请者信息	姓 名	易继财	性 别	男	出生年月	1971 年 10 月	民 族	汉族
	学 位	硕士			职 称	讲师		
	电 话	020-85288399		电子邮箱	jicai@scau.edu.cn			
	传 真			个 人 网 页				
	工 作 单 位	华南农业大学						
	所 在 院 系 所	生命科学学院遗传工程研究室						
依托单位信息	名 称	华南农业大学					代 码	51064201
	联 系 人	陈奕		电子邮箱	kycjkh@scau.edu.cn			
	电 话	020-85280070		网站地址				
合作单位信息	单 位 名 称							代 码
项目基本信息	项 目 名 称	与生长素相关的水稻卷叶突变基因克隆及功能分析						
	资 助 类 别	面上项目			亚 类 说 明	自由申请项目		
	附 注 说 明							
	申 请 代 码	C02020501: 稻类遗传育种学			C011007: 分子遗传学			
	基 地 类 别							
	执 行 年 限	2007.01-2009.12			研究属性	应用基础研究		
	资助经费	24.00 万元						



项目摘要

中文摘要(500 字以内):

水稻叶片适度卷曲在株型改良育种中有重要意义。目前尚未见从水稻中克隆到卷叶相关基因的报道。申请者以 r 射线诱导产生的水稻卷叶突变体 **rl10(t)** 为材料,应用图位克隆方法拟克隆卷叶突变相关基因。前期分析已把卷叶突变座位精细定位于第三染色体,发现候选基因为一个编码生长素合成关键酶的基因。本项目拟通过基因操作技术克隆该基因,并应用转化互补、过量表达、**RNAi** 及反义 **RNA** 抑制,分析其功能,包括基因的时空表达特性、卷叶突变与该基因功能的关系、内源 **IAA** 分析及外源 **IAA** 反应、突变所致的细胞学变化,以阐明水稻卷叶突变的机理及其与该基因调控的关系,为水稻超高产育种中卷叶基因的利用奠定基础。

关键词(不超过 5 个,用分号分开): 水稻;卷叶突变;**IAA**;基因克隆;功能分析

Abstract(limited to 500 words):

Moderately rolling leaf is of significance for improvement of plant-type in rice breeding, and the cloning of gene controlling this trait has not been reported so far. In this research, **rl10(t)**, a rice rolled leaf mutant, induced by r-rays, was used for cloning the gene responding for rolled leaf mutation. The mutation locus in **rl10(t)** has been mapped on chromosome 3 and the most possible candidate gene encoding a key enzyme in **IAA** biosynthesis has been predicted in the primary study. The main objects of this project are to identify this mutated locus, as well as to analyze the gene function by using the transformation complementary experiments, overexpression, **RNAi** and antisense-**RNA** suppression. The analysis of spatial-temporal gene expression characteristics, the changes in endogenous **IAA** content, the responses to exogenous **IAA**, and the cytological changes in mutant, when compared with wild-type variety will be performed to understand the molecular mechanisms of leaf rolling mutation and the relationship with gene regulation. The results from this study will lay the foundation for the utilization of rolling leaf gene in rice breeding.

Keywords(limited to 5 keywords,seperated by;):rice;leaf rolling mutant;**IAA**;gene cloning;functional analysis



经费预算表

(金额单位: 万元)

<p>预算编制说明:</p> <p>1. 在填报本表之前, 请根据项目资助类别认真阅读相关的资助经费管理办法; 经费预算的编制以申请书中的《经费申请表》为基础, 以《国家自然科学基金项目资助批准通知书》中的资助金额为依据;</p> <p>2. 编制经费预算时, 不考虑不可预见因素和前期投入;</p> <p>购置与试制仪器设备在 5 万元以上 (包括 5 万元) 时, 须在报告正文中逐项说明用途和必要性。</p>		
科 目	预算经费	备 注 (计算依据与说明)
一. 研究经费	20.4000	
1. 科研业务费	9.0000	
(1) 测试/计算/分析费	6.0000	DNA 序列分析、IAA 及 IAA 合成中间产物分析等。
(2) 能源/动力费		
(3) 会议费/差旅费	1.5000	参加学术会议等
(4) 出版物/文献/信息传播事务费	1.5000	文章发表、网络使用、文献查询等。
(5) 其它		
2. 实验材料费	10.6500	
(1) 原材料/试剂/药品购置费	7.6500	购买酶、试剂盒、标准品、引物合成、同位素、易耗品等。
(2) 其它	3.0000	田间实验费等
3. 仪器设备费	0.7500	小型电泳仪、电泳槽等。
4. 实验室改装费		
5. 协作费		
二. 国际合作与交流费	0.0000	
1. 项目组成员出国合作交流		
2. 境外专家来华合作交流		
三. 劳务费	2.4000	研究生劳务费
四. 管理费	1.2000	总经费的 5%
合 计	24.0000	
与本项目相关的其他经费来源	国家其他计划资助经费	
	其他经费资助 (含部门匹配)	
	其他经费来源合计	0.0000



报告正文

研究内容和研究目标按照申请书执行。



国家自然科学基金资助项目签批审核表

<p>我接受国家自然科学基金的资助，将按照申请书、项目批准意见和计划书负责实施本项目（批准号：30671279），严格遵守国家自然科学基金委员会关于资助项目管理、财务等各项规定，切实保证研究工作时间，认真开展研究工作，按时报送有关材料，及时报告重大情况变动，对资助项目发表的论著和取得的研究成果按规定进行标注。</p> <p>项目负责人（签章）： 年 月 日</p>		<p>我单位同意承担上述国家自然科学基金项目，将保证项目负责人及其研究队伍的稳定和研究项目实施所需的条件，严格遵守国家自然科学基金委员会有关资助项目管理、财务等各项规定，并督促实施。</p> <p>依托单位（公章） 年 月 日</p>					
本栏目由基金委填写	科学处审查意见：						
	建议年度拨款计划（本栏目为自动生成，单位：万元）：						
	年度	总 额	第一年	第二年	第三年	第四年	第五年
	金额						
本栏目主要用于重大项目等	科学部审查意见：						
	负责人（签章）： 年 月 日						
本栏目主要用于重大项目等	相关局室审核意见：						
	负责人（签章）： 年 月 日						
本栏目主要用于重大项目等	委领导审批意见：						
	委领导（签章）： 年 月 日						



申请代码:	C020205
受理部门:	
收件日期:	
受理编号:	30671257

国家自然科学基金 申 请 书

资助类别: 面上项目

亚类说明: 自由申请项目

附注说明:

项目名称: 与生长素相关的水稻卷叶突变基因克隆及功能分析

申 请 者: 易继财 电话: 020-85288399

依托单位: 华南农业大学

通讯地址: 广州天河五山华南农业大学生命科学学院

邮政编码: 510642 单位电话: 020-85280070

电子邮件: jicai@scau.edu.cn

申报日期: 2006年3月10日

国家自然科学基金委员会



基本信息

申请者信息	姓 名	易继财	性 别	男	出生年月	1971 年 10 月	民 族	汉族
	学 位	硕士	职 称	讲师	主要研究领域			
	电 话	020-85288399		电 子 邮 件	jicai@scau.edu.cn			
	传 真			个 人 网 页				
	工 作 单 位	华南农业大学 / 生命科学学院遗传工程研究室						
	在研项目批准号							
依托单位信息	名 称	华南农业大学				代 码	51064201	
	联 系 人	陈奕		电 子 邮 件	kycjhc@scau.edu.cn			
	电 话	020-85280070		网 站 地 址	http://www.scau.edu.cn			
合作单位信息	单 位 名 称							代 码
项目基本信息	项目名称	与生长素相关的水稻卷叶突变基因克隆及功能分析						
	资助类别	面上项目			亚 类 说 明	自由申请项目		
	附注说明							
	申请代码	C020205:作物遗传育种学			C011007:分子遗传学			
	基地类别							
	预计研究年限	2007 年 1 月 — 2009 年 12 月			研究属性	应用基础研究		
	申请经费	35.0000 万元						
摘要	<p>(限 400 字):</p> <p>水稻叶片适度卷曲在株型改良育种中有重要意义。目前尚未见从水稻中克隆到卷叶相关基因的报道。申请者以 r 射线诱导产生的水稻卷叶突变体 rl10(t)为材料,应用图位克隆方法拟克隆卷叶突变相关基因。前期分析已把卷叶突变座位精细定位于第三染色体,发现候选基因为一个编码生长素合成关键酶的基因。本项目拟通过基因操作技术克隆该基因,并应用转化互补、过量表达、RNAi 及反义 RNA 抑制,分析其功能,包括基因的时空表达特性、卷叶突变与该基因功能的关系、内源 IAA 分析及外源 IAA 反应、突变所致的细胞学变化,以阐明水稻卷叶突变的机理及其与该基因调控的关系,为水稻超高产育种中卷叶基因的利用奠定基础。</p>							
	关键词(用分号分开,最多 5 个)	水稻; 卷叶突变; IAA; 基因克隆; 功能分析						



项目组主要成员（注：项目组主要成员不包括项目申请者，国家杰出青年科学基金类项目不填写此栏。）

编号	姓名	出生年月	性别	职称	学位	单位名称	电话	电子邮件	项目分工	每年工作时间（月）
1	梅曼彤	1942-10-23	女	教授	其他	华南农业大学	020-85280200	mtmei@scau.edu.cn	基因克隆	4
2	周峰	1972-12-27	男	助理研究员	博士	华南农业大学	020-85288399	zhoufeng@scau.edu.cn	功能互补载体及过量表达	6
3	姚涓	1974-4-25	女	实验师	硕士	华南农业大学	020-85280200	yaojuan@scau.edu.cn	RNAi 载体	6
4	刘兰娜	1981-11-8	女	硕士生	学士	华南农业大学	020-85280187	liulanna@sohu.com	反义载体	8
5	曹友培	1982-11-11	男	硕士生	学士	华南农业大学	020-85280187	cyp251@sohu.com	基因转化及转化苗分析	8
6									显微切片 IAA 分析等	
7										
8										
9										

总人数	高级	中级	初级	博士后	博士生	硕士生
6	1	3	0	0	0	2

说明： 高级、中级、初级、博士后、博士生、硕士生人员数由申请者负责填报（含申请者），总人数自动生成。



经费申请表

(金额单位: 万元)

科目	申请经费	备注(计算依据与说明)
一.研究经费	29.7500	
1.科研业务费	11.0000	
(1) 测试/计算/分析费	8.0000	DNA 序列分析、IAA 及 IAA 合成中间产物分析等
(2) 能源/动力费		
(3) 会议费/差旅费	1.5000	参加相关学术会议等
(4) 出版物/文献/信息传播费	1.5000	文章发表、网络使用、文献查询等
(5) 其它		
2.实验材料费	18.0000	
(1) 原材料/试剂/药品购置费	15.0000	购买酶、试剂盒、标准品、引物合成、同位素、易耗品等
(2) 其它	3.0000	田间实验费等
3.仪器设备费	0.7500	
(1) 购置	0.7500	小型电泳仪、电泳槽等
(2) 试制		
4.实验室改装费		
5.协作费		
二.国际合作与交流费	0.0000	
1.项目组成员出国合作交流		
2.境外专家来华合作交流		
三.劳务费	3.5000	研究生生活补贴
四.管理费	1.7500	总经费的 5%
合 计	35.0000	
与本项目相关的 其他经费来源	国家其他计划资助经费	
	其他经费资助(含部门匹配)	
	其他经费来源合计	0.0000



报告正文

(一) 立项依据与研究内容

1、项目的立项依据

培育超高产水稻品种一直是国内外水稻研究上的重点、热点和难点。叶片是植物光合作用器官，是制造光合产物的重要场所，与产量密切相关。在高产育种及株型改良中，叶片性状一直是水稻遗传育种家关注的焦点。袁隆平对水稻超高产育种提出的关于叶部形态的标准：上部3片功能叶要“长、直、窄、凹、厚”（袁隆平，1997），其中的“凹”是指叶片的适度卷曲。适度卷曲是解决叶长与叶挺之间矛盾的有效方法（潘学彪等，2004）。已有的研究表明，叶片适度卷曲有利于保持叶片直立，提高群体光能利用效率，还可以改善水稻生长中后期群体基部的通风透光条件，提高群体的光合作用效率和改善微环境，从而有利于水稻产量的提高（沈福成，1983；陈宗祥等，2001；陈宗祥等，2002；郎有忠等，2004；郎有忠等，2004；陆江锋等，2005）。

迄今关于植物叶片发育机理的知识较少（黄海，2003），而对于水稻卷叶的分子控制机理方面的知识则是空白。目前尚未在水稻中克隆到卷叶基因。

植物叶片的发育与三个方向的轴极性建立和发育有关，即“基-顶”轴、“中-侧”轴、“近-远”轴，其中“近-远”轴极性建立最为关键（Micol et al., 2003）。近年来，已克隆到一些与叶片“近轴面/远轴面”极性建立有关的基因，包括：决定近轴面的基因 PHAN(Waites et al., 1995), AS1(Byrne et al., 2000), AS2(Iwakawa et al., 2002), PHB、PHV、REV(Zhong and Ye, 1999; Ratcliffe et al., 2000; McConnell et al., 2001), RS2(Timmermans et al., 1999), OsPNH1(Nishimura et al., 2002)；决定远轴面的基因YABBY家族成员YAB2、YAB3、FIL和KAN家族成员KAN1、KAN2、KAN3 (Eshed et al., 2001; Bowman et al., 2002; Kerstetter et al., 2001)。这些基因多数都编码转录因子，可能调控下游基因的表达，分别决定近轴面和远轴面的细胞的命运。最近，还发现一些特殊的miRNA对叶片发育也起调控作用(Juarez et al., 2004)。这些轴性决定基因或miRNA发生突变，将会严重影响到植物叶片“近-远”轴极性的建立和叶片的发育，从而导致叶片畸形，其中包括叶片卷曲，如玉米中的 rld_1 卷叶突变体(Juarez et al., 2004)。另外，近年来还分别在拟南芥(Zhao et al., 2001)和矮牵牛(Santamaria et al., 2002)中发现了与生长素有关的卷叶突变体YUCCA和FLOOZY，表明生长素相关的基因也参与了叶发育的调控，但其分子机制尚未得到深入了解。

作为重要的粮食作物及基因组最小的单子叶植物，水稻在经济上及植物功能基因组



研究上的重要性都是不言而喻的。因此,克隆卷叶基因可为水稻超高产育种中卷叶基因的利用奠定基础,相关的研究也可作为卷叶的分子控制机理乃至叶片发育的机理的阐明奠定基础。

迄今为止,在水稻中总共已发现了近11个卷叶基因座位,其中Gramene (www.gramene.org) 网站公布了6个(rl_1 , rl_2 , rl_3 , rl_4 , rl_5 , rl_6), 分别定位在经典遗传图的1, 4, 12, 1, 3, 7号染色体上。另外李仕贵等(1998)、邵元健等(2005)分别在第5染色体上不同位置定位到 rl_7 和 rl_8 。严长杰等(2005)在水稻第9染色体上定位到 $rl_{9(t)}$ 。顾兴友等(1995)在日本流岗卷叶粳中还发现一个不完全显性方式遗传的卷叶基因 $RI_{(t)}$ 。邵元健等(2005)在第2染色体长臂上定位到一个不完全隐性的卷叶基因 $rl_{(t)}$ 。除 rl_7 、 rl_8 、 $rl_{9(t)}$ 和 $rl_{(t)}$ 外,其余的卷叶基因均未定位于分子遗传图上,且尚未见有关这些基因的克隆及功能分析的报道。

我们利用 Co^{60} - γ 射线辐照广东地方品种青粳占,诱导产生出一个稳定的水稻卷叶突变体(图1,见工作基础),经遗传分析,证明该突变性状受单一隐性基因控制,应用 F_2 分离群体已将其精细定位于第三染色体短臂上物理距离约为50kb的范围内,其内包括4个预测基因。虽然已报道的 rl_5 也位于第三染色体(经典遗传图定位),但其位于该染色体的长臂上 $chl1$ 标记基因附近。可推断我们获得的突变体卷叶性状受一新的卷叶基因控制,将其暂命名为 $rl_{10(t)}$ 。经对精细定位区段内基因的初步筛选,发现4个预测基因中的一个基因与生长素色氨酸合成途径中的关键酶有关,且该基因在突变体发生较大片段的缺失,因此推测该基因很可能与卷叶突变有关。

本项目拟继续通过转化互补完成该卷叶突变基因的克隆,并研究其时空表达特性,分析该基因的功能,以及其与IAA的关系,为该基因及突变体在水稻新品种选育上的应用和对卷叶分子调控机理的了解奠定基础。

主要参考文献:

- 李仕贵, 马玉清, 何平, 黎汉云, 陈英, 周开达, 朱立煌。一个未知的卷叶基因的识别和定位。四川农业大学学报, 1998, 16(4): 391~393。
- 严长杰, 严松, 张正球, 梁国华, 陆驹飞, 顾铭洪。一个新的水稻卷叶突变体 $rl_{9(t)}$ 的遗传分析和基因定位。科学通报, 2005, 50 (24): 2757-2762。
- 邵元健, 陈宗祥, 张亚芳, 陈恩会, 祁顶成, 缪进, 潘学彪。一个水稻卷叶主效QTL的定位及其物理图谱的构建。遗传学报, 2005, 32(5): 501~506。
- 邵元健, 潘存红, 陈宗祥, 左示敏, 张亚芳, 潘学彪。水稻不完全隐性卷叶主基因 $rl_{(t)}$ 的精细定位。科学通报, 2005, 50 (19): 2107-2113。
- 陆江锋, 郎有忠, 张祖建, 朱庆森。水稻一组卷叶近等基因系的株形、群体结构和光合特性比较。扬州大学学报(农业与生命科学版), 2005, 26(2): 56-60。
- 陈宗祥, 陈刚, 潘学彪。RI(t)卷叶基因在杂交水稻中的遗传表达及效应研究。作物学报, 2002, 28(6): 847~851。
- 陈宗祥, 潘学彪, 胡俊。水稻卷叶性状与理想株型的关系。江苏农业研究, 2001, 22(4): 88~91。



- 沈福成. 关于水稻卷叶性状在育种中利用的几点看法. 贵州农业科学, 1983(5): 6~8.
- 郎有忠, 张祖建, 顾兴友, 杨建昌, 朱庆森. 水稻卷叶性状生理生态效应的研究 I. 叶片姿态, 群体构成及广分布特征. 作物学报, 2004, 30 (8): 806~810.
- 郎有忠, 张祖建, 顾兴友, 杨建昌, 朱庆森. 水稻卷叶性状生理生态效应的研究 II. 光合特性, 物质生产与产量形成. 作物学报, 2004: 30 (9): 883~887.
- 顾兴友, 顾铭洪. 一种水稻卷叶性状的遗传分析. 遗传, 1995, 17(5): 20~23.
- 袁隆平. 杂交水稻超高产育种. 杂交水稻, 1997, 12 (6): 1-6.
- 黄海. 植物叶发育调控机理研究的进展. 植物学通报, 2003, 20 (4): 416~422.
- 潘学彪, 韩月澎, 陈宗祥, 张洪熙. 水稻植株形态遗传改良的研究进展. 扬州大学学报(农业与生命科学版), 2004, 25(1): 36-40.
- Bowman J L, Eshed Y, Baum S F. Establishment of polarity in angiosperm lateral organs. Trends in Genetics, 2002, 18 : 134~141.
- Byrne M E, Barley R, Curtis M, Arroyo J M, Dunham M, Hudson A, Martienssen R A. Asymmetric leaves1 mediates leaf patterning and stem cell function in Arabidopsis. Nature, 2000, 408 : 967~971.
- Eshed Y, Baum S F, Perea L V, Bowman J L. Establishment of polarity in lateral organs of plants. Current Biology, 2001, 11 : 1251~1260.
- Iwakawa H, Ueno Y, Semiarti E, Onouchi H, Kojima S, Tsukaya H, Hasebe M, Soma T, Ikezaki M, Machida C, Machida Y. The ASYMMETRIC LEAVES2 gene of Arabidopsis thaliana, required for formation of a symmetric flat lamina, encodes a member of a novel family of proteins characterized by cysteine repeats and a leucine zipper. Plant Cell Physiol, 2002, 43 : 467~478.
- Juarez M T, Kui J S, Thomas J, Heller B A, Timmermans M C P. microRNA-mediated repression of rolled leaf1 specifies maize leaf polarity. Nature, 2004, 428 : 84~88.
- Kerstetter R A, Bollman K, Taylor R A, Bombliks K, Poethig R S. KANADI regulates organ polarity in Arabidopsis. Nature, 2001, 411 : 706~709.
- McConnell J R, Emery J, Eshed Y, Bao N, Bowman J, Barton M K. Role of PHABULOSA and PHAVOLUTA in determining radial patterning in shoots. Nature, 2001, 411 : 709~713.
- Micol J L and Hake S. The development of plant leaves. Plant Physiology, 2003, 131: 389-394.
- Nishimura A, Ito M, Kamiya N, Sato Y, Matsuoka M. OsPNH1 regulates leaf development and maintenance of the shoot apical meristem in rice. The Plant Journal, 2002, 30 (2) : 189~201.
- Ratcliffe O J, Riechmann J L, Zhang J Z. INTERFASCICULAR FIBERLESS1 is the same gene as REVOLUTA. Plant Cell, 2000, 12 : 315~317.
- Santamaria R T, Bliet M, Ljung K, Sandberg G, Joseph N.M. Mol, Souer E, and Koes R. FLOOZY of petunia is a flavinmono-oxygenase-like protein required for the specification of leaf and flower architecture. GENES & DEVELOPMENT, 2002, 16: 753~763.
- Timmermans M C P, Hudson A, Becraft P W, Nelson T. ROUGH SHEATH2 : a Myb protein that represses knox homeobox genes in maize lateral organ primordia. Science, 1999, 284 : 151~153.
- Waites R, Hudson A. phantastica: a gene required for dorsoventrality of leaves in Antirrhinum majus. Development, 1995, 121 : 2143-2154.
- Zhao Y, Christensen S K, Fankhauser C, Cashman J R, Cohen J D., Weige D, Chory J. A Role for Flavin Monooxygenase-Like Enzymes in Auxin Biosynthesis. SCIENCE, 2001, 291: 306-309.
- Zhong R, Ye Z H. IFL, a gene regulating interfascicular fiber differentiation in Arabidopsis, encodes a homeodomain-leucine zipper protein. Plant Cell, 1999, 11 : 2139~2152.



2、项目的研究内容、研究目标，以及拟解决的关键问题。

研究内容：

经对精细定位区段内基因的初步筛选，发现 4 个预测基因（ORF）中的一个基因与生长素色氨酸合成途径的关键酶有关，且该基因在突变体中发生较大片段的缺失，测序分析表明其它 3 个基因在突变体和原种间没有差异（详见工作基础），因此将该基因定为候选的致卷叶突变基因。

（1）候选的致卷叶突变基因 *rl1000* 的克隆：

- a. 从原种的基因组中扩增出候选基因并测序验证
- b. 转化互补试验：构建功能互补表达载体，转化卷叶株，确认该基因的功能。
- c. 构建过量表达载体，转化正常粳稻品种，了解该基因上调表达对叶型的影响。
- c. 构建 RNA 干涉（RNAi）载体，转化正常粳稻品种，了解该基因下调表达对叶型的影响。
- d. 构建不同长度的反义 RNA 载体，转化正常粳稻品种，了解该基因下调表达的程度对叶型的影响。

（2）致卷叶突变基因 *rl1000* 的功能分析

- a. 该基因的时空表达特性分析：应用 Northern 杂交和 RT-PCR 分析，了解不同时期、不同组织内该基因的 RNA 转录差异。
- b. 卷叶突变与 IAA 的关系
比较分析原种、突变体及转化植株的外源 IAA 生理反应及内源 IAA 含量。
比较分析原种、突变体及转化植株内生长素合成途径中的某些中间产物含量。
通过以上分析，进一步确认该基因与 IAA 合成的关系。
- c. 突变体、原种及转化体叶片切片显微观察，了解该基因导致卷叶的细胞学机理。

研究目标：

从水稻卷叶突变材料克隆致卷叶突变基因 *rl1000*，通过功能互补、过量表达和表达抑制(RNAi 和反义 RNA)了解其功能，确认该基因与卷叶突变的关系，阐明生长素的合成与水稻叶片正常发育和异常发育（卷叶突变）的关系，并进而探讨调控该基因表达的途径，为该基因及突变体在水稻新品种选育中应用奠定基础。



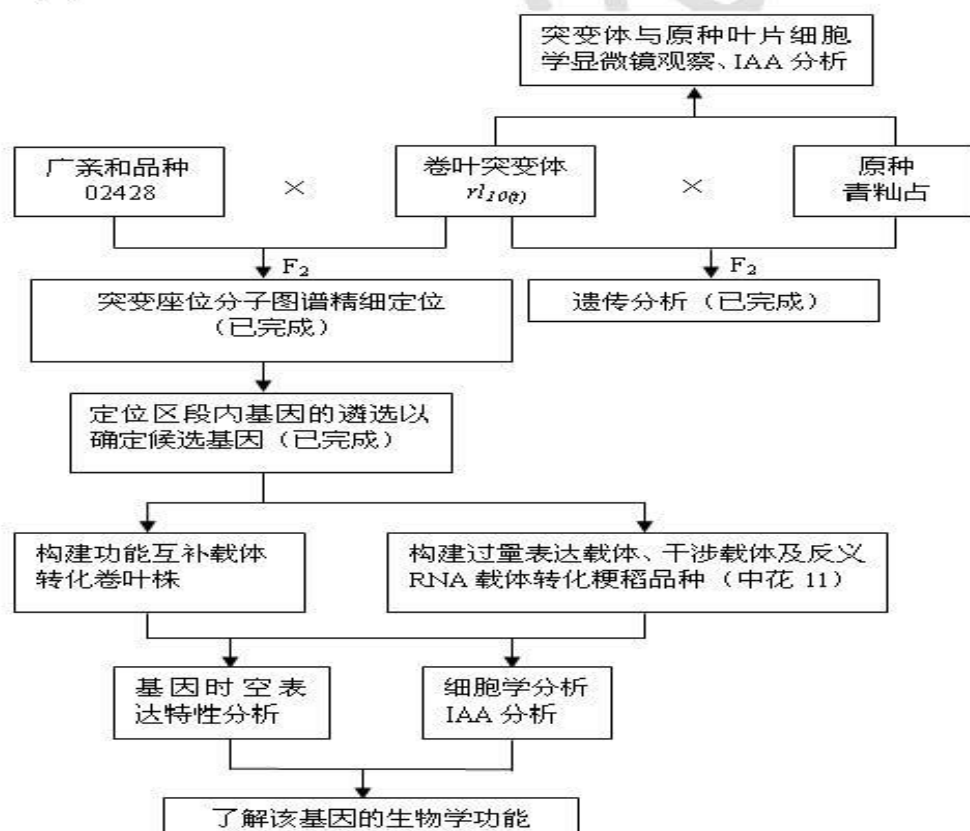
拟解决的关键问题:

(1) 首先要确定精细定位区段 (~50kb) 内候选的卷叶基因以供转化功能鉴定, 此部分工作已完成。在定位区域内预测的基因中, 有一个基因编码生长素合成的关键酶。已确定该基因为候选的致卷叶突变基因。

(2) 转化互补试验是确认基因的主要依据。作为籼稻品种突变体 *rl₁₀₀* 的转化难度较大, 我们将同时以突变体 *rl₁₀₀* 和梗稻品种杂交的后代分离株中选择一些卷叶株 (含有约 1/2 梗稻核背景) 为转化材料, 有利于转化。另外, 结合采用构建过量表达载体、RNAi 载体和反义 RNA 表达载体转化梗稻的方法来验证基因的功能。

3、拟采取的研究方案及可行性分析

技术路线:





研究方案:

- (1) 利用 PCR 和 RT-PCR 及测序分析, 对精细定位区段 (~50kb) 内预测的基因遴选以供转化互补用, 此部分工作已完成 (详见工作基础部分), 其中有一个基因编码生长素色氨酸合成途径的关键酶, 将其定为候选基因。
- (2) 利用网站公布的水稻基因组序列数据, 根据 Blast 比对结果设计合适的引物, 在原种中克隆该基因, 并测序验证。
- (3) 转化互补实验: 构建自身启动子驱动的候选基因功能互补载体, 转化卷叶株, 观察能否回复正常表型, 以确认致卷叶突变的基因。
- (4) 构建 Ubi 强启动子驱动的候选基因过量表达载体, 转化再生能力强的粳稻品种如中花 11 等, 观察成功转化植株当代及后代的表型变化, 了解该基因上调表达对叶型的影响。
- (5) 构建候选基因的 RNAi 载体, 转化再生能力强的粳稻品种如中花 11 等, 观察成功转化植株当代及后代的表型变化, 了解该基因下调表达对叶型的影响。
- (6) 构建候选基因的不同长度的反义 RNA 表达载体, 转化再生能力强的粳稻品种如中花 11 等, 观察成功转化植株当代及后代的表型变化, 了解该基因不同程度的下调表达对叶型的影响。
- (7) 卷叶基因 *rl10(t)* 的功能分析
 - a. 植株不同时期、不同组织的 RT-PCR 分析和 Northern 分析, 以了解该基因的时空表达特性。
 - b. 用气 (液) 相色谱/质谱连用分析原种、突变体及转化植株的不同组织 (叶片, 根, 幼穗等) 内源 IAA 含量, 以及它们对外源 IAA 的生理反应, 以了解该突变基因与 IAA 调控的关系。
 - c. 用气 (液) 相色谱/质谱连用分析原种、突变体及转化植株内生长素色氨酸合成途径中的某些中间产物含量, 以了解该基因与 IAA 合成的关系。
 - d. 显微观察原种、突变体及转化植株的叶片细胞生长变化, 以了解该基因导致卷叶的细胞学机理。

综合上述结果, 确定 *rl10(t)* 卷叶突变基因的功能及生物学意义。



可行性分析

(1) 我们已将 *rl10q* 座位精细定位于第三染色体短臂上约 50kb 范围内, 通过 Southern 杂交分析发现 1 个基因在突变体有较大片段的缺失, 序列分析表明该基因编码生长素合成的关键酶 (详见工作基础)。因此本项目有较好的前期工作基础。

(2) 转化互补试验能否完成是验证基因功能的关键。由于部分籼稻品种转化、再生难度大, 为保证转化互补的成功, 本项目设计了两套方案, 即 a. 转化 *rl10q* (籼稻) 和平均含有 1/2 粳稻背景的杂种后代卷叶植株, 检测其能否回复正常表型; b. 用 RNAi 载体转化粳稻品种 (中花 11), 从正常基因的失活来说明基因的功能, 任一方案的完成均可达到阐明基因功能的目的。

(3) 申请者所在的广东省植物功能基因组学与生物技术重点实验室的刘耀光研究员、庄楚雄研究员以及本课题组主要成员梅曼彤教授均具有水稻基因克隆的丰富经验及成熟的相关技术, 能为本项目的实施提供各方面的帮助。

4、本项目的特色与创新之处

(1) 本项目所用材料为申请者所在研究组选出, 据查未有从水稻第三染色体短臂的相同区域定位卷叶相关基因的报道, 故本基因的成功克隆具有完全自主知识产权, 可申请专利, 并可进一步应用到水稻育种实践。

(2) 植物叶片发育受多种机制调控, 目前尚未见任何水稻卷叶相关基因的克隆及功能分析的报道, 本项目从分子生物学、细胞学、生理学等多个层次对卷叶与 IAA 的关系进行研究, 对阐明单子叶植物中生长素调控途径有重要的理论意义。

5、年度研究计划及预期研究结果

2007 年度: 候选卷叶突变基因的克隆及测序验证

候选基因功能互补载体、过量表达载体、RNAi 载体和反义 RNA 载体构建

2008 年度: 候选基因功能互补载体转化卷叶株

过量表达载体、RNAi 载体及反义 RNA 载体转化粳稻 (中花 11)
突变体与原种内源 IAA 含量分析以及对外源 IAA 的生理反应



突变体与原种叶片切片的显微镜比较观察

2009 年度：转化体的转基因和卷叶性状的共分离分析

IAA 含量分析、IAA 合成中间产物分析

叶片切片观察等

不同时期及组织中的基因表达特性分析

结果整理及撰写论文

预期研究结果：

- (1) 克隆获得水稻 *rl₁₀₀* 卷叶突变基因并申请基因专利
- (2) 了解该基因的功能及时空表达特性，阐明 IAA 合成与叶片发育的关系。
- (3) 培养硕士研究生 2~3 人
- (4) 发表 SCI 论文 1~2 篇

(二) 研究基础与工作条件

1、工作基础

申请人参加了本实验室刘耀光研究员、庄楚雄研究员、梅曼彤教授主持的多项科研项目，熟练掌握了本研究所需的实验技术。本研究的前期工作已获得实质性进展。

本项目的前期工作已从 ^{60}Co - γ 射线处理籼稻品种青籼占种子的后代中选出卷叶突变体 *rl₁₀₀*。该突变体叶片适度内卷（图 1）。2004 年夏，我们应用 *rl₁₀₀* 与 02428 杂交的 F_2 群体，通过 SSR、SNP 和 InDel 标记分析，已将其卷叶突变座位定于第三染色体短臂的约 50kb 的范围内（图 2）。通过 RiceGAAS 水稻基因注释系统预测定位区段内有 4 个基因（ORF），接着应用 PCR 及杂交分析进行遴选，发现其中一个基因（ORF2）在原种青籼占和突变体 *rl₁₀₀* 的基因组之间存在差异，即有较大片段的缺失（图 3）。该 ORF 编码生长素色氨酸合成途径的一个关键酶。测序分析表明其它 3 个 ORF 在突变体和原种间没有差异。因此将该基因做为该卷叶突变的候选突变基因。我们还对幼苗期（二叶一心）叶片进行了生长素含量测定，发现突变体的生长素含量明显降低；还初步观察了灌浆后期剑叶的显微横切片（图 4），发现突变体的剑叶中部中脉组织周围维管束数目相对



减少，气腔发育相对滞后；另外成熟期考种数据统计分析表明突变体的分蘖显著增多。近年来许多研究表明，生长素在叶中维管束的建成以及禾本科植物分蘖的发生过程中都有调控作用（Mattsson J et al., 2003；梁振兴等, 1998；李春喜等, 2000），故推测 $rl_{10(t)}$ 突变体的卷叶与生长素合成有关。

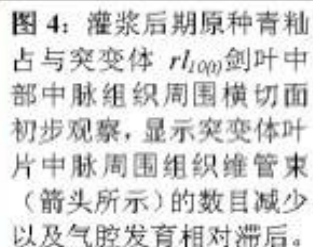
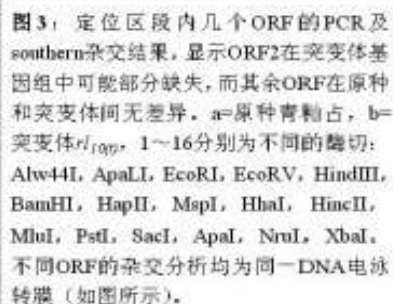
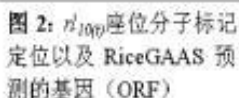
上述前期工作为本项目提供了较坚实的基础。

李春喜，赵广才，代西梅，姜丽娜，尚玉磊。小麦分蘖动态与内源激素的研究。作物学报，2000，26（6）：963~968。

梁振兴，马兴林。冬小麦分蘖过程中内源激素作用的研究。作物学报，1998，24（6）：788~792。

Mattsson J, Ckurshumova W and Berleth T. Auxin Signaling in Arabidopsis Leaf Vascular Development. Plant Physiology, 2003, 131: 1327~1339.







申请者所在的遗传工程研究室是仪器设备齐全的实验室。其中有大中型控温高速离心机、台式离心机、分光光度仪、基因枪、电激仪、PCR 仪、脉冲电场电泳仪、BioRad FX 分子磷屏成像分析系统、超低温冰箱、普通显微镜和荧光显微镜、切片机、细菌和植物组织培养所需的各种装置、人工气候室以及同位素操作室等。本项目全部工作可在本实验室完成。另外我校分析测试中心配备有气（液）相色谱和质谱仪，可用于 IAA 含量及 IAA 合成中间代谢产物的分析。

2、工作条件

申请者所在的遗传工程研究室，经广东省教育厅及学校多年投资，已配备进行基因克隆、遗传转化以及组织切片与显微观察所需的仪器设备及实验室条件，2004 年已获批准建设广东省教育厅植物功能基因组重点开放实验室，由省财政厅投资 600 万元，故项目承担单位已具有供本项目需求的研究条件。

3、申请者简历

申请者**易继财**简历：

男，1971 年 10 月出生，讲师，1996 年 7 月于华南农业大学生命科学学院生物化学专业毕业，获硕士学位，现于生命科学学院遗传工程研究室工作。曾参加刘耀光研究员、梅曼彤教授以及庄楚雄研究员的课题组，从事水稻基因克隆和功能分析的科研工作，参加多项国家基金、863 等项目研究。现为在职博士研究生，导师梅曼彤教授，论文研究题目为：r 射线诱导的水稻卷叶突变体的分子标记定位与分子生物学研究。近年来的主要研究工作包括空间辐射和 Co^{60} - γ 射线诱导产生的水稻突变体筛选、分子标记分析以及相关突变座位的定位克隆和功能分析等。在本项目中负责项目的总体设计和统筹协调，具体承担基因表达特性分析、转化、结果分析等工作。主要发表文章：

(1) **易继财**，庄楚雄，姚涓，王慧，陈志强，梅曼彤。空间搭载诱导水稻种子突变的分子标记多态性分析。生物物理学报，2002，18(4)：478-483。

(2) 周峰，**易继财**，张群宇，王慧，梅曼彤。水稻空间诱变后代的微卫星多态性分析。华南农业大学学报，2001，22（4）：55-57。



(3) 余红兵, 周峰, 姚涓, **易继财**, 庄楚雄, 骆艺, 梅曼彤。高空气球搭载水稻种子后代诱变的研究。核农学报, 2004, 18 (4): 276-279。

(4) **易继财**, 徐凤彩。萝卜溶菌酶活性中心残基的初步研究。生物化学与生物物理学报, 1997, 29 (4): 377-382。

(5) 穆虹, 廖毅, 梁雪芬, **易继财**。萝卜溶菌酶制剂配制的研究。华南农业大学学报, 1997, 18 (3): 86-90。

(6) M. Mei Y.Qiu, Y.Sun, R.Huang, J.Yao, Q.Zhang, M.Hong & **J.Ye**. Morphological and molecular changes of maize plants after seeds been flown on recoverable satellite . Adv. Space Res. 1998, 22(12): 1691-1697.

(7) **J.C.Yi**, F.Zhou, C.X.Zhuang, M.T.Mei, H.Wang, and Z.Q.Chen. Morphological and molecular changes of rice plants after seeds been flown on recoverable satellite. 4th International rice genetics symposium, 2000, Oct.22-27, P195. Los Banos, Laguna, PHILIPPINES.

项目组成员**梅曼彤**教授简历:

1965年毕业于华南农学院农业生物物理专业; 1983-1985年公派赴美国加利福尼亚大学劳伦斯伯克利研究所进行放射细胞生物学及分子生物学研究; 1989年开始承担国家自然科学基金项目、美国洛克菲勒基金水稻生物技术国际合作项目, 开展水稻重要农艺性状基因的分子图谱定位及高能重离子辐射对植物的诱变效应、诱变机理等方面的研究。1998年开始承担国家高技术航天领域项目, 主要从事空间辐射诱变效应及分子生物学研究。现为华南农业大学遗传工程研究室主任、教授、博士生导师, 其主持的“重离子辐射对水稻及玉米生物学效应研究”(国家自然科学基金资助项目)1996年获广东省自然科学三等奖。在本项目中主要负责基因克隆方面的工作。主要发表文章:

(1) **Mei MT** et al. Construction of a lychee genetic linkage map based on RAPD markers. Acta Hort, 2003, 625: 131-136.

(2) Zhuang CX, Fu Y, Zhang GQ, **Mei MT** and Lu YG. Molecular Mapping of S-c, an F1 pollen sterility in rice. Euphytica, 2002, 127: 133-138.

(3) **M. Mei**, Y.Qiu, Y.Sun, R.Huang, J.Yao, Q.Zhang, M.Hong & J.Ye. Morphological



and molecular changes of maize plants after seeds been flown on recoverable satellite. Adv. Space Res, 1998, 22(12): 1691-1697.

(4) **Mei MT** et al. RFLP tagging of brown planthopper resistance gene in indica rice. Rice Genetics III, 1996, 590-595.

(5) 杨存义, 陈忠正, 庄楚雄, **梅曼彤**, 刘耀光。水稻籼粳杂种不育基因座 *Sc* 的遗传图和物理图精细定位。科学通报, 2004, 49 (13): 1273-1277。

(6) 姜大刚, 卢森, 周海, 武小金, 庄楚雄, 刘耀光, **梅曼彤**。用 EST 和 SSR 标记定位水稻温敏不育基因 *tms5*。科学通报, 2006, 51 (2): 148-151。

(7) 庄楚雄, **梅曼彤**, 张桂权, 卢永根。用 RAPD 标记对栽培稻 F1 花粉不育基因座 *S-b* 定位。遗传学报, 2002, 29 (8): 700-705。

(8) **梅曼彤**。《空间生命》第五篇, 科学空间与应用。科学出版社, 2001, ISBN 7-03-009254-6。

(9) 庄楚雄, 张桂权, **梅曼彤**, 卢永根。栽培稻 F1 花粉不育基因 *S-a* 的分子标记定位。遗传学报, 1999, 26(3): 213-218。

项目组成员**周峰**简历:

助理研究员, 1996年毕业于安徽大学生物化学专业, 获学士学位, 毕业后工作于安徽生物药厂。1999~2004年于华南农业大学作物遗传育种专业攻读博士学位, 学位论文题目为“辐射诱发水稻矮化突变体 *dwarf69-6* 的遗传学与分子生物学分析”, 2004年6月获得农学博士学位。2004年7月开始在华南农业大学生命科学学院遗传工程研究室工作。主要研究方向为基因工程在作物遗传育种中的应用。已熟练掌握基因操作有关的多项技能, 在本项目中承担功能互补载体和过量表达载体的构建。已发表论文:

(1) **周峰**, 易继财, 张群宇, 王慧, 梅曼彤。水稻空间诱变后代的微卫星多态性分析。华南农业大学学报, 2001, 22 (4): 55-57。

(2) 姚涓, 赵均良, 陈金顶, 穆虹, **周峰**, 姜大刚, 梅曼彤。转基因耐除草剂大豆及产品中外源成分检测方法的建立。华南农业大学学报, 2005, 26(4): 67-72。



项目组成员**姚涓**简历:

实验师, 1996年毕业于华南农业大学土壤农化专业, 获学士学位。毕业留校在华南农业大学生命科学学院遗传工程研究室工作。2000~2004年在职华南农业大学攻读生物化学与分子生物专业硕士学位, 学位论文题目为“转基因大豆及其产品外源基因检测体系的建立”, 2004年6月获得理学硕士学位。在本项目中承担RNAi载体和反义RNA载体的构建。主要发表文章:

(1) **姚涓**, 赵均良, 陈金顶, 穆虹, 周峰, 姜大刚, 梅曼彤。转基因耐除草剂大豆及产品中外源成分检测方法的建立。华南农业大学学报, 2005, 26(4): 67-72。

(2) 余红兵, 周峰, **姚涓**, 易继财, 庄楚雄, 骆艺, 梅曼彤。高空气球搭载水稻种子后代诱变的研究。核农学报, 2004, 18(4): 276-279。

(3) 易继财, 庄楚雄, **姚涓**, 王慧, 陈志强, 梅曼彤。空间搭载诱导水稻种子突变的分子标记多态性分析。生物物理学报, 2002, 18(4): 478-483。

(4) Mei M, Qiu Y, Sun Y, Huang R, **Yao J**, Zhang Q, Hong M, Ye J. Morphological and molecular changes of maize plants after seeds been flown on recoverable satellite. Adv. Space. Res, 1998, 22(12): 1691-1697.

4、承担科研项目情况

申请者参加了本实验室多项科研项目, 在部分科研项目中承担了重要任务:

(1) 国家自然科学基金项目‘与油菜素类固醇相关的水稻矮杆突变基因克隆及功能分析’(30571051, 2006-2008) 参加

(2) 863项目‘空间重粒子辐射诱导植物遗传变异规律特点的研究’(2002-2005) 参加

(3) 国家自然科学基金项目‘空间辐射诱变水稻育种的机理及应用研究’(30170534, 2002-2004) 参加

(4) 国家高技术航天领域项目“空间辐射因素对植物种子的诱变效应及其分子生物学研究”(863-2-3-3-1, 1998-2001) 参加



5、完成自然科学基金情况

申请者未主持过国家自然科学基金项目

（三）经费申请说明

本项目申请经费 35 万元，其中科研业务费 11.0 万元，包括测试分析费 8.0 万元，用于委托公司进行 DNA 序列分析、IAA 及 IAA 合成中间产物含量分析等；会议费为 1.5 万元，用于课题组成员参加相关学术会议；出版、文献、信息费用 1.5 万元，用于文章发表、网络使用、文献查询等。实验材料费为 18.0 万元，其中 15.0 万元为购买研究所用酶、试剂盒、标准样品、易耗品、同位素等，及引物合成的费用；3.0 万元用于试验材料的田间种植费用等；0.75 万元用于购买易损耗的小型电泳仪、小型电泳槽等。劳务费为 10%，即 3.5 万元，用于参加本项目研究生的生活补贴。管理费为 5%，即 1.75 万元。经费预算中，申请经费的 85% 将直接用于科研。

（四）其他附件

推荐信 1:

申请者具有较深厚的分子遗传学理论基础，全面掌握了基因工程的各项技术。他 1996 年进入我校生命科学学院遗传工程研究室工作，曾参与了本人主持的 973、863、国家自然科学基金等多项科研项目。他刻苦钻研、勇于实践、治学严谨，不仅娴熟掌握了分子标记定位分析、植物基因转化、分子杂交，生物信息分析等技术，还能够有所创新地应用于研究中，具有相当强的独立研究能力，已作为本实验室的主要力量。他完成了 Co^{60} - γ 射线和空间环境因素诱导产生的突变体筛选及其分子标记定位分析，特别是在 γ 射线诱导水稻产生的卷叶突变体 rl_{100} 的精细定位及所锚定区段内几个基因



(ORF) 的初步筛选等研究中取得重要进展。在本项目中应用 PCR 扩增候选基因, 并应用转化互补试验和 RNA 干涉技术来完成 *rl_{10(t)}* 中卷叶控制基因的克隆, 实验设计合理可行, 可望完成研究的各项内容, 达到预期目标。本研究将为进一步在水稻育种中利用该基因打下基础。申请者所在实验室具有完成本项目所需的各种设备及条件, 本推荐人也将大力支持该项目的工作。

推荐人: 华南农业大学 刘耀光 研究员

签名

推荐信 2:

易继财同志 1996 年 6 月硕士毕业于华南农业大学, 毕业后到生命科学学院遗传工程研究室工作, 从事水稻突变体筛选、分子标记定位分析和水稻基因克隆与功能分析等方面的研究工作, 参加了 973、863、国家自然科学基金等多项研究课题。通过多年的工作和学习, 掌握了扎实的分子生物学等方面的基础理论知识和熟练的基因工程等方面的操作技能, 具有很强的独立科研能力。

本项目是申请者博士学位论文的工作基础, 经 2 年多的研究, 已完成了水稻卷叶基因 *rl_{10(t)}* 的精细定位和突变机理的初步分析, 研究结果显示, 该水稻卷叶突变可能是由 IAA 合成途径中的关键基因缺失所造成的, 为克隆卷叶基因、分析其功能和了解 IAA 对卷叶程度的调控打下了坚实的基础。



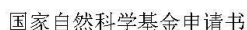
适度的卷叶，有利于改善水稻的群体效应，提高水稻的群体光合作用，从而提供水稻的产量，因此，了解 IAA 对卷叶调控的机理具有重要的应用价值。

申请者具备了申请和从事国家基金相关领域研究的能力，而且本项目的研究基础好，所在的实验室条件优越，为申请者完成申请的研究内容提供很好的保障。所以本人极力推荐易继财同志申请国家自然科学基金。

推荐人：华南农业大学 庄楚雄 研究员

签名

导师同意书：另附页。



申 请 者：易继财
 项目名称：与生长素相关的水稻卷叶突变基因克隆及功能分析
 资助类别：面上项目
 附注说明：

依托单位：华南农业大学
 亚类说明：自由申请项目

我保证申请书内容的真实性。如果获得基金资助,我将履行项目负责人职责,严格遵守国家自然科学基金委员会的有关规定,切实保证研究工作时间,认真开展工作,按时报送有关材料。若填报失实和违反规定,本人将承担全部责任。

签字:

我保证有关申报内容的真实性。如果获得基金资助,我将严格遵守国家自然科学基金委员会的有关规定,切实保证研究工作时间,加强合作、信息资源共享,认真开展工作,及时向项目负责人报送有关材料。若个人信息失实、执行项目中违反规定,本人将承担相关责任。

编号	姓 名	工作单位名称	项目分工	每年工作 时间 (月)	签 字
1	梅曼彤	华南农业大学	基因克隆	4	
2	周峰	华南农业大学	功能互补载体及过量表	6	
3	姚涓	华南农业大学	RNAi 载体反义载体	6	
4	刘兰娜	华南农业大学	基因转化及转化苗分析	8	
5	曹友培	华南农业大学	显微切片 IAA 分析等	8	
6					
7					
8					
9					

已按填报说明对申请人的资格和申请书内容进行了审核。申请项目如获资助,我单位保证对研究计划实施所需要的人力、物力和工作时间等条件给予保障,严格遵守国家自然科学基金委员会有关规定,督促项目负责人和项目组成员以及本单位项目管理部门按照国家自然科学基金委员会的规定及时报送有关材料。

合作单位公章 2

日期:

受理编号: c15140500000559

项目编号: 2015A030313414

文件编号: 粤科规财字[2015]120号



2015A030313414

广东省自然科学基金项目 合同书

项目名称: 水稻mTERF基因v14调控叶绿体发育的分子机理研究

项目类别: 广东省自然科学基金-自由申请

项目起止时间: 2015-08-01 至 2018-08-01

管理单位(甲方): 广东省自然科学基金管理委员会

依托单位(乙方): 华南农业大学

通讯地址: 广东省广州市天河区五山路483号

邮政编码: 510642

单位电话: 020-38632819

项目负责人: 张群宇

联系电话: 02085288395

项目联系人: 张群宇

联系电话: 15918839846

广东省科学技术厅
二〇一四年制

一、主要研究内容和要达到的目标

研究内容：

在已有研究工作基础上，将对以下研究内容进行研究：

a. 以水稻台中65 和突变体v14 不同叶期为材料分析确认mTERF 基因V14 调控的叶绿体靶基因。白化突变体 v14 导致水稻叶绿体发育受阻，通过已有研究工作机构分析发现部分叶绿体基因表达模式发生变化。目前对mTERF 蛋白家族功能研究发现其参与细胞器具有的转录、转录终止或者转录后修饰等调控。我们将构建V14 及一系列突变表达载体（根据V14 氨基酸序列进行生物信息学分析结果）进行体外表达，并与推测的靶基因结合位点序列进行体外结合实验。证明V14 特异性调控的靶基因。

b. 分析V14 蛋白在叶绿体的蛋白复合体成员。

目前对 mTERF 基因复合体的调控机理功能报道较少，如仅有动物mTERF-4 与Msun4 (5-methylcytosine RNA methyltransferase 4) 组成复合体结合线粒体核糖体大亚基，从而调控线粒体核糖体的成熟。因此分析 V14 复合体对了解和解释该复合体调控靶基因表达的机理具有重要的意义，本研究将利用酵母双杂交和免疫共沉淀方法（V14 特异抗体）分析V14 蛋白复合体，在研究内容1 确认靶基因的基础上解释该复合体调控靶基因表达的机理。

c. 水稻mTERF 基因家族成员间关系的初步分析。

将筛选得到的在高温下弥补 V14 蛋白的家族成员R-v14s 编码区序列和V14 基因启动子序列构建植物转化载体并转化到v14 突变体材料。通过分析R-v14s 转基因材料，确认该家族成员弥补v14的功能。

研究目标：

申请人在克隆水稻白化突变基因 v14 的研究工作基础上，将通过水稻芯片杂交、定量RT-PCR和Western blot 等方法分析该mTERF 基因家族成员调控的水稻叶绿体候选靶基因，并通过进一步确认靶基因和验证其结合位点，深入阐述V14 对水稻叶绿体发育的调控机理。

二、研究成果及形式

论文及专著情况	国家统计局刊物以上刊物 发表论文（篇）		2		专著（册）		0	
专利情况(项)	发明专利		实用新型专利		外观设计专利		国外专利	
	申请	授权	申请	授权	申请	授权	申请	授权
	0	0	0	0	0	0	0	0
其他								

三、项目进度和阶段目标

1. 项目起止时间： 2015-08-01 至 2018-08-01		
2. 项目实施进度及阶段主要目标：		
开始日期	结束日期	主要工作内容
2015-08-01	2016-07-31	1. 利用水稻芯片杂交（重复验证）、定量RT-PCR 和Western Blot 等方法确认V14 调控的叶绿体靶基因。以台中 65 和v14 突变体不同温度处理的不同苗期叶片为材料，分析水稻mTERF 基因家族成员表达模式，推测在高温下弥补V14 蛋白的家族成员R-v14。
2016-08-01	2017-07-31	2. 通过 GO 富集和KEGG 通路分析V14 调控途径的功能，利用实时定量RT-PCR 确认候选基因的表达变化。将筛选得到的在高温下弥补 V14 蛋白的家族成员R-v14s 编码区序列和V14 基因启动子序列构建植物转化载体并转化到v14 突变体材料。
2017-08-01	2018-08-01	3. 完成酵母双杂交和免疫共沉淀实验，筛选并确认 V14 复合体的组成，双分子荧光互补验证得到的互作基因，解释V14 对叶绿体发育途径的调控机理。预期获得V14 复合体的组成。

四、项目总经费及省科技厅经费预算

1. 省科技厅经费下达总额：（大写）壹拾万圆整；（小写）10.00万元；					
2. 省科技厅经费年度下达计划：					
年度	2015 年	年	年	年	年
经费(万元)	10.00				
3. 总经费开支预算计划：					
经费筹集情况：					(单位：万元)
省科技厅经费	自筹资金				合计
	自有资金	贷款	地方政府投入	其它	
10.00					10.00
政府部门、境外资金及其他资金投入情况说明：	<div style="text-align: center; font-size: 2em; opacity: 0.3; transform: rotate(-30deg);">2015A030313414</div>				

经费预算				(单位: 万元)
	总投入经费		省科技厅经费	
支出经费	经费额	用途说明	经费额	用途说明
科研业务费:	3.20	测试费, 差旅费等支出	3.20	测试费, 差旅费等支出
实验材料费:	3.90	购买实验试剂等支出	3.90	购买实验试剂等支出
仪器设备费:	0	无	0	无
实验室 改装费:	0	无	0	无
协作费:	0	无	0	无
人员费:	2.40	研究生补助	2.40	研究生补助
专家咨询费:	0	无	0	无
国际合作 与交流费:	0	无	0	无
管理费:	0.50	项目管理费	0.50	项目管理费
合计:	10.00		10.00	

五、人员信息

项目负责人								
姓名	证件号码	年龄	性别	职称	学历	在项目中承担的任务	所在单位	签名
张群宇	413001197308073036	42	男	副研究员	博士研究生	研究项目实验设计, 指导等	华南农业大学	

项目组主要成员								
姓名	证件号码	年龄	性别	职称	学历	在项目中承担的任务	所在单位	签名
周峰	340104197212273037	43	男	助理研究员	博士研究生	基因克隆	华南农业大学	
王曼	410802197203152026	43	女	讲师	博士研究生	水稻生理指标检测	华南农业大学	
戟志程	421127198910033938	26	男	未取得	本科	V14基因表达分析	华南农业大学	
贾春阳	413001198905112034	26	男	未取得	本科	水稻转基因转化	华南农业大学	

六、依托单位与合作单位的合作协议

1. 依托单位与合作单位的工作分工：	
2. 经费分配：	
依托单位（盖章）：	华南农业大学
合作单位1（盖章）：	
合作单位2（盖章）：	

七、合同条款

第一条 甲方与乙方根据《中华人民共和国合同法》及国家有关法规和规定，为顺利完成（2015）年水稻mTERF基因v14调控叶绿体发育的分子机理研究 专项项目（文件编号：粤科规财字[2015]120号）经协商一致，特订立本合同，作为甲乙双方在项目实施管理过程中共同遵守的依据。

第二条 甲方的权利义务：

1. 按合同书规定进行经费核拨的有关工作协调。
2. 根据甲方需要，在不影响乙方工作的前提下，定期或不定期对乙方项目的实施情况和经费使用情况进行检查或抽查。
3. 根据《广东省科技计划项目信用管理办法(试行)》对乙方进行科技计划信用管理。

第三条 乙方的权利义务：

1. 确保落实自筹经费及有关保障条件。
2. 按合同书规定，对甲方核拨的经费实行专款专用，单独列账，并随时配合甲方进行监督检查。
3. 使用财政资金采购设备、原材料等，按照《广东省实施〈中华人民共和国招标投标法〉办法》有关规定，符合招标条件的须进行招标。
4. 项目实施完成或实施到一定程度，须按照《广东省省级科技计划项目结题管理的实施细则（试行）》提出验收或终止结题的申请，并按甲方要求做好项目结题工作。
5. 在每年规定时间内向甲方如实提交上年度工作情况报告，报告内容包含上年度项目进展情况、经费决算和取得的成果等。
6. 按照国家和省有关规定，提交科技报告及其他材料。

第四条 在履行本合同的过程中，如出现广东省相关政策法规重大改变等不可抗力情况，甲方有权对所核拨经费的数量和时间进行相应调整。

第五条 对分年度拨款（滚动资助）项目，甲方有权利根据项目研究进展或中期考核情况变更或中止项目后续资助经费数额。

第六条 在履行本合同的过程中，当事人一方发现可能导致项目整体或部分失败的情形时，应及时通知另一方，并采取适当措施减少损失，没有及时通知并采取适当措施，致使损失扩大的，应当就扩大的损失承担责任。

第七条 本项目技术成果的归属、转让和实施技术成果所产生的经济利益的分享，除双方另有约定外，按国家和广东省有关法规执行。

第八条 根据项目具体情况，经双方另行协商订立的附加条款，作为本合同正式内容的一部分，与本合同具有同等效力。

第九条 本合同一式三份，各份具有同等效力。甲、乙方及课题负责人各执一份，三方签字、盖章后即生效，有效期至项目结题后一年内。各方均应负合同的法律责任，不应受机构、人事变动的影响。

第十条 乙方必须接受甲方聘请的本项目合同监理单位的监督和管理。监理单位按照甲方赋予的权利对本项目合同的履行进行审核、进度调查，对项目合同变更、经费使用情况进行监督管理及组织项目验收。

说明：1. 本合同书中，凡是当事人约定无需填写的内容，应在空白处划（/）。

2. 委托代理人签订本合同书的，应出具合法、有效的委托书。

2015A030313414

八、本合同签约各方

管理单位（甲方）：广东省自然科学基金管理委员会（盖章）		
法定代表人（或法人代理）：	_____	（签章）
		年 月 日
依托单位（乙方）：华南农业大学（盖章）		
法定代表人（或法人代理）：	陈晓阳 _____	（签章）
联系人（项目主管）姓名：	华南农业大学科技处 _____	（签章）
	Email: kjcgxk@scau.edu.cn	
	电话：020-85283435	
开户单位名称：	华南农业大学	
开户银行名称：	广东广州工行五山支行	
开户银行帐号：	3602002609000310520	
		年 月 日
联系人（课题负责人）姓名：张群宇（签名）		
	Email: zqy@scau.edu.cn	
	电话：02085288395	
		年 月 日

SCAUJIB202518697

检索证明

根据委托人提供的论文材料，委托人华南农业大学生命科学学院 周峰 1 篇论文收录情况如下表。

序号	论文名称	发表刊物及发表的年月卷期/页码等	作者排名	论文等级	作者文中单位	收录情况	影响因子	中科院大类分区
1	Multiscale simulation of elastic modulus of rice stem	BIOSYSTEMS ENGINEERING 出版年：2019 出版日期：NOV 卷期：187 页码：96-113 文献类型：Article	第一作者	A 类	华南农业大学 生命科学学院	SCI	IF2-year=3.215 IF5-year=3.417 (2019)	农林科学 2 区 Top 期刊：否 (2019)

说明：论文等级和中科院大类分区按《华南农业大学学术论文评价方案（试行）》划分。

报告免责声明：如未盖章，报告无效



SCAULIB202518690

检索证明

根据委托人提供的论文材料，委托人华南农业大学生命科学学院 周峰 1 篇论文收录情况如下表。

序号	论文名称	发表刊物及发表的年月卷期/页码等	作者排名	论文等级	作者文中单位	收录情况	影响因子	中科院大类分区
1	A rice mTERF protein V14 sustains photosynthesis establishment and temperature acclimation in early seedling leaves	BMC PLANT BIOLOGY 出版年: 2021 出版日期: SEP 6 卷期: 21 1 页码: - 文献号: 406 文献类型: Article	并列第一作者	A 类	华南农业大学 生命科学学院	SCI	IF2-year=5.26 IF5-year=5.761 (2021)	生物学 2 区 Top 期刊: 否 (2021)

说明: 论文等级和中科院大类分区按《华南农业大学学术论文评价方案(试行)》执行

报告免责声明: 如未盖章, 报告无效



SCAULIB202518691

检索证明

根据委托人提供的论文材料，委托人华南农业大学生命科学学院 周峰 1 篇论文收录情况如下表。

序号	论文名称	发表刊物及发表的年月卷期/页码等	作者排名	论文等级	作者文中单位	收录情况	影响因子	中科院大类分区
1	The ties of brotherhood between japonica and indica rice for regional adaptation	SCIENCE CHINA-LIFE SCIENCES 出版年: 2022 出版日期: JUL 卷期: 65 7 页码: 1369-1379 文献类型: Article	共同第一作者	T2 类	华南农业大学 生命科学学院	SCI	IF2-year=9.1 IF5-year=7.1 (2022)	生物学 1 区 Top 期刊: 是 (2022)

说明: 论文等级和中科院大类分区按《华南农业大学学位论文评价方案(试行)》划分。

报告免责声明: 如未盖章, 报告无效



Available online at www.sciencedirect.com

ScienceDirect

journal homepage: www.elsevier.com/locate/issn/15375110

Research Paper

Multiscale simulation of elastic modulus of rice stem

Feng Zhou^a, Jiale Huang^{b,c,*}, Wangyu Liu^{b,**}, Tao Deng^b, Zhikang Jia^b^a Guangdong Provincial Key Laboratory of Protein Function and Regulation in Agricultural Organisms, College of Life Sciences, South China Agricultural University, Guangzhou, 510642, People's Republic of China^b School of Mechanical and Automotive Engineering, South China University of Technology, Wushan Road, Tianhe District, Guangzhou, 510641, People's Republic of China^c Department of Mechanical and Electrical Engineering, Xiamen University, Xiamen, 361005, People's Republic of China

ARTICLE INFO

Article history:

Received 15 January 2019

Received in revised form

21 August 2019

Accepted 2 September 2019

Published online 18 September 2019

Keywords:

Rice stem

Multiscale simulation

Mechanical properties

Sensitivity analysis

The objective was to obtain a quantitative relationship between the multiscale structural parameters and the elastic modulus of rice stem. Anisotropic elastic properties of rice stem were calculated via multiscale simulation. The elastic constants of the sub-layers of cell wall were calculated by the Halpin-Tsai equations and the rule of mixtures. Cellular structure of stem cross section was reconstructed via a skeletonisation method and used to create the finite element models. The influence of multiscale structural parameters, including the volume fractions of skin and vascular bundle, the cell wall thickness of different types of cells, the volume fraction and stiffness of compound composition, the volume fraction of S2 layer and the microfibril angle (MFA) in the layer, on the overall stiffness of rice stem was determined. Numerical results showed that if the volume fraction and stiffness of each cell wall component are assumed to be constant, increasing the volume fraction of the mechanical tissue layer, thickening the fibre cell wall and decreasing the MFA in S2 layer are the most effective ways to increase the longitudinal tensile modulus of rice stem. Changing the cell wall thickness and the volume fraction of vascular bundle is useful for controlling the tangential modulus. However, more effective is to change the cell wall thickness of parenchyma cell and the volume fraction of the vascular bundle for controlling the radial tensile modulus of rice stem.

© 2019 IAGrE. Published by Elsevier Ltd. All rights reserved.

1. Introduction

In the field of rice breeding, it would be advantageous to predict the plant stability by theoretical or numerical

methods instead of experimental tests. The elastic modulus of rice stem determines the stability of a whole plant (McMahon, 1973). Moreover, the rice straw granules can be used as reinforcing fillers in the polymer composite. In agricultural engineering, knowledge of crop stem stiffness is

* Corresponding author. School of Mechanical and Automotive Engineering, South China University of Technology, Wushan Road, Tianhe District, Guangzhou, 510641, People's Republic of China.

** Corresponding author.

E-mail addresses: scutjlhuang@163.com (J. Huang), scutwyliu@163.com (W. Liu).

<https://doi.org/10.1016/j.biosystemseng.2019.09.003>

1537-5110/© 2019 IAGrE. Published by Elsevier Ltd. All rights reserved.

Nomenclature			
Abbreviations			
CT	Cell wall thickness	$E_{xi}(x_1, x_2, \dots, x_n)$	Partial derivative of the normalised elastic modulus function of rice stem
CTFC	Cell wall thickness of the fibre cell	F_i	Reaction force at the restricted end, N
CTPC	Cell wall thickness of parenchyma cell	G_{12}, G_{13}, G_{23}	Shear moduli of the composite along different directions, Pa
LVB	Large vascular bundle	G_{12}^P	Shear modulus of the P layer, Pa
MC	Moisture content	G_{H12}, G_{H23}	Shear moduli of hemicellulose along longitudinal and transverse directions, Pa
MFA	Microfibril angle	G_{L12}, G_{L23}	Shear moduli of lignin along longitudinal and transverse directions, Pa
MLM	Multilayer model	H-cE	Changes of the elastic modulus of hemicellulose, Pa
MT	Mechanical tissue layer	H-cV	Changes of the volume fraction of hemicellulose, %
RVE	Representative volume element	K_S	Sensitivity coefficient
Sv	Transverse sectional area occupied by vessels and phloem tissue	L-cE	Changes of the elastic modulus of lignin, Pa
SvL	Transverse sectional area occupied by vessels and phloem tissue in large vascular bundle	L-cV	Changes of the volume fraction of lignin, %
SvS	Transverse sectional area occupied by vessels and phloem tissue in small vascular bundle	L_i	Length of rice stem along the loading direction, m
SVB	Small vascular bundle	L_r	Total length of the cell wall in the region, m
VBS	Vascular bundle sheath	$Q_{11}, Q_{12}, Q_{22}, Q_{66}$	Stiffness coefficients of the composite, Pa
VBSL	Vascular bundle sheath in large vascular bundle	S_i	Stem cross-sectional area perpendicular to loading direction, m ²
VBSS	Vascular bundle sheath in small vascular bundle	S_r	Region area, m ²
Symbols		t_1	Average thickness of the double cell wall, m
A, A_f, A_m	Elastic properties of the composite, fibre and matrix in Halpin-Tsai equations, Pa	t_p	Thickness of the P layer, m
C_{c1}, C_{n1}, C_{l1}	Volume fractions of the components in the S1 layers, %	t_{s2}	Thickness of the S2 layer, m
C_{c2}, C_{n2}, C_{l2}	Volume fractions of the components in the S2 layers, %	u_i	Displacement along loading directions, m
C-cE	Changes of the elastic modulus of cellulose, Pa	$v_{12}, v_{21}, v_{13}, v_{23}$	Poisson's ratios of the composite along different directions
C-cV	Changes of the volume fraction of cellulose, %	V_f	Volume fraction of the fibre, %
$C_{ic(i)}, C_{m(i)}, C_{n(i)}$	Volume fractions of the components in the i interlayer, %	v_{f12}	Longitudinal Poisson's ratio of the fibre
E_1, E_2, E_3	Elastic moduli of the composite along different directions, Pa	v_{m12}, v_{m23}	Poisson's ratios of the matrix along longitudinal and transverse directions
E_1^P, E_2^P	Elastic moduli of the P layer along longitudinal and transverse directions, Pa	V_{mH}, V_{mL}	Volume fractions of the hemicellulose and the lignin in the matrix, %
Ecore	Elastic modulus of parenchyma tissue, Pa	VS2	Volume fraction of S2 layer in the cell wall, %
E_{f1}	Longitudinal elastic modulus of the fibre, Pa	Vskin	Volume fraction of skin mechanical tissue layer, %
E_{H1}, E_{H2}	Elastic moduli of hemicellulose along longitudinal and transverse directions, Pa	Vvb	Volume fraction of vascular bundle, %
E_i	Elastic modulus of rice stem, Pa	Greek symbols	
E_{L1}, E_{L2}	Elastic moduli of lignin along longitudinal and transverse directions, Pa	ΔE	Relative change of tensile modulus, Pa
E_{lvb}	Elastic modulus of large vascular bundle, Pa	ΔS	Relative change of variable
E_{m1}, E_{m2}, E_{m3}	Elastic moduli of the matrix along different directions, Pa	Δx_i	The change of each normalised factor
E_{pred}	Predicted elastic modulus of rice stem, Pa	ζ	A measure of reinforcement geometry which depends on loading condition
E_{refe}	Elastic modulus of the referential rice stem, Pa	η	Parameter calculated by the ratio of Elastic properties of fibre and matrix
Eskin	Elastic modulus of mechanical tissue layer, Pa	θ_1, θ_2	Microfibril angles in the S1 and S2 layers, °
Esvb	Elastic modulus of small vascular bundle, Pa	$\theta_i(i)$	Microfibril angle in the i interlayer, °
		ρ_r	Average relative density of the cellular structure of each region, kg m ⁻³

useful for the efficiency improvement and energy conservation of straw choppers and balers (Igathinathane, Womac, & Sokhansanj, 2010; Tumuluru, Tabil, Song, Iroba, & Meda, 2014). Therefore, the accurate prediction of rice stem stiffness is needed.

Similar to other biological materials, a large range of stiffness was found in rice stem (Chuanren, Bochu, Pingqing, Daohong, & Shaoxi, 2004; Huang, Liu, Zhou, & Peng, 2018). The variation is attributed to the wide range of structural parameters at different length scales (Brule, Rafsanjani,

Pasini, & Western, 2016; Gibson, 2012). Rice stem is composed of fibre and parenchyma cells. The cell wall can be regarded as fibre-reinforced composite lamina where the cellulose microfibrils are embedded into the matrix of hemicellulose and lignin. Therefore, the elastic constant of rice stem is affected by the mechanical properties and arrangement of each component, the sequence and thickness of each sub-layer of cell wall and the morphology of the cells. The moisture content also influences the stiffness of living plant due to the fact that the water can lower the rigidity of the cell wall (Wang, Liu, & Lai, 2014b).

To fully understand the mechanical properties of rice stem, it is essential to establish the quantitative relation between the multiscale structural parameters and the elastic modulus of rice stem. Meanwhile, such quantitative relation can also be used to tailor the stiffness of rice stem (Brule et al., 2016). Plant breeders can obtain the suitable anisotropic elastic modulus of the rice stem through exactly controlling the structural parameters at different length scales. However, the length scales of different structural parameters of rice stem range from nanometre to centimetre, leading to the difficulty in theoretical or numerical prediction.

Multiscale modelling is a suitable way to capture the relationship between the multiscale structural parameters and the macro elastic modulus of biological materials. The procedure of the multiscale simulation of plant materials is usually divided into two steps. Firstly, the cross section of the cellular structure should be accurately obtained via Voronoi tessellation (Faisal et al., 2012, 2014; Wang, Liu, Huang, & Ma, 2014a) or image-based reconstruction methods (Astley, Harrington, & Stol, 1997; Huang, Liu, Zhou, & Peng, 2017; Nienga & Béakou, 2011), and then it is used to create the finite element models. Sometimes, the cross section of the plant tissue can even be regarded as periodic polygons to simplify the calculation (Chen, Li, He, & Han, 2015; Magistris & Salmén, 2008; Malek & Gibson, 2017; Qing & Mishnaevsky, 2009). The geometric accuracy of meso-scale finite element model is based on the precision of reconstruction. Secondly, the elastic properties of the cell wall are captured via the theory of composite (Astley et al., 1997; Magistris & Salmén, 2008; Muzamal, Gamstedt, & Rasmuson, 2014; Wang et al., 2014a) or the finite element method (Chen et al., 2015; Malek & Gibson, 2017; Qing & Mishnaevsky, 2009). The calculated elastic properties of cell wall can be served as the input parameters of the meso-scale finite element model. The first step makes a connection between the macro-scale and meso-scale parameters, whilst the second step links the meso-scale and the micro-scale parameters. Once the connections of parameters at different length scales are obtained, the relationship between the multiscale structural parameters and the overall macro elastic modulus can be determined through this method.

This study tries to establish the precise relation between the multiscale structural parameters and the macro elastic modulus of rice stem. Tensile moduli of rice stem along different directions are calculated via numerical simulation. The influences of multiscale structural parameters, including the volume fractions of skin and vascular bundle, the cell wall thickness of different types of cells, the volume fraction and stiffness of compound composition, the volume

fraction of S2 layer and the microfibril angle (MFA) in S2 layer, on the tensile modulus of rice stem are determined and fully discussed.

2. Methods

2.1. Anatomical structures of rice stem

Three different anatomical tissues are distinguished in the rice stem: mechanical tissue layer (MT), small/large vascular bundle (SVB and LVB) and parenchyma tissue, as shown in Fig. 1. The mechanical tissue layer and vascular bundle consist of thick fibre cells, whereas the parenchyma tissue consists of parenchyma cells. According to the density of the fibre cells, the cross section of vascular bundle can also be divided into two different regions: the vascular bundle sheath (VBS) and the transverse sectional area occupied by vessels and phloem tissue (Sv). Moreover, air chambers with irregular shape may exist in the parenchyma tissue, influencing the mechanical properties of rice stem.

2.2. Reconstruction of stem wall

The acquisition of accurate plant tissue microstructure is crucial for numerical simulation. Microstructures of rice stems are not uniform, as shown in Fig. 2b. A large cell area gradient (the transitional regions between different tissues) and concave polygon feature (air chambers) are found in the stem. A skeletonisation method is a suitable way to capture these features (Fig. 2d). Hualiangyou 689 hybrid rice was used as an example in this study. The 3D finite element models were extruded from the framework of rice stem along the longitudinal direction (500 μm). A detailed introduction to the skeletonisation method are referred to in our previous study (Huang et al., 2017).

2.3. Mechanical properties of each sub-layer of cell wall

Two distinct types of cells can be found in the rice stem: the fibre cell and the parenchyma cell. The fibre cell wall is made up of a primary wall (P) and several secondary walls (S1, S2 and S3). Each of the sub-layer of cell wall is considered as the fibre reinforced composite with different orientation arrangements of cellulose microfibrils (Fig. 1g), whereas the parenchyma cell wall only consists of primary wall. Adjacent cells are connected by the middle lamella (M). The primary wall and secondary walls are mainly composed of cellulose, hemicellulose and lignin. The elastic properties of hemicellulose and lignin are decreased as the moisture content (MC) increases (Cousins, 1976, 1978), whilst the elastic properties of cellulose almost remain constant when the moisture content varies. Furthermore, the volume fraction of each component changes with moisture content. Above two factors simultaneously decrease the stiffness of cell wall. Here, we assume that the relative humidity (RH) of the fresh cell wall is around 80%. According to the method proposed by Marklund and Varna (2009), the concentric cylinder model was used to calculate the volume fractions of each component of different sub-layers for fresh cell wall. The mechanical properties and

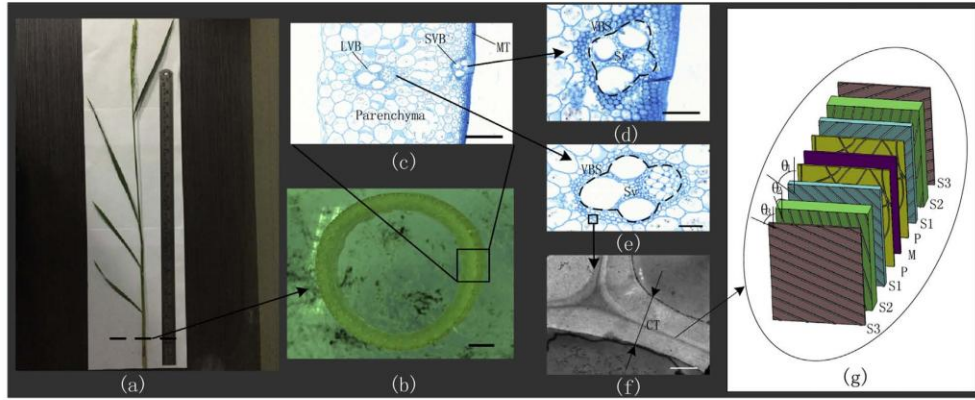


Fig. 1 – Anatomical structures of rice stem (Huang et al., 2018), a whole stem, b stem cross section, c anatomical structure of rice stem wall, d small vascular bundle, e large vascular bundle, f fibre cell wall, g sub-layers of cell wall, LVB large vascular bundle, SVB small vascular bundle, MT mechanical tissue layer, VBS vascular bundle sheath, Sv transverse sectional area occupied by vessels and phloem tissue, CT cell wall thickness (scale bars b = 1 mm, c = 200 μ m, d, e = 50 μ m, f = 1 μ m).

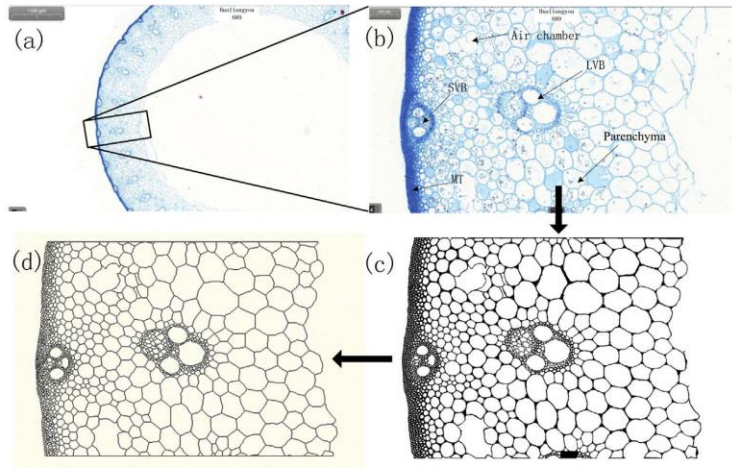


Fig. 2 – Reconstruction of the cross section of rice stem via skeletonisation method, a cross section of stem wall obtained by an optical microscope, b representative volume element (RVE) of stem wall, c binary image of stem wall and d the final DXF file reconstructed by straight lines.

volume fraction of dry and fresh cell wall components are showed in Tables 1 and 2.

The fibre cell wall can be regarded as the cellulose microfibril in a matrix of hemicellulose and lignin. The composite mechanical properties of the matrix were obtained by the rule of mixtures (Magistris & Salmén, 2008; Muzamal et al., 2014) as follows:

$$E_{m1} = \frac{V_{mH}}{V_m} E_{H1} + \frac{V_{mL}}{V_m} E_{L1} \quad (1)$$

$$\frac{1}{E_{m2}} = \frac{V_{mH}}{V_m E_{H2}} + \frac{V_{mL}}{V_m E_{L2}} \quad (2)$$

$$\frac{1}{G_{m12}} = \frac{V_{mH}}{V_m G_{H12}} + \frac{V_{mL}}{V_m G_{L12}} \quad (3)$$

$$\frac{1}{G_{m23}} = \frac{V_{mH}}{V_m G_{H23}} + \frac{V_{mL}}{V_m G_{L23}} \quad (4)$$

$$V_{m12} = \frac{V_{mH}}{V_m} \nu_{H12} \frac{V_{mL}}{V_m} \nu_{L12} \quad (5)$$

$$V_{m23} = \frac{E_{m2} E_{m3}}{G_{23} (E_2 + E_3)} - 1 \quad (6)$$

Table 1 – The mechanical properties of dry and fresh cell wall components (RH = 0% and RH = 80%, respectively) used in the this study, the dry data are obtained from references (Bergander & Salmén, 2002; Cousins, 1976, 1978; Magistris & Salmén, 2008; Marklund & Varna, 2009) and the wet data are calculated by the concentric cylinder model (Marklund & Varna, 2009).

Elastic constant	Cellulose		Hemicellulose		Lignin	
	dry	wet	dry	wet	dry	wet
E_1 (GPa)	134	134	8	1.936	6	3.081
E_2 (GPa)	27.2	27.2	3.4	0.823	6	3.081
G_{12} (GPa)	4.4	4.4	1.2	0.29	2.26	1.158
ν_{12}	0.1	0.1	0.33	0.33	0.33	0.33
ν_{23}	0.5	0.5	0.43	0.43	0.33	0.33

where E_{m1} , E_{m2} , G_{m12} , G_{m23} , ν_{m12} and ν_{m23} are the elastic properties of the matrix. V_{mH} and V_{mL} are the volume fraction of hemicellulose and lignin in the matrix, respectively. E_{H1} and E_{L1} are the longitudinal elastic moduli, E_{H2} and E_{L2} are the transverse elastic moduli, ν_{H12} and ν_{L12} are the Poisson's ratio in the longitudinal direction, G_{H12} and G_{L12} are the longitudinal shear moduli, and G_{H23} and G_{L23} are the transverse shear moduli of the hemicellulose and lignin, respectively. The elastic properties of M layer were directly calculated by the Eqs. (1)–(6).

For the secondary walls (S1, S2 and S3), the longitudinal modulus and Poisson's ratio are calculated as follows:

$$E_1 = E_{f1}V_f + E_{m1}V_m \quad (7)$$

$$\nu_{12} = \nu_{f12}V_f + \nu_{m12}V_m \quad (8)$$

where E_1 and E_{f1} are the longitudinal elastic moduli and ν_{12} and ν_{f12} are the longitudinal Poisson's ratio of the composite and the fibre, respectively. V_f is the volume fraction of the fibre.

The transverse and shear elastic properties of the secondary walls can be obtained by the Halpin-Tsai equations (Halpin & Kardos, 1976) as follows:

$$\frac{A}{A_m} = \frac{1 + \xi \eta V_f}{1 - \eta V_f}, \quad \eta = \frac{A_f/A_m - 1}{A_f/A_m + 1} \quad (9)$$

where A is one of the elastic properties (E_2 , G_{12} and G_{23}) listed in Table 3. A_f and A_m are the corresponding elastic properties

of fibre and matrix. ξ is the parameter influenced by the fibre shape, fibre arrangement and the loading condition. For the fibre which is cylinder shape and square arrangement, the values of ξ are given in Table 3.

The relation between ν_{12} and ν_{21} is shown as follow:

$$\frac{\nu_{12}}{E_1} = \frac{\nu_{21}}{E_2} \quad (10)$$

The in plane Poisson's ratio of the composite is calculated as follows:

$$\nu_{23} = \frac{E_2 E_3}{G_{23}(E_2 + E_3)} - 1 \quad (11)$$

Assuming $E_2 = E_3$, $\nu_{12} = \nu_{13}$ and $G_{12} = G_{13}$, all the elastic constants of the secondary walls can be determined.

Combining the mechanical properties and the volume fraction of the cell wall components (Tables 1 and 2), the total elastic constants of each secondary wall can be obtained via the Halpin-Tsai equations and the rule of mixtures.

AFM pictures indicated that P layer is a long random fibre reinforced composite (Ding, Zhao, & Zeng, 2013). Therefore, the elastic properties of P layer can be calculated as follows:

$$Q_{11} = \frac{E_1}{1 - \nu_{12}\nu_{21}} \quad (12)$$

$$Q_{22} = \frac{E_2}{1 - \nu_{12}\nu_{21}} \quad (13)$$

Table 2 – The volume fraction of dry and fresh cell wall components at different sublayers of cell wall, the dry data are obtained from reference (Bergander & Salmén, 2002) and the wet data are calculated by the concentric cylinder model (Marklund & Varna, 2009).

Sublayers	Cellulose		Hemicellulose		Lignin	
	dry	wet	dry	wet	dry	wet
M (%)	0	0	44	45.7	56	54.3
P (%)	15	13.3	33	35.3	52	51.4
S1 (%)	28	25.2	31	33.8	41	41
S2 (%)	50	46.1	31	34.6	19	19.3
S3 (%)	48	43.9	36	39.9	16	16.2

Table 3 – Parameter of ξ for different elastic constants in Halpin-Tsai equations (Halpin & Kardos, 1976).

Elastic constant	E_2	G_{12}	G_{23}
ξ	2	1	$\{1 + \nu_{m23}\} / \{3 - \nu_{m23} - 4\nu_{m12} \cdot \nu_{m21}\}$ where ν_{m12} , ν_{m21} and ν_{m23} are the Poisson's ratio of the matrix. For the incompressible isotropic matrix materials, $\xi \leq 1$

$$Q_{12} = \frac{E_2 \nu_{12}}{1 - \nu_{12} \nu_{21}} \quad (14)$$

$$Q_{66} = G_{12} \quad (15)$$

$$E_1^P = E_2^P = \frac{1}{8} (3Q_{11} + 3Q_{22} + 2Q_{12} + 4Q_{66}) (1 - \nu_{12} \nu_{21}) \quad (16)$$

$$G_{12}^P = \frac{1}{8} (Q_{11} + Q_{22} - 2Q_{12} + 4Q_{66}) \quad (17)$$

where E_1 , E_2 , ν_{12} , ν_{21} , G_{12} can be obtained from Eqs. (7)–(10). E_1^P , E_2^P and G_{12}^P are the elastic properties of P layer. The final calculating results of each sub-layer of cell wall are shown in Table 4.

2.4. Finite element analysis models of rice stem

According to the anatomic structure and the cell type in the stem cross section, the cross section of 3D finite element analysis models is divided into six regions: the mechanical tissue layer (MT, thick fibre cell), the parenchyma tissue (parenchyma cell), the vascular bundle sheath in small vascular bundle (VBSS, thick fibre cell), the transverse sectional area occupied by vessels and phloem tissue in small vascular bundle (SvS, thin fibre cell), the vascular bundle sheath in large vascular bundle (VBSL, thick fibre cell) and the transverse sectional area occupied by vessels and phloem tissue in large vascular bundle (SvL, thin fibre cell), as shown in Fig. 3. The thicknesses of each sub-layer of fibre cell and parenchyma cell are shown in Table 5.

Table 5 – The thickness and MFA of each sub-layer of cell wall (Huang et al., 2018).

Sub-layer of cell wall	Fibre cell (nm)	Parenchyma cell (nm)	MFA (°) ^b
M	62.47	62.47	–
P	134.16	$0.5 \times (t_1 - 62.47)$	Random
S1	114.83	–	70
S2	$0.5 \times (t_1 - 858.89)^a$	–	17.71
S3	149.22	–	70

^a t_1 is the average thickness of the double cell wall in different regions.

^b Data are obtained from references (Bergander & Salmén, 2002; Huang et al., 2018).

The average thickness of the double cell wall is calculated as follows:

$$t_1 = \rho_r \cdot \frac{S_r}{L_r} \quad (18)$$

where ρ_r is the average relative density of the cellular structure of each region, S_r and L_r are the region area and total length of the cell wall in the region, respectively. S_r and L_r are measured from the DXF file of the reconstructed image (Fig. 2d). ρ_r is obtained from the optical image (Fig. 2b). The thicknesses of S2 layer of fibre cell, P layer of parenchyma cell and the total thickness of cell wall (t_{s2} , t_p and t_1 , respectively) for different regions of Hualiangyou 689 rice are calculated from Eq. (18) and Table 5, as shown in Table 6.

Table 4 – The elastic properties of each sub-layer of cell wall at RH = 80%, data are calculated by using the Eqs. (7)–(17).

Sub-layer	E_1 (GPa)	E_2 (GPa)	E_3 (GPa)	G_{12} (GPa)	G_{13} (GPa)	G_{23} (GPa)	ν_{12}	ν_{13}	ν_{23}
M	2.559	1.368	1.368	0.490	0.490	0.486	0.33	0.33	0.406
P	8.760	8.760	8.760	2.958	2.958	2.958	0.481	0.481	0.481
S1	35.685	2.519	2.519	0.741	0.741	0.723	0.272	0.272	0.742
S2	63.041	3.430	3.430	0.894	0.894	0.868	0.224	0.224	0.976
S3	60.138	3.066	3.066	0.808	0.808	0.778	0.229	0.229	0.970

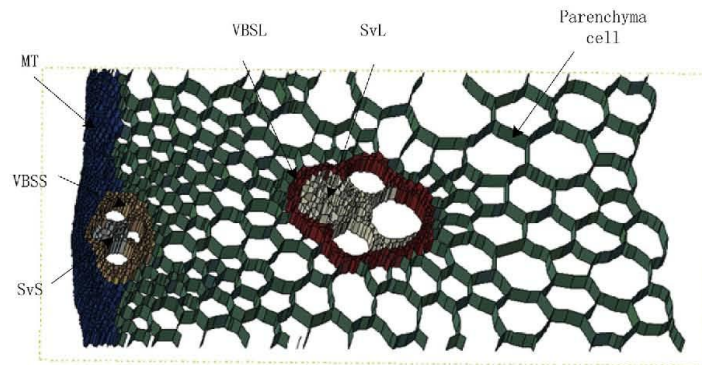


Fig. 3 – Different regions in the cross section of rice stem.

Table 6 – The thicknesses of S2 layer, P layer and the total thickness of cell wall for different regions of Hualiangyou 689 rice, data are calculated by using the Eq. (18) and the data of Table 5.

Region	MT	VBSS	SvS	VBSL	SvL	Parenchyma cell
t_1 (μm)	3.795	2.699	1.386	2.196	1.386	1.292
t_{s2} (μm)	1.468	0.92	0.264	0.669	0.264	—
t_p (μm)	—	—	—	—	—	0.615

2.5. Load cases and boundary conditions

To calculate the macro elastic constants of the rice stem, the 3D finite element model is restricted at one end, while a displacement (u_i) is applied to the other end. The elastic modulus of the rice stem is calculated as follows:

$$E_i = \frac{F_i L_i}{S_i u_i} \quad (19)$$

where F_i is the reaction force at the restricted end, L_i is the length of the rice stem along the loading direction, and S_i is the stem cross-sectional area perpendicular to loading direction. In this study, the unit strains along different directions ($u_i = L_i$) are applied to the model to calculate the elastic modulus.

2.6. Convergence analyses

The S4R elements in Abaqus/CAE 6.14-1 were used in this study. Convergence analyses were carried out to guarantee the accuracy the results, as shown in Fig. 4. The plot shows that when the global mesh seed size decreases from 0.04 mm to 0.005 mm, the total mesh number increases around 55%, however, the calculated tensile modulus is almost the same, indicating that the simulated results are independent of the mesh size. Considering the accuracy and the calculation time, the global mesh seed size is set as 0.01 mm in this study.

2.7. Prediction of elastic properties of different species of rice stem based on the total differential equation

The sensitivity coefficient K_s is calculated as follows:

$$K_s = \frac{\Delta E}{\Delta S} \quad (20)$$

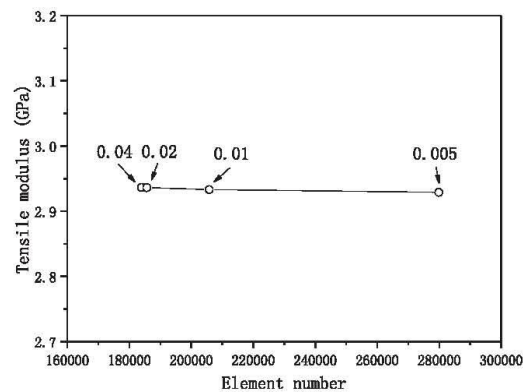


Fig. 4 – The relationship among the total mesh seed size, the mesh number and the final calculation results.

where ΔE (%) is the relative change of tensile modulus when the variable changes ΔS (%).

The sensitivity coefficients can be used to approximately predict the anisotropic elastic properties of different species of rice stem based on the total differential equation as follows.

$$\Delta E = E_{x1}(x1, x2, \dots, xn)\Delta x1 + E_{x2}(x1, x2, \dots, xn)\Delta x2 + \dots + E_{xn}(x1, x2, \dots, xn)\Delta xn \quad (21)$$

where ΔE is the complete increment of the normalised elastic modulus, $E_{xi}(x1, x2, \dots, xn)$ and Δxi ($i = 1, 2, \dots, n$) are the partial derivative of the normalised elastic modulus function of rice stem and the change of each normalised factor, respectively. $E_{xi}(x1, x2, \dots, xn)$ can be approximately evaluated by the Eq. (20). Then, the predicted elastic properties of rice stem E_{pred} can be obtained as follows:

$$E_{pred} = E_{refe} \cdot (1 + \Delta E) \quad (22)$$

where E_{refe} is the elastic modulus of the referential rice stem.

3. Results and discussions

3.1. Modelling result and comparisons with experiments

The numerical result calculated by the aforementioned multilayer model (MLM) is shown in Fig. 5. The simulated longitudinal tensile modulus is 3.16 GPa, which is in accordance with the experiment (2.87 GPa). Therefore, the multilayer model is suitable for predicating the elastic modulus of rice stem. However, the finite element analysis (FEA) result is still 10.1% higher than the experiment. Previous literatures

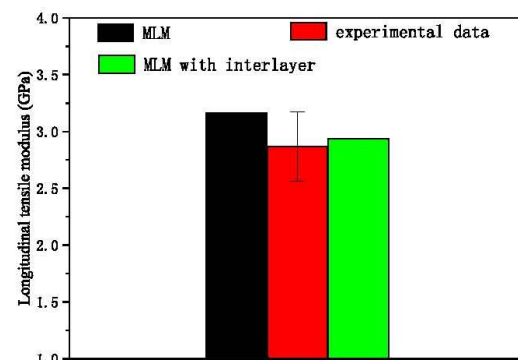
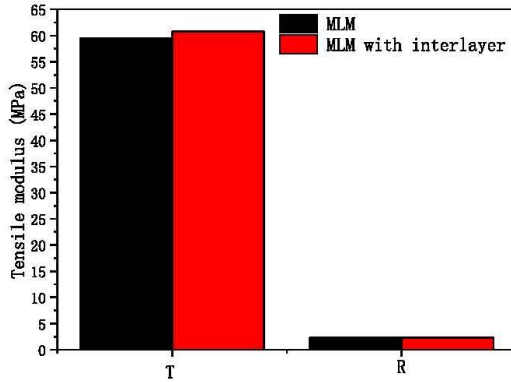
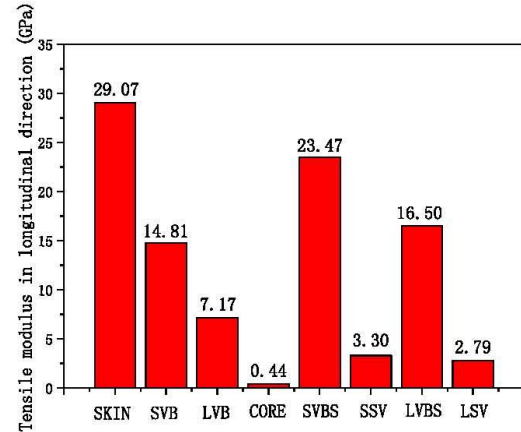


Fig. 5 – Numerical and experimental results of the longitudinal tensile modulus of rice stem. Experimental data are extracted from reference (Huang et al., 2018).

Table 7 – Elastic properties and MFA of each sub-layer of the interlayer at RH = 80% (the INT-01 and the S2 layers are adjacent).

Interlayer	E ₁ (GPa)	E ₂ (GPa)	E ₃ (GPa)	G ₁₂ (GPa)	G ₁₃ (GPa)	G ₂₃ (GPa)	ν_{12}	ν_{13}	ν_{23}	MFA (°)
INT-01	62.761	3.42	3.42	0.892	0.892	0.866	0.224	0.224	0.973	18.23
INT-02	60.524	3.338	3.338	0.879	0.879	0.853	0.228	0.228	0.956	22.42
INT-03	56.075	3.18	3.18	0.852	0.852	0.828	0.236	0.236	0.920	30.78
INT-04	49.467	2.955	2.955	0.814	0.814	0.792	0.248	0.248	0.865	43.33
INT-05	40.779	2.675	2.675	0.767	0.767	0.748	0.263	0.263	0.789	60.06

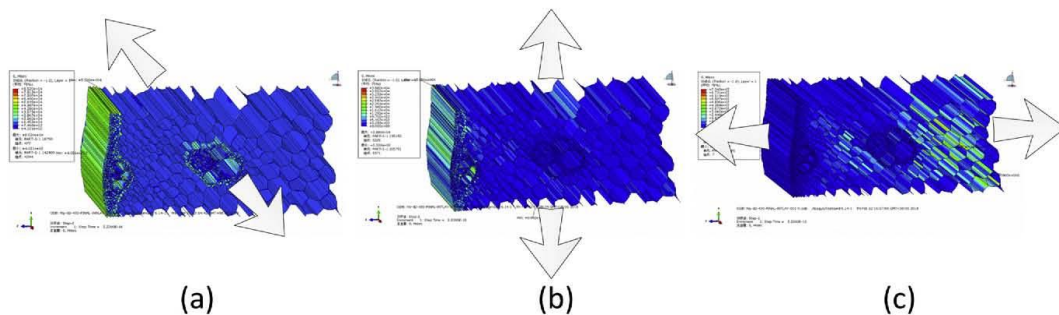
**Fig. 6 – Numerical results of tangential (T) and radial (R) tensile moduli of rice stem.****Fig. 8 – Longitudinal tensile modulus of each elementary tissue.**

showed that the simulation of the fibre cell wall stiffness calculated by the MLM is higher than the experiment (Bergander & Salmén, 2002), which may be attributed to the inaccurate division of the S1 and S2 layers. Our previous studies found that the prediction accuracy of the fibre cell wall will increase significantly if a gradual transition zone (interlayer) is introduced into the cell wall between the S1 and S2 layers during the fibre cell wall modelling (Wang, Liu, & Peng, 2013). Since the accurate thickness of the interlayer cannot be observed by the experiment, here, it is assumed that the thickness ratio of the interlayer to the total thickness of the S1 and S2 layers is equal to the optimised configuration result (around 28.6%) in the reference (Wang et al., 2013). In order to

simulate the gradual transition properties of the interlayer in ABAQUS, the interlayer is discretised into 5 sub-layers with the same thickness. The gradual transitions of the mechanical properties and MFA of the interlayer are described by the quadratic function as follows.

$$\theta_i = \theta_1(i) = (\theta_1 - \theta_2) \cdot \left(\frac{2i-1}{10}\right)^2 + \theta_2 \quad (23)$$

$$C_{ic} = C_{ic}(i) = (C_{c1} - C_{c2}) \cdot \left(\frac{2i-1}{10}\right)^2 + C_{c2} \quad (24)$$

**Fig. 7 – The stress contour of rice stem at different tensile directions, a longitudinal b tangential and c radial tensile directions.**

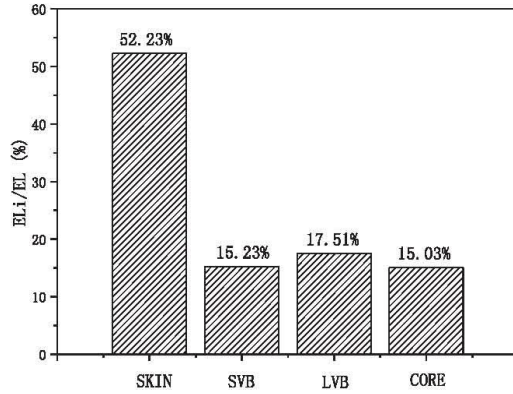


Fig. 9 – Contribution of each elementary tissue to the overall macro elastic modulus of rice stem.

$$C_{ih} = C_{ih}(i) = (C_{h1} - C_{h2}) \cdot \left(\frac{2i-1}{10}\right)^2 + C_{h2} \quad (25)$$

$$C_{ii} = C_{ii}(i) = (C_{i1} - C_{i2}) \cdot \left(\frac{2i-1}{10}\right)^2 + C_{i2} \quad (26)$$

where $\theta_i(i)$, $C_{ic}(i)$, $C_{ih}(i)$ and $C_{ii}(i)$ are the MFA and volume fractions of the components in the i interlayer. θ_1 , C_{c1} , C_{h1} , C_{i1}

and θ_2 , C_{c2} , C_{h2} , C_{i2} are the MFA and volume fractions of the components in the S1 and S2 layers, respectively. Detailed properties of each sub-layer are shown in Table 7.

Since the thicknesses of the S1 and S2 layers of the thin fibre cell is small, which has a small influence on the final results of the simulation, we only consider the interlayer in the thick fibre cell (including the fibre cells in MT, VBSS and VBSL). The calculated result is also shown in Fig. 5. The plot shows that the calculated value of the multilayer model with interlayer (MLM with interlayer) is 2.93 GPa, which is only slightly higher than the experiment (2.87 GPa), indicating that the input parameters of the cell wall and the multilayer model with interlayer are reasonable for the multiscale modeling of rice stem. Therefore, the following calculations are all based on this model.

Figure 6 shows the transverse and radial tensile moduli simulated by the models of MLM and the MLM with interlayer. Due to the fact that the transverse and radial dimensions of the rice stem are small, the results cannot be validated by the experiment. Thus, for the transverse and radial tensile moduli, only the numerical results are discussed. Figure 6 shows that the transverse tensile modulus (T) slightly increases from 59.59 MPa to 60.79 MPa when considering the interlayer in the thick fibre cell wall. However, the radial tensile modulus (R) almost keeps constant (only increases from 2.317 MPa to 2.319 MPa).

The stress contours of rice stem at different tensile directions are shown in Fig. 7. The plot shows that the stress

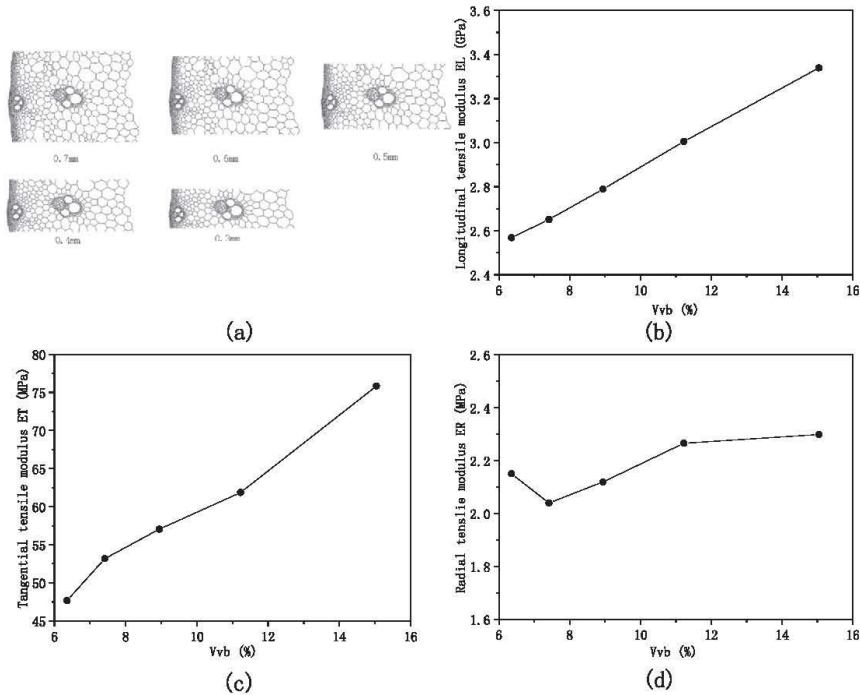


Fig. 10 – Effect of the volume fraction of vascular bundle (Vvb) on the stiffness of rice stem.

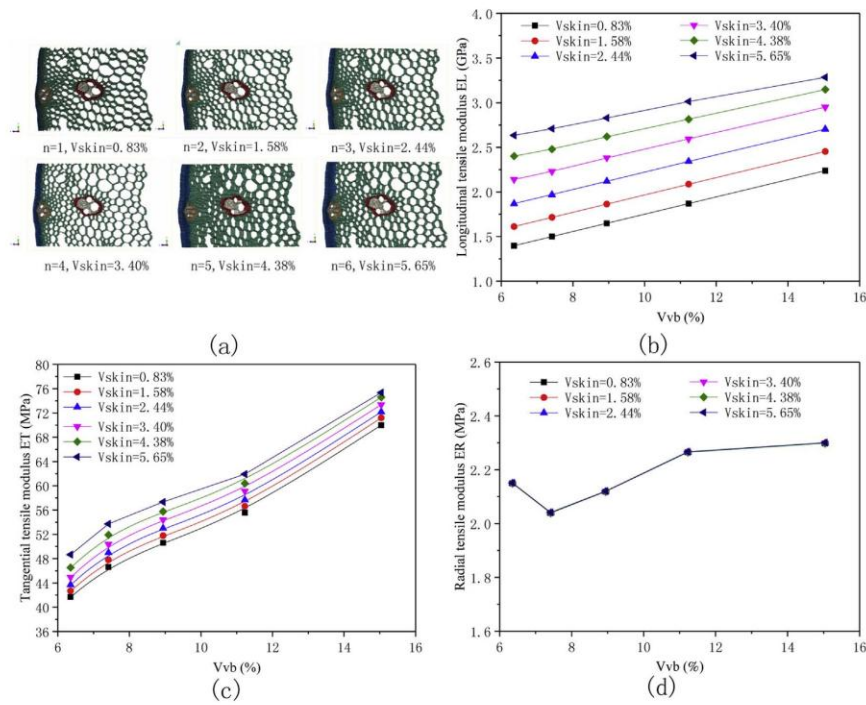


Fig. 11 – Combined effect of the volume fractions of skin mechanical tissue layer and vascular bundle (Vskin and Vvb) on the stiffness of rice stem.

concentrates in the regions of the MT, SVB and LVB during the longitudinal stretch, indicating that the mechanical tissue layer and vascular bundles are the main supporting tissues during growth. For the tangential stretch, the high stress locates at the MT and the SVB. However, for the radial stretch, the stress concentrates at the parenchyma cell, indicating the maximum influence of the parenchyma cell on the radial tensile modulus. These results also explain the phenomenon that the longitudinal tensile modulus increases significantly while the radial tensile modulus almost keeps constant when considering the interlayer of the cell wall.

3.2. Elastic modulus of different tissues in rice stem

As aforementioned description, rice stem is composed of MT, SVB, LVB and parenchyma tissue. Therefore, the elastic properties and the volume fraction of the elementary tissues determine the total mechanical properties of rice stem. Due to the small size of the rice stem, it is difficult to separate and test the properties of each elementary tissue. However, based on the multiscale simulation, this problem can be easily solved. From Fig. 8, it can be observed that the rank order of the elastic modulus is $E_{skin} > E_{svb} > E_{lvb} > E_{core}$ for the elementary tissues. The stiffness of the MT, SVB and LVB ranges from 7 GPa to 30 GPa, which is much higher than that of the parenchyma tissue (E_{core} , 0.44 GPa), suggesting that these tissues are important for the stiffness of rice stem. Combining

the elastic properties and the position of elementary tissues in the stem cross section, we can find that the stiffness of the elementary tissue presents a decreased gradient distribution from the skin to the core. Moreover, this gradient distribution also appears in the cross section of vascular bundle (Fig. 8). As a consequence, the macro elastic properties of rice stem present high anisotropy.

The contribution of each elementary tissue to the overall macro elastic modulus of rice stem is shown in Fig. 9. The plot shows that the MT contributes 52.23% to the overall stiffness of rice stem, but its volume fraction only occupies 5.12% in the stem. The SVB and LVB contribute 32.74% to the overall stiffness and their volume fractions occupy 10.44%, whereas the volume fraction of parenchyma tissue occupies 84.44% in rice stem, but it only contributes 15.03% to the overall stiffness. Thus, it can be inferred that compared to the SVB and LVB, MT is more important for the stiffness of rice stem, and the parenchyma tissue exerts the least influence on the longitudinal tensile modulus, which is in accordance with our previous study (Huang et al., 2018).

3.3. Effects of mesoscale parameters (tissue level) on the overall macro elastic modulus of the rice stem

In order to determine the effect of the volume fraction of vascular bundle (Vvb) on the mechanical properties of rice stem, we adjust the volume fraction of the vascular bundle by

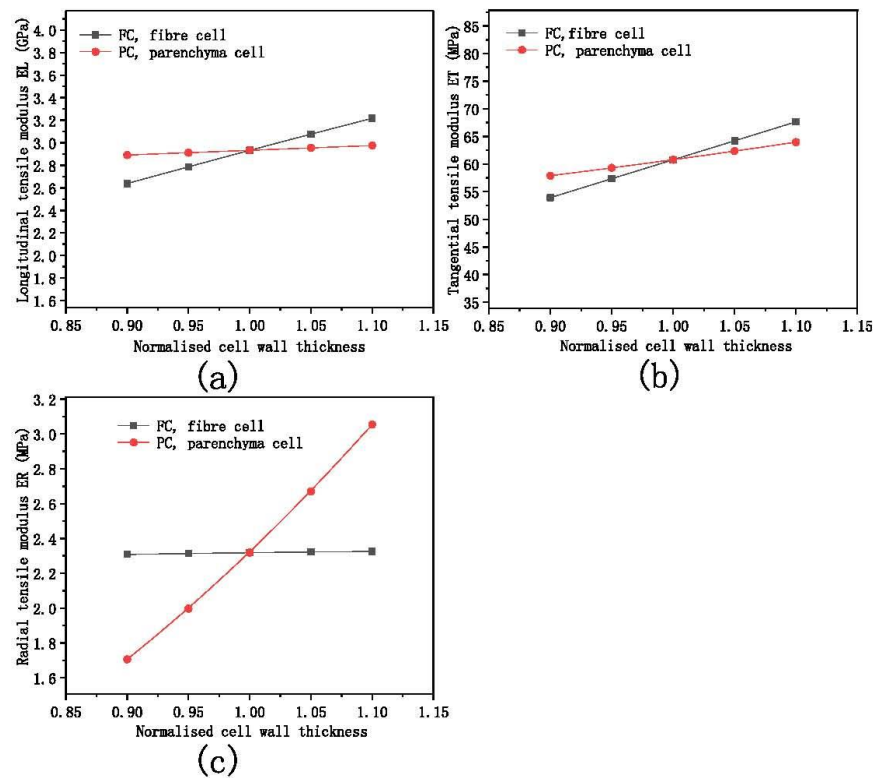


Fig. 12 – Relation between the tensile moduli of rice stem and normalised cell wall thickness of different types of cells.

changing the width of the finite element model, as shown in Fig. 10. The plot shows that the longitudinal and tangential tensile moduli increase with the increase of the fibre volume fraction, whereas the radial tensile modulus changes irregularly. When the volume fraction of the vascular bundle increases from 6.36% to 15.04%, the longitudinal tensile modulus increases around 30%, whereas the tangential tensile modulus increases around 59.1%, indicating that the volume fraction of vascular bundle exerts a greater influence on the tangential tensile modulus.

In addition to the Vvb, the volume fraction of MT also influences the tensile modulus of rice stem at tissue level. We change the quantity of the skin fibre cell layers ($n = 1-6$) to control the volume fraction of MT (Fig. 11a). The combined effect of the volume fractions of MT, SVB and LVB on the mechanical properties of rice stem is shown in Fig. 11. The plot shows that similar to the fibre volume fraction, the longitudinal and tangential tensile moduli increase with the increase of the volume fraction of MT. Taking the fibre volume fraction of 8.94% as an example, when the volume fraction of MT increases from 0.83% to 5.65%, the longitudinal tensile modulus increases around 71.5%, whereas the tangential tensile modulus only increases around 13.3%. Therefore, the volume fraction of MT exerts a greater influence on the longitudinal tensile modulus. Moreover, when the fibre volume

fraction is fixed, the increased values of the tensile moduli are almost the same. This phenomenon may be attributed to the weak mutual influences between the mechanical tissue layer and vascular bundle on the tensile moduli of rice stem.

3.4. Effects of microscale parameters on the overall macro elastic modulus of the rice stem

In addition to the volume fraction of different tissues at meso-scale, the microscale structural parameters, including the cell wall thickness, the volume fraction and stiffness of compound composition, the volume fraction of S2 layer and the MFA in S2 layer, directly dominate the mechanical properties of tissue, and therefore influencing the macro stiffness of the rice stem.

The tissues of rice stem are mainly composed of fibre cell and parenchyma cell. Effect of normalised cell wall thickness on the tensile modulus of rice stem is shown in Fig. 12. It can be seen that the longitudinal and tangential tensile moduli increase with the increase of cell wall thickness of fibre cell, whereas the radial tensile modulus almost keeps constant. The plot also shows that increasing the cell wall thickness of parenchyma cell can significantly increase the radial modulus and slightly increase the tangential modulus of rice stem. However, the longitudinal modulus is independent of the cell

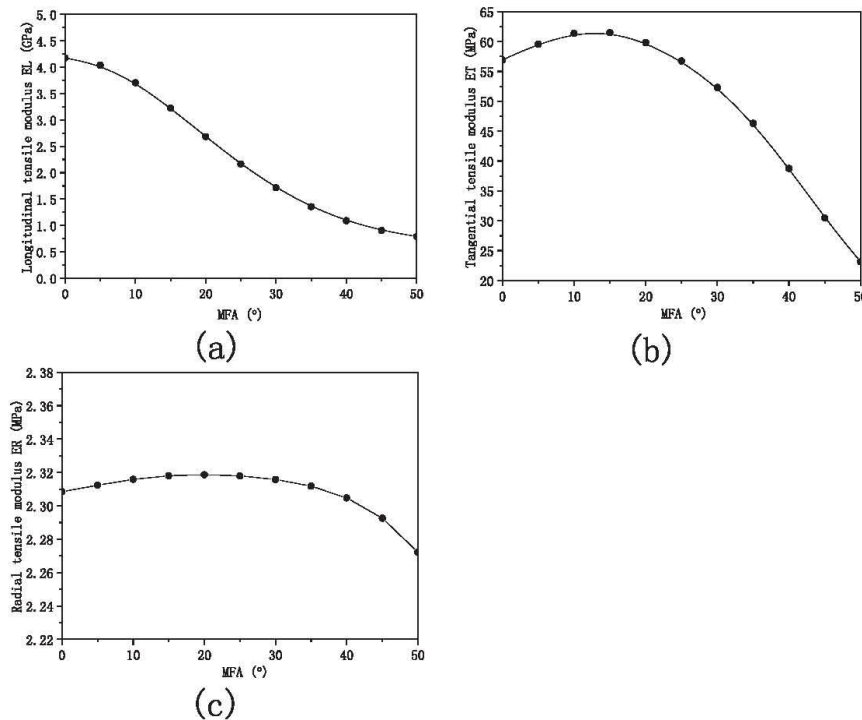


Fig. 13 – Effect of the MFA in S2 layer on the tensile moduli of rice stem.

wall thickness of parenchyma cell. Therefore, the fibre cell dominates the longitudinal modulus and the parenchyma cell determines the radial modulus of rice stem, whereas the fibre cell and parenchyma cell simultaneously affect the overall tangential modulus. Compared to the parenchyma cell, fibre cell exerts a greater influence on the tangential modulus of rice stem.

Effect of the MFA in S2 layer on the mechanical properties of rice stem is shown in Fig. 13. Similar to the wood materials, the longitudinal tensile modulus decreases as the MFA increases. However, the tangential and radial tensile moduli increase initially then decrease rapidly beyond the point of 20°. Due to the fact that the radial tensile modulus spans from 2.271 MPa–2.319 MPa when the MFA changes, the effect of MFA in S2 layer on the radial tensile modulus can be neglected.

The relative thickness of the S2 layer influences the modulus of the fibre cell wall. In order to quantitatively study the effect of relative thickness of the S2 layer on the mechanical properties of rice stem, we assumed that the thicknesses of M and P layers and the total thickness of the cell wall keep constant, and the thicknesses of S1 and S3 layers vary with the change of the thickness of S2 layer. Meanwhile, the thickness ratio of S1 to S3 keeps constant. The numerical results are shown in Fig. 14. Since the S2 layer of the

fibre cell is the main supporting structures of rice stem under the longitudinal and tangential tension, the longitudinal and tangential tensile moduli increase with the increase of relative volume fraction of S2 layer in the fibre cell wall. The radial tensile modulus is determined by the mechanical properties of parenchyma tissue. Therefore, it is independent of the relative volume fraction of S2 layer in the fibre cell wall.

As the fundamental elements of the cell wall, the mechanical properties and the relative content of each component are closely correlated to the stiffness of the rice stem. Figure 15 shows that the elastic properties of cellulose has a greater influence on the longitudinal and radial tensile moduli of rice stem, and the stiffness change of lignin has pronounced effect on the tangential tensile modulus. However, the effect of stiffness variation of lignin on the mechanical properties of rice stem can be neglected. The relation between the overall tensile modulus of rice stem and the normalised change of volume fraction of each component is shown in Fig. 16. Since plant cellulose always has the greatest influence on the mechanical properties of cell wall, increasing the volume fraction of cellulose can directly increase the stiffness of rice stem at all directions. The decrease of the volume fractions of hemicellulose and lignin is equivalent to increase the volume fraction of cellulose, leading to the increase of stiffness of rice stem.

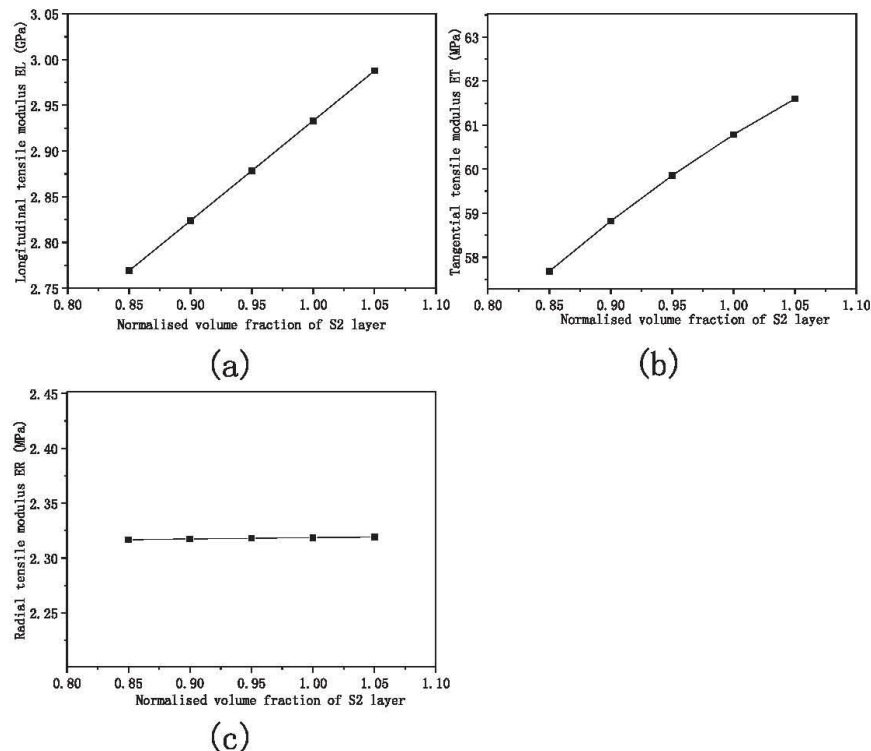


Fig. 14 – Effect of the relative thickness of S2 layer on the mechanical properties of rice stem.

3.5. Sensitivity analysis of multiscale structural parameters on the stiffness of rice stem

The effects of normalised multiscale structural parameters on the mechanical properties of rice stem are shown in Fig. 17. From the slopes of the lines, one can obtain the relative influenced degree of each factor on the stiffness of rice stem.

In addition to the normalization of each factor, we also used the sensitivity analysis to reflect the influenced degree of the multiscale structural parameters on the overall stiffness. The sensitivity coefficient K_s is calculated by Eq. (20). Since the responses of tensile modulus to different factors are not always linear, the value of K_s may change as the value of ΔS varies. However, it can be still used directly to describe the influenced degree of each factor. Assuming the value of ΔS is -10% , the sensitivity coefficient of each factor is shown in Table 8 based on the data of Fig. 17.

Generally, large absolute value of sensitivity coefficient reflects the high sensitivity of tensile modulus to the factor. The longitudinal tensile modulus is highly sensitive to the cell wall thickness of fibre cell (CTFC) and the volume fraction and stiffness variation of cellulose (C-cV and C-cE). The less important factors are the MFA, the volume fraction of hemicellulose (H-cV) and the volume fraction of skin mechanical tissue layer (Vskin). Other factors have minor effect on the longitudinal stiffness of rice stem, especially for the stiffness

variations of hemicellulose and lignin (H-cE and L-cE). For the tangential tensile modulus, the cell wall thickness of fibre cell (CTFC), the volume fractions of cellulose and hemicellulose (C-cV and H-cV) and the stiffness variation of hemicellulose (H-cE) are the most sensitive factors. The less important factors are the cell wall thickness of parenchyma cell (CTPC) and the volume fractions of vascular bundle (Vvb). The effects of other factors on the tangential tensile modulus can be neglected. The cell wall thickness of parenchyma cell (CTPC) exerts the greatest influence on the radial tensile modulus. The less important factors are the volume fraction and stiffness variation of cellulose (C-cV and C-cE) and the volume fractions of vascular bundle, hemicellulose and lignin (Vvb, H-cV and L-cV). The contributions of other factors to the radial tensile modulus can be neglected. Therefore, the influenced degree of multiscale structural parameters on the macro stiffness of rice stem can be directly compared through Table 8.

Since the lodging resistance of rice stem is closely correlated to its elastic properties, it is crucial to control the stem stiffness for the breeding of rice cultivar with high ability of lodging resistance. Some of these structural parameters, such as the stiffness and volume fraction of each component in cell wall, may be the intrinsic properties, which are difficult to change. However, the MFA in S2 layer, the cell wall thickness and the volume fractions of mechanical tissue layer and

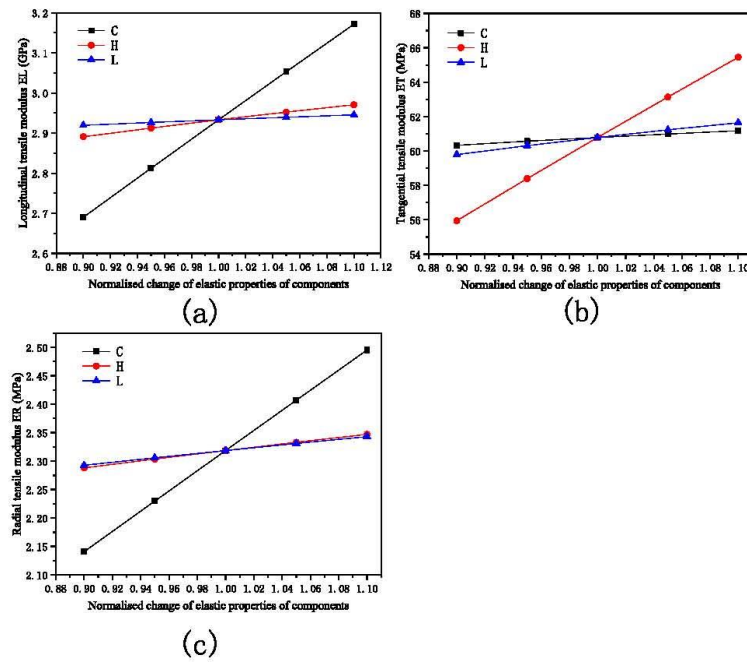


Fig. 15 – Relation between the tensile modulus of rice stem and normalised elastic properties of each component, C: cellulose, H: hemicellulose and L: lignin.

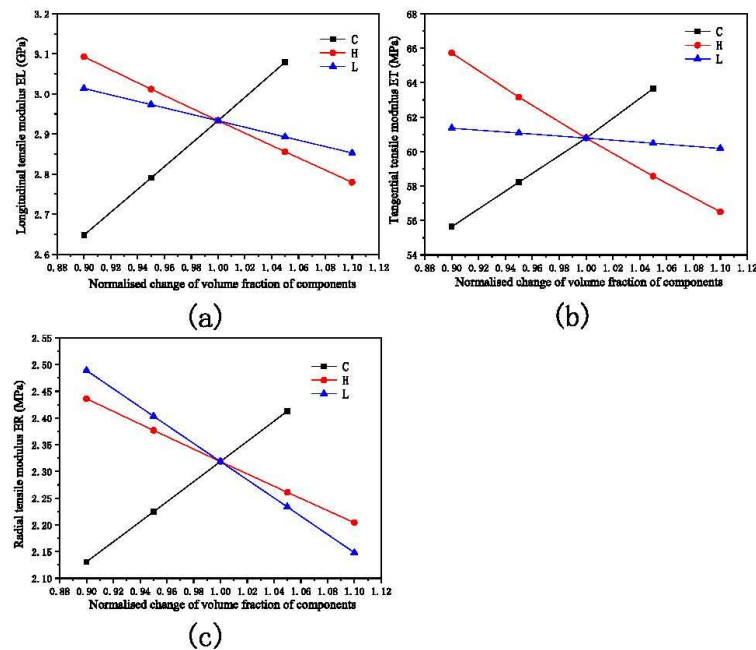


Fig. 16 – Relation between the tensile modulus of rice stem and the normalised change of volume fraction of each component, C: cellulose, H: hemicellulose and L: lignin.

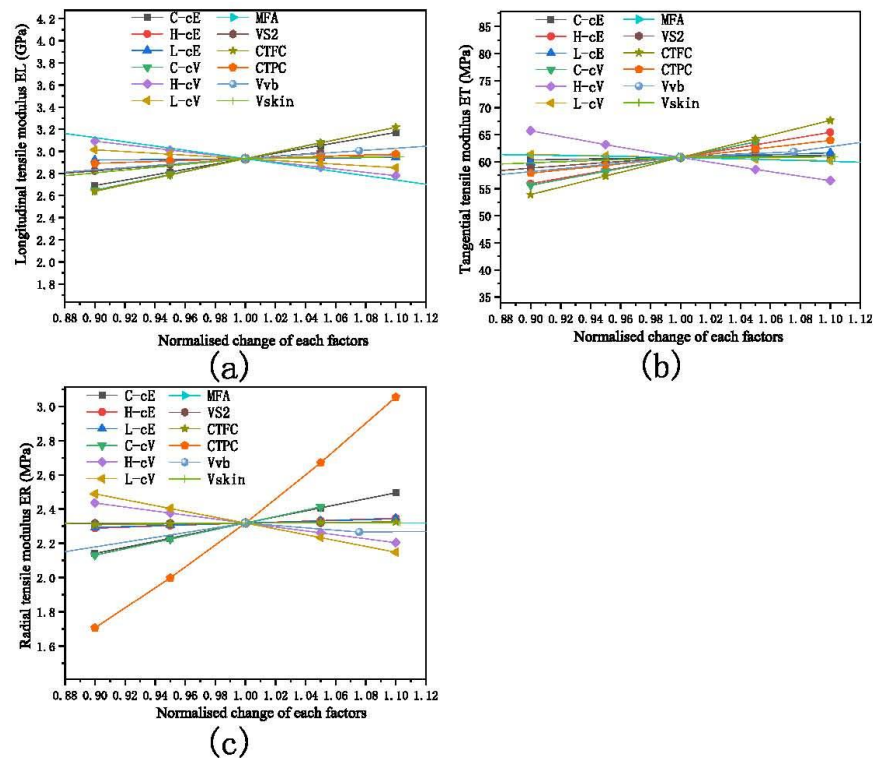


Fig. 17 – Effects of normalised multiscale structural parameters on the mechanical properties of rice stem, MFA microfibril angle, VS2 volume fraction of S2 layer in the cell wall, CTFC cell wall thickness of the fibre cell, CTPC cell wall thickness of parenchyma cell, Vvb volume fraction of vascular bundle, Vskin volume fraction of skin mechanical tissue layer, C-cE, H-cE and L-cE change of the elastic moduli of each component, C-cV, H-cV and L-cV change of the volume fraction of each component.

Table 8 – Sensitivity coefficients of multiscale structural parameters, data are calculated by using the Eq. (20).

Length scale	Factor	Sensitivity coefficient		
		L	T	R
Tissue level	Vskin	0.437261	0.166797	0.001286
Micro level	Vvb	0.343531	0.430743	0.600101
	CTFC	1.00552	1.129889	0.043433
Ultrastructural level	CTPC	0.14442	0.477084	2.643011
	VS2	0.372881	0.3236	0.005176
	MFA	−0.64847	−0.07431	0.00155
	C-cV	0.971904	0.84588	0.810082
	H-cV	−0.54256	−0.81215	−0.50657
	L-cV	−0.27391	−0.0932	−0.73508
	C-cE	0.828949	0.074694	0.767124
	H-cE	0.143875	0.796193	0.130945
	L-cE	0.046197	0.163901	0.111622

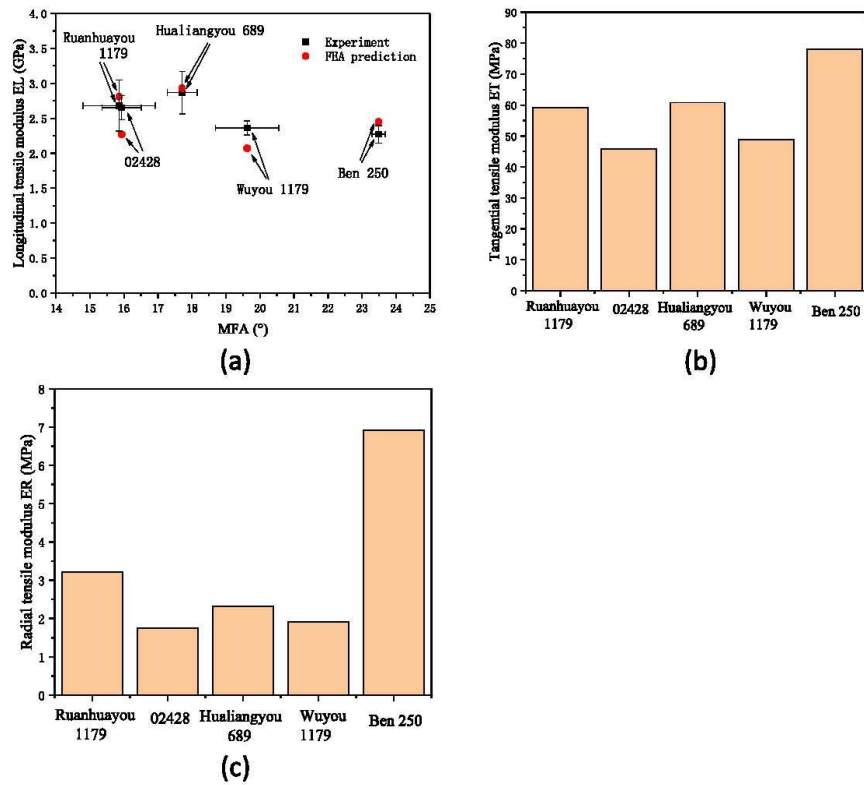
vascular bundle may be adjusted through changing the growth rate (Herman, Dutilleul, & Avella-Shaw, 1999), the water and fertiliser conditions (Zhang et al., 2016a, 2016b), using the phytohormones (Okuno et al., 2014; Rani Sinniah,

Wahyuni, Syahputra, & Gantait, 2012) or controlling the related gene (Li, 2003; Ookawa et al., 2014). Increasing the volume fraction of the mechanical tissue layer, thickening the fibre cell wall and decreasing the MFA in S2 layer are the most effective way to increase the longitudinal tensile modulus of rice stem. For controlling the tangential modulus, changing the cell wall thickness and the volume fraction of vascular bundle is useful. However, it is more practical to change the cell wall thickness of parenchyma cell and the volume fraction of vascular bundle for controlling the radial tensile modulus of rice stem.

In the field of plant breeding, plant breeders can regulate the cell wall components, cell wall thickness or other traits through gene mutation (Fan et al., 2017, 2018; Li et al., 2017). However, the existing gene regulation is still a qualitative method, lacking of quantitative prediction. We establish the precise relation between the multiscale structural parameters and the macro elastic modulus of rice stem in this paper. This relationship is useful for guiding the selection of mutants which can custom-tailor the mechanical properties of plant stem. For example, according to the sensitivity coefficients in Table 8, if we want to enhance the radial tensile modulus of

Table 9 – The change of some normalised factors of different rice stems, data are calculated from the reference (Huang et al., 2018).

	Ruanhuayou1179	02428	Hualiangyou689	Wuyou1179	Ben250
Vskin	−0.08715	−0.24077	0	−0.19202	−0.03397
VF	−0.07254	−0.34404	0	−0.29948	−0.12539
MFA	−0.10446	−0.10051	0	0.10785	0.32637
VS2	−0.13586	−0.15665	0	−0.1205	−0.03198
CTFC	−0.01895	−0.00669	0	0.00746	0.00423
CTPC	0.1651	−0.01299	0	0.00329	0.77952

**Fig. 18** – Tensile modulus of different kinds of rice stem, experimental data are obtained from reference (Huang et al., 2018).

rice stem, we should select the gene mutants which can increase the cell wall thickness of parenchyma cell or increase the volume fraction of vascular bundle (assuming the volume fraction and stiffness of each cell wall component keep constant). It is the first step to establish the quantitative relationship between the parameters and performance. In the future, it is necessary to combine with the existing gene regulation results in order to achieve the accurate regulation.

Moreover, these sensitivity coefficients also can be used to approximately predict the anisotropic elastic properties of different species of rice stem. Taking Hualiangyou 689 as the referential rice stem, the elastic properties of four different kinds of rice stems, including Ruanhuayou 1179 (hybrid rice), 02428 (japonica rice), Wuyou 1179 (hybrid rice) and Ben 250

(indica type rice), were calculated according to the Eqs. (21) and (22). The change of some normalised factors of these rice stems (Δx_i) is shown in Table 9. The final calculating results based on Tables 8 and 9 are showed in Fig. 18. The plot shows that the predictions are in close agreement with the experiments (Fig. 18a). In addition, the tangential and radial tensile moduli of rice stems can be easily and fast determined by using the Eqs. (21) and (22), as shown in Fig. 18b and Fig. 18c.

4. Conclusions

In this work, the mechanical properties of rice stem are calculated via numerical multiscale simulation. The elastic

constants of the sub-layers of cell wall were calculated by the Halpin-Tsai equations and the rule of mixtures. Cellular structure of stem cross section was reconstructed via skeletonisation method and used to create the finite element models. The predicted longitudinal tensile modulus is in good agreement with the experiment. Effects of multiscale structural parameters, including the volume fractions of mechanical tissue layer and vascular bundle, the stiffness and volume fractions of each component, MFA, cell wall thickness and the volume fraction of S2 layer in the cell wall, on the overall macro stiffness of rice stem are investigated. If we assume the volume fraction and stiffness of each cell wall component keep constant, the sensitivity analysis results show that increasing the volume fraction of the mechanical tissue layer, thickening the fibre cell wall and decreasing the MFA in S2 layer are the most effective way to increase the longitudinal tensile modulus of rice stem. Changing the cell wall thickness and the volume fraction of vascular bundle is useful for controlling the tangential modulus. However, it is more practical to change the cell wall thickness of parenchyma cell and the volume fraction of vascular bundle for controlling the radial tensile modulus of rice stem. The results of sensitivity analysis also can be used to approximately predict the anisotropic elastic properties of different species of rice stem. These results can be used in guiding the stiffness tailoring of rice stem.

Acknowledgement

The authors gratefully acknowledge the financial support from the National Natural Science Foundation of China (No. 11572128) and the China Postdoctoral Science Foundation (No. 2019TQ0180).

REFERENCES

- Astley, R. J., Harrington, J. J., & Stol, K. A. (1997). Mechanical modelling of wood microstructure, an engineering approach. *IPENZ Transactions*, 24, 21–29.
- Bergander, A., & Salmén, L. (2002). Cell wall properties and their effects on the mechanical properties of fibers. *Journal of Materials Science*, 151–156.
- Brule, V., Rafsanjani, A., Pasini, D., & Western, T. L. (2016). Hierarchies of plant stiffness. *Plant Science International Journal of Experimental Plant Biology*, 250, 79–96.
- Chen, L., Li, A., He, X., & Han, L. (2015). A multi-scale biomechanical model based on the physiological structure and lignocellulose components of wheat straw. *Carbohydrate Polymers*, 133, 135–143.
- Chuanren, D., Bochu, W., Pingqing, W., Daohong, W., & Shaoli, C. (2004). Relationship between the minute structure and the lodging resistance of rice stems. *Colloids and Surfaces B Biointerfaces*, 35, 155–158.
- Cousins, W. J. (1976). Elastic modulus of lignin as related to moisture content. *Wood Science and Technology*, 10, 9–17.
- Cousins, W. J. (1978). Young's modulus of hemicellulose as related to moisture content. *Wood Science and Technology*, 12, 161–167.
- Ding, S.-Y., Zhao, S., & Zeng, Y. (2013). Size, shape, and arrangement of native cellulose fibrils in maize cell walls. *Cellulose*, 21, 863–871.
- Faisal, T. R., Hristozov, N., Rey, A. D., Western, T. L., & Pasini, D. (2012). Experimental determination of *Philodendron melinonii* and *Arabidopsis thaliana* tissue microstructure and geometric modeling via finite-edge centroidal Voronoi tessellation. *Physical Review E Statistical Nonlinear and Soft Matter Physics*, 86, 031921.
- Faisal, T. R., Hristozov, N., Western, T. L., Rey, A. D., & Pasini, D. (2014). Computational study of the elastic properties of Rheum rhabarbarum tissues via surrogate models of tissue geometry. *Journal of Structural Biology*, 185, 285–294.
- Fan, C., Feng, S., Huang, J., Wang, Y., Wu, L., Li, X., et al. (2017). AtCesA8-driven OsSUS3 expression leads to largely enhanced biomass saccharification and lodging resistance by distinctively altering lignocellulose features in rice. *Biotechnology and Biofuels*, 10, 221.
- Fan, C., Li, Y., Hu, Z., Hu, H., Wang, G., Li, A., et al. (2018). Ectopic expression of a novel OsExtensin-like gene consistently enhances plant lodging resistance by regulating cell elongation and cell wall thickening in rice. *Plant Biotechnology Journal*, 16, 254–263.
- Gibson, L. J. (2012). The hierarchical structure and mechanics of plant materials. *Journal of the Royal Society Interface*, 9, 2749–2766.
- Halpin, J. C., & Kardos, J. L. (1976). The Halpin-Tsai equations: A review. *Polymer Engineering Science*, 16, 344–352.
- Herman, M., Dutilleul, P., & Avella-Shaw, T. (1999). Growth rate effects on intra-ring and inter-ring trajectories of microfibril angle in Norway spruce (*Picea abies*). *IAWA Journal*, 20, 3–21.
- Huang, J., Liu, W., Zhou, F., & Peng, Y. (2017). Stiffness variability analysis of maize fiber bundles via multiscale simulation. *Journal of Materials Science*, 52, 7917–7928.
- Huang, J., Liu, W., Zhou, F., & Peng, Y. (2018). Effect of multiscale structural parameters on the mechanical properties of rice stems. *Journal of the Mechanical Behavior of Biomedical Materials*, 82, 239–247.
- Igathinathan, C., Womac, A. R., & Sokhansanj, S. (2010). Corn stalk orientation effect on mechanical cutting. *Biosystems Engineering*, 107, 97–106.
- Li, Y. (2003). Brittle culm1, which encodes a cobra-like protein, affects the mechanical properties of rice plants. *The Plant Cell Online*, 15, 2020–2031.
- Li, F., Xie, G., Huang, J., Zhang, R., Li, Y., Zhang, M., et al. (2017). OsCESA9 conserved-site mutation leads to largely enhanced plant lodging resistance and biomass enzymatic saccharification by reducing cellulose DP and crystallinity in rice. *Plant Biotechnology Journal*, 15, 1093–1104.
- Magistris, F. D., & Salmén, L. (2008). Finite Element modelling of wood cell deformation transverse to the fibre axis. *Nordic Pulp and Paper Research Journal*, 23, 240–246.
- Malek, S., & Gibson, L. J. (2017). Multi-scale modelling of elastic properties of balsa. *International Journal of Solids and Structures*, 113–114, 118–131.
- Marklund, E., & Varna, J. (2009). Modeling the hygroexpansion of aligned wood fiber composites. *Composites Science and Technology*, 69, 1108–1114.
- McMahon, T. (1973). Size and shape in biology. *Science*, 179, 1201–1204.
- Muzamal, M., Gamstedt, E. K., & Rasmuson, A. (2014). Modeling wood fiber deformation caused by vapor expansion during steam explosion of wood. *Wood Science and Technology*, 48, 353–372.
- Ntenga, R., & Béakou, A. (2011). Structure, morphology and mechanical properties of *Rhectophyllum camerunense* (RC) plant-fiber. Part I: Statistical description and image-based reconstruction of the cross-section. *Computational Materials Science*, 50, 1442–1449.
- Okuno, A., Hirano, K., Asano, K., Takase, W., Masuda, R., Morinaka, Y., et al. (2014). New approach to increasing rice lodging resistance and biomass yield through the use of high gibberellin producing varieties. *PLoS One*, 9, e86870.

- Ookawa, T., Inoue, K., Matsuoka, M., Ebitani, T., Takarada, T., Yamamoto, T., et al. (2014). Increased lodging resistance in long-culm, low-lignin *gh2* rice for improved feed and bioenergy production. *Scientific Reports*, 4, 6567.
- Qing, H., & Mishnaevsky, L. (2009). Moisture-related mechanical properties of softwood: 3D micromechanical modeling. *Computational Materials Science*, 46, 310–320.
- RaniSinniah, U., Wahyuni, S., Syahputra, B. S. A., & Gantait, S. (2012). A potential retardant for lodging resistance in direct seeded rice (*Oryza sativa* L.). *Canadian Journal of Plant Science*, 92, 13–18.
- Tumuluru, J. S., Tabil, L. G., Song, Y., Iroba, K. L., & Meda, V. (2014). Grinding energy and physical properties of chopped and hammer-milled barley, wheat, oat, and canola straws. *Biomass and Bioenergy*, 60, 58–67.
- Wang, N., Liu, W., Huang, J., & Ma, K. (2014a). The structure-mechanical relationship of palm vascular tissue. *Journal of the Mechanical Behavior of Biomedical Materials*, 36, 1–11.
- Wang, N., Liu, W., & Lai, J. (2014b). An attempt to model the influence of gradual transition between cell wall layers on cell wall hygroelastic properties. *Journal of Materials Science*, 49, 1984–1993.
- Wang, N., Liu, W., & Peng, Y. (2013). Gradual transition zone between cell wall layers and its influence on wood elastic modulus. *Journal of Materials Science*, 48, 5071–5084.
- Zhang, W.-j., Wu, L.-m., Ding, Y.-f., Weng, F., Wu, X.-r., Li, G.-h., et al. (2016a). Top-dressing nitrogen fertilizer rate contributes to decrease culm physical strength by reducing structural carbohydrate content in japonica rice. *Journal of Integrative Agriculture*, 15, 992–1004.
- Zhang, W., Wu, L., Wu, X., Ding, Y., Li, G., Li, J., et al. (2016b). Lodging resistance of japonica rice (*Oryza Sativa* L.): Morphological and anatomical traits due to top-dressing nitrogen application rates. *Rice*, 9, 31.

RESEARCH

Open Access



A rice mTERF protein V14 sustains photosynthesis establishment and temperature acclimation in early seedling leaves

Man Wang^{1,2†}, Feng Zhou^{1,2†}, Hong Mei Wang^{1,2}, De Xing Xue¹, Yao-Guang Liu^{1,2,3*} and Qun Yu Zhang^{1,2,3*}

Abstract

Background: Plant mitochondrial transcription termination factor (mTERF) family members play important roles in development and stress tolerance through regulation of organellar gene expression. However, their molecular functions have yet to be clearly defined.

Results: Here an mTERF gene *V14* was identified by fine mapping using a conditional albino mutant *v14* that displayed albinism only in the first two true leaves, which was confirmed by transgenic complementation tests. Subcellular localization and real-time PCR analyses indicated that *V14* encodes a chloroplastic protein ubiquitously expressed in leaves while spiking in the second true leaf. Chloroplastic gene expression profiling in the pale leaves of *v14* through real-time PCR and Northern blotting analyses showed abnormal accumulation of the unprocessed transcripts covering the *rpoB-rpoC1* and/or *rpoC1-rpoC2* intercistronic regions accompanied by reduced abundance of the mature *rpoC1* and *rpoC2* transcripts, which encode two core subunits of the plastid-encoded plastid RNA polymerase (PEP). Subsequent immunoblotting analyses confirmed the reduced accumulation of RpoC1 and RpoC2. A light-inducible photosynthetic gene *psbD* was also found down-regulated at both the mRNA and protein levels. Interestingly, such stage-specific aberrant posttranscriptional regulation and *psbD* expression can be reversed by high temperatures (30 ~ 35 °C), although *V14* expression lacks thermo-sensitivity. Meanwhile, three *V14* homologous genes were found heat-inducible with similar temporal expression patterns, implicating their possible functional redundancy to *V14*.

Conclusions: These data revealed a critical role of *V14* in chloroplast development, which impacts, in a stage-specific and thermo-sensitive way, the appropriate processing of *rpoB-rpoC1-rpoC2* precursors and the expression of certain photosynthetic proteins. Our findings thus expand the knowledge of the molecular functions of rice mTERFs and suggest the contributions of plant mTERFs to photosynthesis establishment and temperature acclimation.

Keywords: mTERFs, *rpoB-rpoC1-rpoC2* operon, Chloroplast development, Temperature response, Rice

* Correspondence: ygliu@scau.edu.cn; zqy@scau.edu.cn

†Man Wang and Feng Zhou contributed equally to this work.

¹State Key Laboratory for Conservation and Utilization of Subtropical Agro-bioresources, College of Life Sciences, South China Agricultural University, Guangzhou 510642, China

Full list of author information is available at the end of the article



© The Author(s). 2021 **Open Access** This article is licensed under a Creative Commons Attribution 4.0 International License, which permits use, sharing, adaptation, distribution and reproduction in any medium or format, as long as you give appropriate credit to the original author(s) and the source, provide a link to the Creative Commons licence, and indicate if changes were made. The images or other third party material in this article are included in the article's Creative Commons licence, unless indicated otherwise in a credit line to the material. If material is not included in the article's Creative Commons licence and your intended use is not permitted by statutory regulation or exceeds the permitted use, you will need to obtain permission directly from the copyright holder. To view a copy of this licence, visit <http://creativecommons.org/licenses/by/4.0/>. The Creative Commons Public Domain Dedication waiver (<http://creativecommons.org/publicdomain/zero/1.0/>) applies to the data made available in this article, unless otherwise stated in a credit line to the data.

Background

The mitochondrial transcription termination factor (mTERF) family consists of a group of nucleic acid binding proteins with so-called mTERF repeats of ~31 amino acids forming three helices [1, 2]. Similarity searches and phylogenetic analysis demonstrated that the mTERF family exists only in eukaryotes except for fungi [3]. All these proteins are predicted to localize to mitochondria and/or chloroplasts. Mammal genomes encode only four mTERFs (MTERF1–4) [4], while higher plants harbor approximately 30 members [5]. The mammalian mTERFs regulate mitochondrial gene expression. Human MTERF1, the first identified mTERF, functions in terminating L-strand transcription at the 16S rRNA/leucyl-tRNA boundary [6], transcription activation [7, 8], and DNA replication [9], followed by the discoveries of the roles of MTERF2 in restraining replication fork progression [10], MTERF3 in transcription suppression, replication [11], and ribosomal biogenesis [12], and MTERF4 in transcription activation [13] and ribosomal biogenesis [14]. Plant mTERFs, by contrast, are barely understood for their roles in the regulation of organellar gene expression. Of the 35 mTERFs in *Arabidopsis*, 11 are chloroplast-localized [15]. SOLDAT10, the first mTERF characterized in higher plants, participates in stress acclimation response and affects the abundance of 16S and 23S rRNA and ClpP protease mRNA [16] in chloroplasts. BSM (RUG2) is targeted to both mitochondria and chloroplasts and is required for the maintenance of the constant accumulation of transcripts in these two organelles [15, 17], which includes splicing of the *clpP* group IIA intron [15]. Two comparative analyses of two other chloroplastic mTERFs, mTERF5 (MDA1) and mTERF9 (TWIRT1), indicated a functional relationship between them, that they share some common targets in gene expression regulation, both respond to salt and osmotic stresses, and both are functionally related to the plastid-encoded plastid RNA polymerase (PEP) [18]. Also, TWIRT1 is likely required for plastid ribosomal stability and/or assembly [19], and MDA1 positively regulates *psbEFLJ* transcription as a transcriptional pausing factor [20], stimulates *psbE* and *ndhA* transcription, and promotes the stabilization of the 5'-ends of processed *psbE* and *ndhA* mRNA [21]. A recent report further found that transcription termination of *psbJ* in the *psbEFLJ* polycistron also involved another PEP-associated mTERF, mTERF8/*PTAC15*, which specifically binds to the 3' terminal region of *psbJ* [22]. In addition to the studies on chloroplastic mTERFs, two mitochondrial mTERFs in *Arabidopsis*, mTERF18 (SHOT1) and mTERF15, were found to interfere in retrograde signaling for heat tolerance [23], and splicing of the *nad2* intron-3 [24], respectively. Meanwhile, a few studies provided some clues to the action modes of plant

mTERFs. Zm-mTERF4, the BSM ortholog in maize, directly binds the group II introns in certain chloroplastic transcripts and interacts with some of the known chloroplastic splicing factors, thus promoting the splicing of such transcripts, including *trnI-GAU*, *trnA-UGC*, and *rpl2* [25]. Later, two studies of *Arabidopsis* mTERF6 demonstrated its DNA-binding activity in vivo, which is required for the transcription termination at a specific site in *trnI-GAU* and at the 3'-end of *rpoA* polycistron in chloroplasts [26, 27]. Recently, mitochondrial *ZmSmk3* was found involved in the splicing of *nad4* intron 1 and *nad1* intron 4 in maize [28], and *Arabidopsis* mTERF9 was shown to promote chloroplast ribosome assembly and translation by interacting with 16S and 23S rRNAs [29]. Despite these advances, the molecular mechanism by which plant mTERFs regulate organellar gene expression is still far from full understanding, and it is not clear if mTERFs involve in processing organellar polycistronic transcripts. Moreover, little information has been provided so far for the impact of mTERFs on chloroplast and mitochondrion development in rice (*O. sativa* L.), a model crop species.

Derived from a cyanobacterial ancestor, the chloroplast holds many genes organized in gene clusters. Chloroplast mRNA maturation includes multiple steps, which are precursor transcription, 5' and 3' end processing, intercistronic cleavage, 5' and 3' end maturation and editing, and intron removal [30]. At least two distinct RNA polymerases, PEP and the nucleus-encoded RNA polymerase (NEP), are responsible for plastid gene transcription during all phases of chloroplast development and in non-green plastid types [31]. The gene encoding the α subunit of PEP, *rpoA*, is clustered with multiple ribosomal protein-encoding genes in the *rpoA* operon, while the genes encoding the β , β' and β'' subunits of PEP, *rpoB*, *rpoC1*, and *rpoC2*, respectively, form a separate operon. Both of the *rpoA* and *rpoB* operons are transcribed by NEP [31–33]. On the other hand, photosynthetic genes, such as *psbA*, *psbD*, and *psaB*, are PEP-dependent. The association between PEP and the promoter regions of most of these genes is significantly increased in the light [34]. For example, a light-responsive promoter was identified between *psbI* and *psbD* in the *psbK-psbI-psbD-psbC* operon, which accounts for the transcription of the dicistronic *psbD-psbC*. Two other standard PEP promoters residing upstream of *psbK* and the light-responsive promoter, respectively, otherwise produce five different overlapping transcripts including *psbK-psbI-psbD-psbC*, *psbK-psbI*, and *psbD-psbC* [35]. The light-induced *psbD-psbC*, which was undetectable in the dark, was abundantly accumulated in green rice seedlings [35].

Here we described the effects of a rice mTERF, V14, on appropriate intercistronic cleavage of the polycistronic

rpoB-rpoC1-rpoC2 precursor in chloroplasts and accumulations of certain photosystem proteins, for example PsbD, during early stage of seedling leaf development. Intriguingly, this regulation pattern is growth stage-specific and temperature-sensitive. We thus suggest a role of V14 in chloroplast development and adaptation to temperature.

Results

V14 is a chloroplastic protein critical to early stage of leaf development

The *V14* locus was previously mapped as a 162-kb region on chromosome 7, using a stage-conditional *virescent-14* (*v14*) mutant of Taichung 65 (T65), a *japonica* cultivar [36]. This mutant develops albinism in the first two true leaves at 25 °C and returns green thereafter [30]. Subsequent fine mapping narrowed down the *V14*

locus to a 30-kb region containing two protein-coding genes (Additional file 1). One of which, *Os07g0583200*, had a 1283-bp deletion in the promoter and 5' untranslated/coding regions (−1245 ~ +38) in the mutant [36]. Indeed, deficiencies of *Os07g0583200* mRNA [36] and its protein product (Fig. 1A) were observed in *v14*. This gene encodes a putative chloroplastic protein (Refseq, <https://www.ncbi.nlm.nih.gov>), and its chloroplast localization was verified in rice leaf protoplasts expressing a *Os07g0583200*-fused *eGFP* construct (Fig. 1B). These data suggested that *Os07g0583200* was a strong candidate for the *V14* locus. Transcripts of this gene were observed in all analyzed stages of leaves (Fig. 1C), and their products bear seven consecutive MTERF repeats at the C-terminus [36], which is annotated by Refseq as a rice MTERF9. We further performed transgenic complementation and RNA interference (RNAi) to

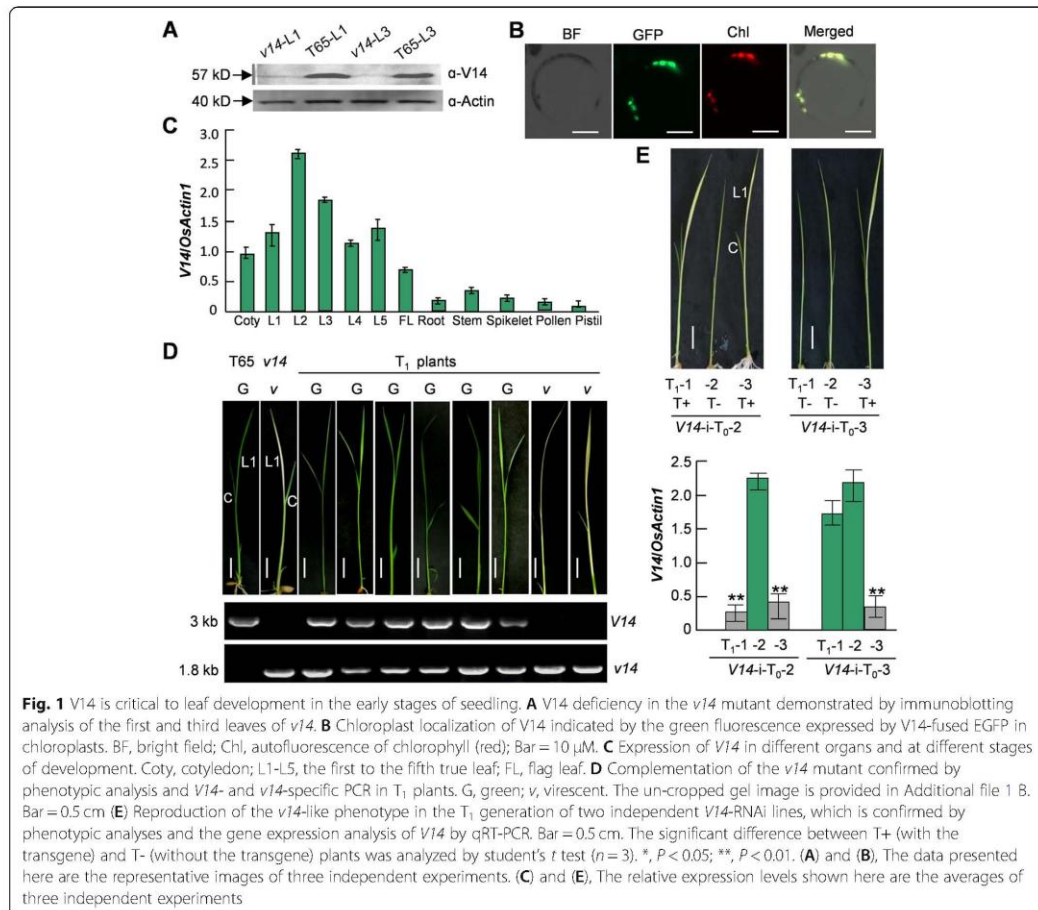


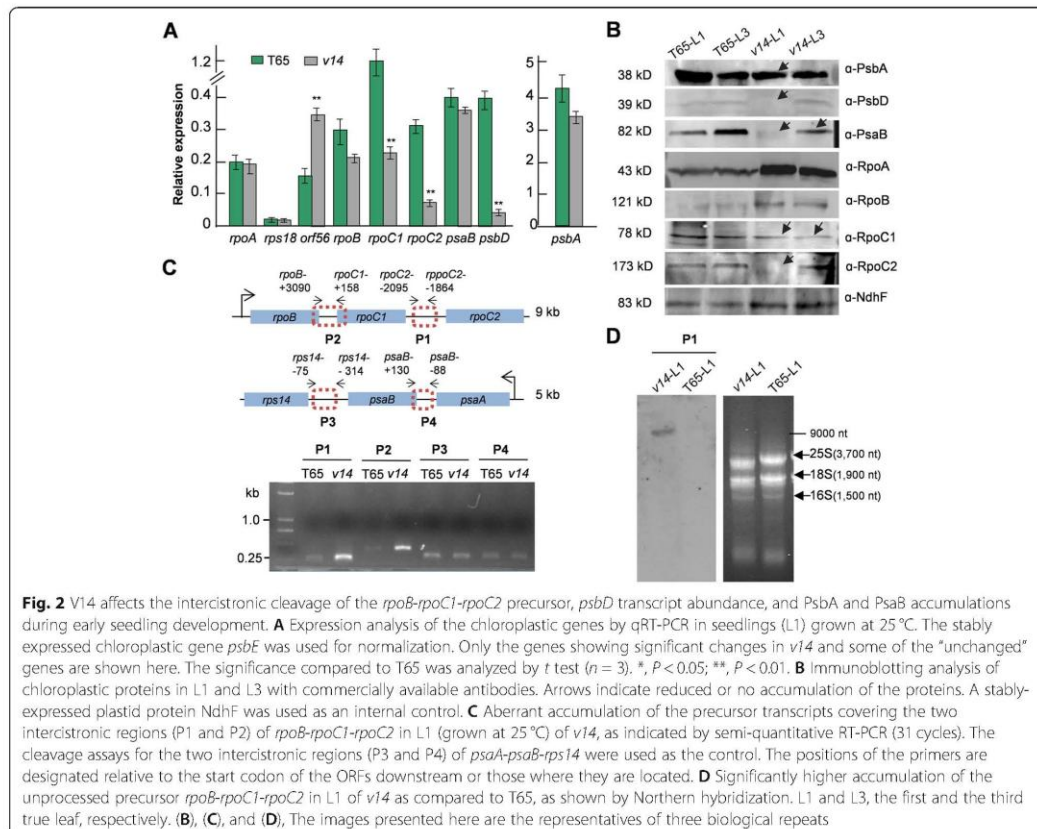
Fig. 1 V14 is critical to leaf development in the early stages of seedling. **A** V14 deficiency in the *v14* mutant demonstrated by immunoblotting analysis of the first and third leaves of *v14*. **B** Chloroplast localization of V14 indicated by the green fluorescence expressed by V14-fused GFP in chloroplasts. BF, bright field; Chl, autofluorescence of chlorophyll (red); Bar = 10 μ m. **C** Expression of V14 in different organs and at different stages of development. Coty, cotyledon; L1–L5, the first to the fifth true leaf; FL, flag leaf. **D** Complementation of the *v14* mutant confirmed by phenotypic analysis and V14- and *v14*-specific PCR in T₁ plants. G, green; v, virescent. The un-cropped gel image is provided in Additional file 1 B. Bar = 0.5 cm **E** Reproduction of the *v14*-like phenotype in the T₁ generation of two independent V14-RNAi lines, which is confirmed by phenotypic analyses and the gene expression analysis of V14 by qRT-PCR. Bar = 0.5 cm. The significant difference between T+ (with the transgene) and T- (without the transgene) plants was analyzed by student's *t* test (*n* = 3). *, *P* < 0.05; **, *P* < 0.01. (A) and (B), The data presented here are the representative images of three independent experiments. (C) and (E), The relative expression levels shown here are the averages of three independent experiments

confirm *Os07g0583200* represents the *V14* locus. Successful complementation of the albinism was achieved in those transgenic *v14*-T₁ plants carrying an *Os07g0583200*-containing fragment with its native promoter (Fig. 1D). Simultaneously, the *v14*-like phenotype was reproduced in the RNAi plants manifesting down-regulated *Os07g0583200* expression (Fig. 1E). We therefore assigned *V14* to this gene thereafter.

V14 sustains functional chloroplasts via posttranscriptional precursor cleavage

Our prior knowledge of *v14* indicates an arrest of chloroplast development in the first two true leaves, as is evident from the absence of mature thylakoids and starch grains [36]. We thus posited transcription deficiency residing in the chloroplasts of the chlorotic leaves. To determine the chloroplastic genes affected, we first used qRT-PCR to assess the difference between *v14* and T65 in transcript abundance of all 62 chloroplastic genes in the first true leaves. The results revealed

significant gene expression changes (2 fold minimum) in *v14* as compared to the wild-type T65, which involved two genes encoding the β' - and β'' -subunits of PEP, *rpoC1* and *rpoC2*, a photosynthetic gene *psbD*, and a rice-exclusive gene *orf56* [37, 38] encoding a truncated NdhH [39] (Fig. 2A). The transcripts *rpoC1*, *rpoC2*, and *psbD* were considerably down-regulated in *v14*, whilst *orf56* was up-regulated (Fig. 2A). Further semi-quantitative RT-PCR analysis of the overlapping region across the coding sequences of *psbD* and *psbC* revealed its absence in *v14* (Additional file 2A), confirming the significant reduction in *psbD* mRNA abundance. Given the important roles of the nucleus-encoded sigma factors in PEP activation, the expression of all five sigma factors was also analyzed by qRT-PCR. The results indicated that none of them were affected by *V14* deficiency (Additional file 2B). Subsequent immunoblotting analysis confirmed the protein deficiency of RpoC1, RpoC2, and PsbD in *v14* (Fig. 2B, Additional file 2C). In addition, the protein levels of some other photosynthetic



proteins were assessed with commercially available antibodies. We found that two other photosystem proteins PsbA and PsbB also decreased in *v14* (Fig. 2B, Additional file 2C), even though their transcript abundance was unchanged (Fig. 2A). In contrast, RpoA and RpoB were more abundant in *v14* than in T65 (Fig. 2B, Additional file 2C). This might be attributed to the feedback inhibition of translation that has been observed in bacteria [40].

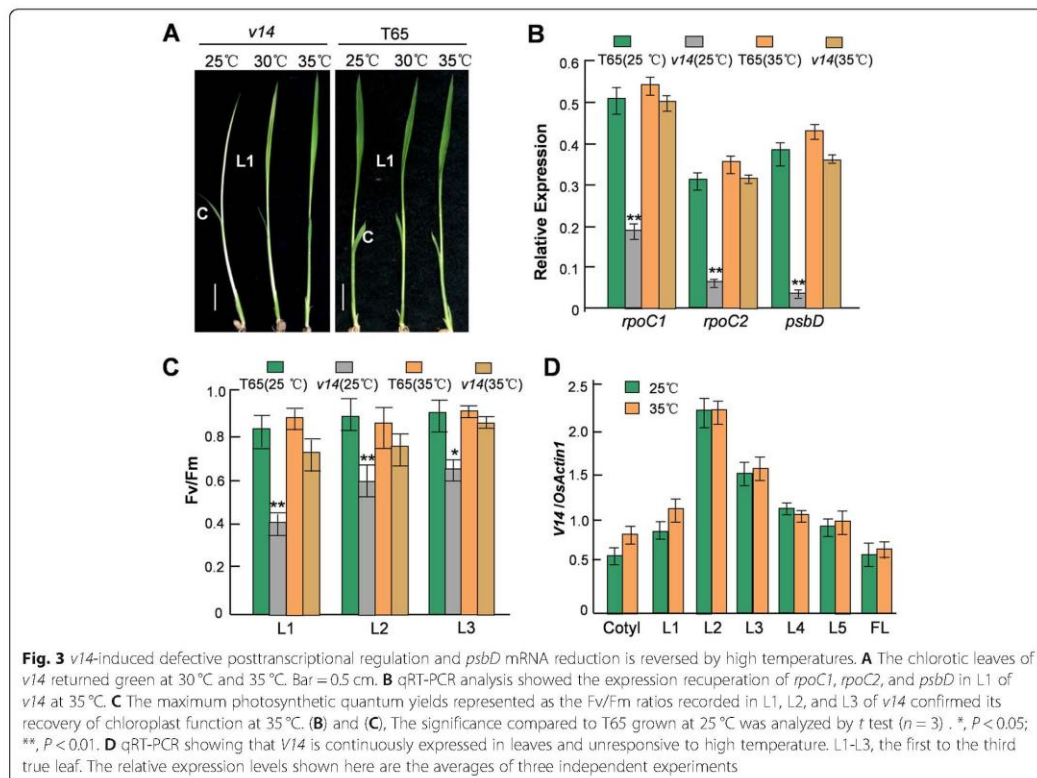
We next analyzed how V14 influences mRNA levels in chloroplasts. We noted that the V14 target genes are organized in co-transcribed gene clusters with other non-targeted genes. In light of the role of maize ZmTERF4 in intron splicing [25], we hypothesized that V14 may intervene in either precursor cleavage or RNA stabilization. To explore the behavior of V14, the abundance of the two intercistronic regions (P1 and P2) from the polycistronic *rpoB-rpoC1-rpoC2* precursor (Fig. 2C) were analyzed by semi-quantitative RT-PCR in the first two true leaves of *v14* and T65, using the two intercistronic regions (P3 and P4) from the polycistronic *psaA-psaB-rps14* precursor (Fig. 2C) as controls. We found that the chlorotic leaves boasted higher amounts of the

unprocessed transcripts including the *rpoB-rpoC1* and/or *rpoC1-rpoC2* regions as compared to the wild-type (Fig. 2C, Additional file 2D). No significant changes were observed for the P3 and P4 regions in *v14* (Fig. 2C, Additional file 2D). Using P1 as a probe for Northern hybridization, we also detected a ~9-kb precursor transcript containing *rpoB*, *rpoC1*, and *rpoC2* only in *v14* (Fig. 2D).

Taken together, these data reflect the effects of V14 on the appropriate intercistronic cleavage of polycistronic *rpoB-rpoC1-rpoC2* and *psbD* mRNA, PsbA, and PsbB accumulations. Given that light regulates expression of the PEP components in the first phase of photosynthesis establishment and *psbD* mRNA, PsbA, and PsbB abundance [41–44], V14 may play a key role in light signaling through chloroplast development.

The albinism phenotype of *v14* is temperature-dependent

Similar to the three temperature-conditional rice virescents reported previously [45], *v14* developed green leaves at permissive temperatures, 30 °C and 35 °C (Fig. 3A). To ascertain this full recovery at high temperatures, we first evaluated the expression levels of *rpoC1*,



rpoC2, and *psbD* in the first true leaves of the *v14* plants grown at 25 °C and 35 °C. The RT-PCR analysis showed that the abundance of these transcripts at 35 °C could reach a level comparable to their counterparts in T65 (Fig. 3B). Indeed, the appropriate cleavages of the two intergenic regions of *rpoB-rpoC1-rpoC2* were retrieved in these green-recovered *v14* plants (Additional file 3). We further assessed chloroplast function in the *v14* plants grown at 35 °C by gauging the Fv/Fm ratio (the maximum photosynthetic quantum yield), a measurement representing Photosystem II efficiency, in the first, second, and third true leaves. In agreement with the expression recuperation of *rpoC1*, *rpoC2*, and *psbD*, the Fv/Fm values recorded in the 35 °C-growing *v14* plants showed no significant difference from those in the T65s grown either at 25 °C or 35 °C (Fig. 3C). By contrast, the 25 °C-growing *v14* plants still could not fully retrieve the power of photosynthesis in their third leaves even though they returned green (Fig. 3C). Interestingly, *V14* mRNA expression in T65 was neither heat-sensitive nor stage-specific, albeit relatively high in the second true leaf (Figs. 1C, 3D).

We thus postulated that there may be unknown *V14* parallel factor(s) acting at high temperatures while *V14* is inactive. Our similarity searches on NCBI identified 30 other *V14*-homologs in rice (Additional file 4). Expression analysis of these genes in 25 °C- and 35 °C-growing T65s showed that three of them, *Os07g0134700*, *Os08g0528700*, and *Os02g0602400*, were significantly up-regulated at 35 °C in the second true leaf where *V14* expression reaches its peak (Fig. 4A, Additional files 5, 6 and 7). *Os07g0134700* and *Os02g0602400* are predicted to encode chloroplastic mTERFs (annotated as rice MTERF2 and MTERF5 homologs, respectively, by Refseq), while *Os08g0528700* encodes an unannotated mTERF-like protein.

Discussion

The mTERF family earned its name from its founding member, human MTERF1 [6], as a group of transcription termination factors 31 years ago, but more molecular functions have since been linked to it, such as transcription initiation, DNA replication, and intron splicing. Our data presented here extend the understanding of the molecular functions of mTERFs, which may regulate intergenic cleavage of polycistronic precursors. We showed that *V14* is required for the appropriate intergenic cleavage of *rpoB-rpoC1-rpoC2* precursor, thus regulating the abundance of mature *rpoC1* and *rpoC2* mRNAs that encode two core subunits of PEP. The expression of *rpoB*, however, is not targeted by *V14*. Since *rpoB* is co-transcribed with *rpoC1* and *rpoC2* by NEP [31–33], this result indicates that *V14* specifically regulates precursor processing but not

precursor transcription for the *rpoB-rpoC1-rpoC2* operon. Despite reduced expression of mature *rpoC1* and *rpoC2* mRNAs in *v14*, expression of the PEP-dependent genes is unaffected except for *psbD*, implicating that low levels of PEP in the proplastids can maintain the expression of most of these genes. This observation is consistent with the developmental and gene-specific regulation of PEP transcription proposed in wheat seedlings [43]. In developing chloroplasts the light-independent PEP functions in the dark as well as in the light for the PEP-dependent genes including *psbA*, *psbC*, *psbE*, and *rnn16*, except for *psbD*, whilst the light-dependent PEP selectively transcribes *psbA* and *psbD* in mature chloroplasts [43]. A light-responsive promoter producing a precursor including *psbD* and *psbC* has also been identified in the *psbK-psbI-psbD-psbC* gene cluster [46]. Considering *psbC* showed no expression change in *v14* while being co-transcribed with *psbD*, we speculated that *V14* may be crucial for *psbD* mRNA stability in a light-dependent way. We also noted that two other photosystem proteins *PsbA* and *PsaB* also decreased because of the *V14* deficiency even without alterations in their transcript abundance, which can be explained by the facts that translation and stability of proteins encoded by *psbA* and *psaB* are light-dependent during chloroplast development [41]. Furthermore, a light response model established in *Arabidopsis* indicates that light signals precede plastid signals, where the first phase of photosynthesis establishment relies on light and triggers changes that will initiate chloroplast development, and more importantly initiates expression of the PEP components [47]. This model supports the impaired processing of *rpoB-rpoC1-rpoC2* precursor and reduced accumulations of *psbD*, *PsbA*, and *PsaB* observed in the chlorotic leaves of *v14*, suggesting that *V14* is essential for light signaling during chloroplast development. *V14* might not act directly on its molecular targets, such as the *rpoB-rpoC1-rpoC2* precursor, but interfere in a key step during chloroplast development that introduces these changes, which needs further investigations.

We showed that *v14* was rescued by higher temperatures, and that the defective intergenic cleavage of the *rpoB-rpoC1-rpoC2* precursor is temperature-dependent (Fig. 3B, Additional file 3). However, the expression of *V14* per se in wild-type is not temperature-sensitive (Fig. 3D). Considering *V14* might act via phytohormone-mediated thermosensory pathways [48, 49], we examined the response of *v14* seedlings to various phytohormone treatments (Additional file 8). However, none of such treatments could restore the albinism observed at 25 °C, suggesting that *V14* is insensitive to phytohormones. We further identified three mTERF genes showing a similar temporal expression pattern to *V14* that were significantly up-regulated by

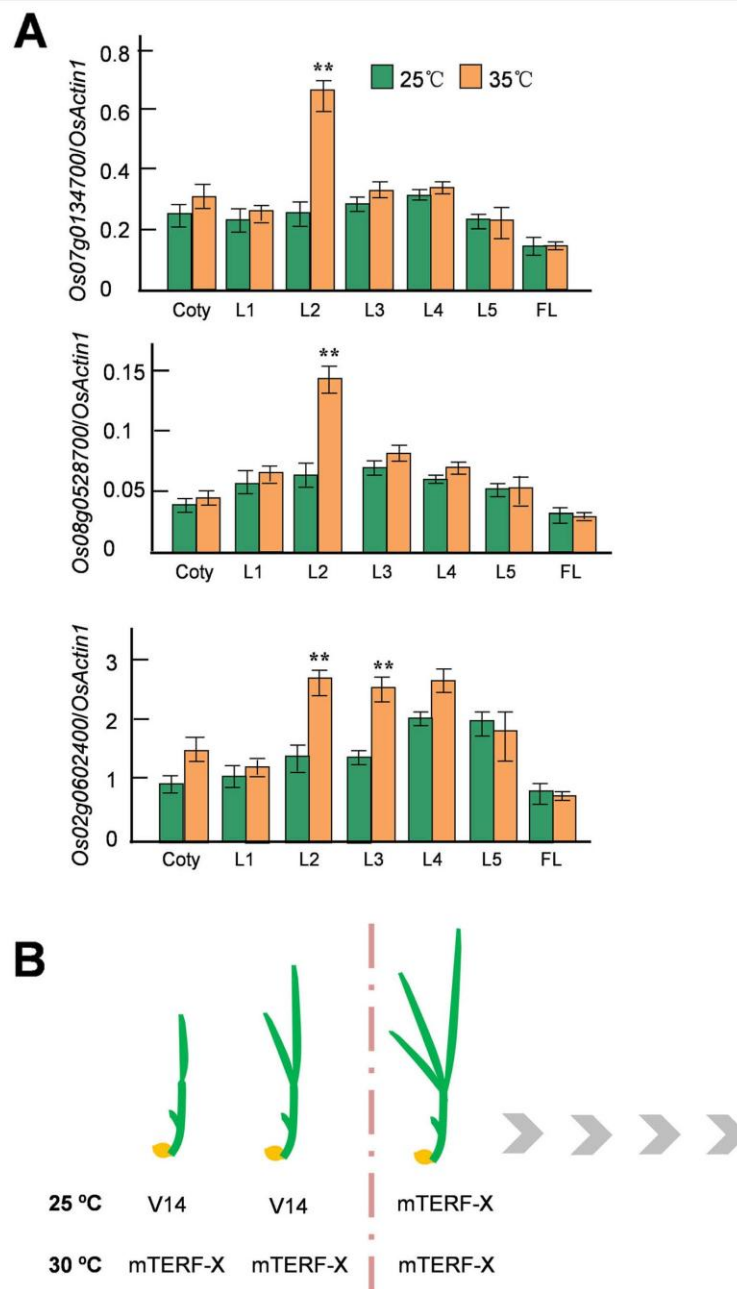


Fig. 4 A Three rice mTERF genes are heat-inducible, as indicated by qRT-PCR. The significant difference in expression between growth at 35 °C and 25 °C was analyzed by *t* test ($n = 3$). *, $P < 0.05$; **, $P < 0.01$. **B** The effects of V14 on chloroplast development are stage-specific and thermo-sensitive

high temperatures in the second leaf (Fig. 4A), suggesting that these genes may be potential candidates for the unknown *V14* parallel(s) whose functions compensate for the *V14* deficiency at high temperatures. These data support the notion that plants have evolved functionally redundant members of gene families, by which certain members can be replaced by some other members in a conditional manner.

Conclusion

V14 is an essential transcriptional and translational regulator in chloroplasts supporting chloroplast biogenesis in the first two true leaves. While *V14* expression is neither stage-specific nor thermo-sensitive, the *V14*-mediated regulation is stringently modulated by developmental stages and temperature (Fig. 4B). The roles of *V14* in chloroplast development are just beginning to emerge. Further studies are needed to dissect the molecular functions of *V14* in intergenic cleavage, mRNA stability, and translational/posttranslational regulation, and to define how such regulations respond to temperature, thus helping to understand the contributions of organellar gene expression to photosynthesis establishment and temperature acclimation.

Methods

Plant materials and treatment

The seeds of T65 were obtained from Dr. Chuxiong Zhuang's lab at South China Agricultural University. The seedlings were grown in growth chambers under 16-h light/8-h dark cycles at 25 °C. Details for the positional mapping of the *V14* locus were provided in a previous study [36]. For the temperature treatments, the seedlings were grown under 16-h light/8-h dark cycles at 25 °C, 30 °C or 35 °C.

Intracellular localization of eGFP fusions

For eGFP visualization, a cDNA fragment of *V14* was obtained from T65 using the primers V14-xho5 and V14-spe3 (Additional file 9), and fused with the coding sequence of *eGFP* in a pUC18-based vector to create the construct *P35S::V14-eGFP*. The construct was then transiently transformed into rice leaf protoplasts following the protocol described previously [50]. The images were collected in the 500- to 550-nm (eGFP fluorescence), and 670- to 750-nm (chlorophyll autofluorescence) ranges with a laser confocal scanning microscope fitted with a 40 × water immersion objective (7 DUO; Zeiss).

Genetic transformation

For complementation test of the *v14* mutant, a genomic fragment containing the promoter, gene body, and a 914-bp 3' UTR region was amplified from T65 genomic DNA using the primers V14P5 and V14P3 (Additional

file 9, and cloned into a plant expression vector pCAMBIA 1380 with Gibson Assembly® Master Mix (New England Biolabs). The success of the complementation was confirmed by phenotypic analysis and PCR using the *V14*-specific primers as described in a previous study [36]. For generation of the *V14*-RNAi plants, a cDNA fragment was obtained from T65 using two primer pairs (Additional file 9), V14i-5-1 and V14i-3-1, and V14i-5-2 and V14i-3-2, and cloned into a plant expression vector pCAMBIA 1301 with Gibson Assembly® Master Mix. The complementation construct was introduced into *v14*, and the RNAi one was transferred into T65, by *Agrobacterium*-mediated transformation.

Chloroplast isolation

Chloroplasts were prepared as previously published [51]. In brief, 10 g of fresh seedling leaves were frozen in liquid nitrogen and gently ground into fine powder. The powder was then suspended in 100 ml of Medium A (50 mM HEPES-KOH pH 8.0, 330 mM sorbitol, 2 mM EDTA- Na_2 , 5 mM ascorbic acid, 5 mM cysteine, 0.05% BSA) and the suspension was filtered through two layers of gauze and then two layers of Miracloth (Merck). This filtrate was subjected to centrifugation (1300×g, 4 °C, 5 min) to collect chloroplast pellets followed by sucrose density gradient centrifugation (30, 40, 55% sucrose density gradient in Medium B, 30000×g, 4 °C, 1 h) using the pellets suspended in 200 µl of Medium B (50 mM HEPES-KOH pH 8.0, 330 mM sorbitol, 2 mM EDTA- Na_2). The green band at the 30 and 40% sucrose interface was collected and rinsed twice with 75 mL of Medium B through centrifugation (2000×g, 4 °C, 15 min). Finally, the pellets were resuspended in 50 µl of TRIzol™ Reagent (ThermoFisher Scientific) for RNA extraction.

Nucleic acid extraction, qRT-PCR, northern blot and immunoblotting

Genomic DNA was isolated from leaves with a DNeasy Plant Mini Kit (Qiagen). Total RNA was extracted from leaves or chloroplasts following the instruction of TRIzol® Reagent. DNase I (Invitrogen) digestion was applied prior to reverse transcription. For assessment of the abundance of nuclear transcripts, Oligo (dT)₂₀ (50 µM) was used for the synthesis of first-strand cDNA from total RNA extracted from leaves. For assessment of the amounts of all chloroplastic transcripts, Random Hexamers (50 ng/µL) was used for the synthesis of first-strand cDNA from total RNA extracted from chloroplasts. The primers for the nucleus-encoded sigma factors were shown in Additional file 9. All the primer sequences for detecting chloroplastic transcripts were listed in Additional file 10, except for those for amplifying the intergenic regions (P1-P4), the overlapping

region across *psbD* and *psbC*, and a region downstream of *psbC* (Additional file 2 A), which were given in Additional file 9. Northern blot analysis was performed using total RNA as previously published [52]. The probe P1 was labeled with 0.01 μM digoxigenin (DIG)-deoxyuridine triphosphate by PCR. To extract proteins, seedling leaves were homogenized in $2 \times$ SDS sample buffer (62.5 mM Tris-HCl, pH 6.8, 20% [v/v] glycerol, 4% [w/v] SDS, 100 mM dithiothreitol, and 0.05% [w/v] Bromophenol Blue), incubated at 95 °C for 5 min, and centrifuged at the maximum speed for 20 min. The samples were quantified and subjected to SDS-PAGE (12%) followed by wet transfer to PVDF membranes (Millipore). The membranes were then incubated with the antibodies against V14, RpoA, RpoB, RpoC1, RpoC2, PsbA, PsbD, PsbB, or NdhF. All these antibodies were obtained from BGI, except for the V14 antibody, which was developed by Abmart using a synthetic peptide EGRQPKTRDRC as the immunogen. All the protein levels were normalized to NdhF by ImageJ, which is shown in Additional file 2C.

Chlorophyll fluorescence analysis

The experiments were performed following the protocol published previously [53] with some minor modifications. Six plants for each group were dark-adapted for 20 min before taking measurements with a PAM fluorometer (Walz). All measurements were taken at the same time during the day. A saturating pulse of radiation ($2700 \mu\text{mol m}^{-2} \text{s}^{-1}$) was applied to record the maximum fluorescence yield (F_m), and a weak modulating radiation ($0.5 \mu\text{mol m}^{-2} \text{s}^{-1}$) was used to measure the minimum fluorescence yield (F_0). The maximum photosynthetic quantum yield was then calculated as F_v (variable fluorescence yield)/ $F_m = (F_m - F_0)/F_m$.

Abbreviations

mTERF: Mitochondrial transcription termination factor; PEP: The plastid-encoded plastid RNA polymerase; NEP: The nucleus-encoded RNA polymerase; F_v : Variable fluorescence yield; F_m : The maximum fluorescence yield; F_0 : The minimum fluorescence yield; NCBI: National Center for Biotechnology Information

Supplementary Information

The online version contains supplementary material available at <https://doi.org/10.1186/s12870-021-03192-2>.

Additional file 1. (A) Fine mapping of the V14 locus on chromosome 7. The dashed line represents the genomic deletion in the promoter and 5' untranslated and coding regions (−1245 ~ +38) in the v14 mutant. Arrows indicate primers for detecting the endogenous and transgenic fragments of V14 and v14 as shown in Fig. 1D. (B) Complementation of the v14 mutant confirmed by V14- and v14-specific PCR in T₁ plants.

Additional file 2. Analysis of the *psbD*-containing transcripts by semi-quantitative RT-PCR (31 cycles) (A), expression analysis of the rice sigma factors by qRT-PCR (B), quantification of the immunoblotting analysis shown in Fig. 2B by ImageJ (C), and analysis of the two intergenic regions (P1 and P2) of *rpoB-rpoC1-rpoC2* in the second true leaves (grown

at 25 °C) of v14 by semi-quantitative RT-PCR (31 cycles) (D). (A), The positions of the primers are designated relative to the start codon of the ORFs where they are located. (B), The significance compared to T65 was analyzed by t test ($n = 3$). (C), All the protein levels were normalized to NdhF. (D), The two intergenic regions (P3 and P4) of *psaA-psaB-rps14* were used as the control. (A) and (D), The images presented here are the representatives of three biological repeats.

Additional file 3. High temperature (35 °C) rescued the cleavage of the two intergenic regions (P1 and P2) of the *rpoB-rpoC1-rpoC2* precursor in L1 of v14. The semi-quantitative RT-PCR was carried out by 31 cycles. L1, the first leaf. P3 and P4 are the two spacer regions in the *psaA-psaB-rps14* operon shown in Fig. 2C. The image presented here is the representative of three biological repeats.

Additional file 4. Phylogenetic analysis of V14 in rice. The neighbor-joining tree was built on protein sequences using the software PHYLIP (version 3.66) and visualized with the software TreeView and MEGA5. Arrows indicate the three genes with temperature-sensitive expression in the second leaf (Fig. 4).

Additional file 5. Gene expression profiles of the other 27 V14-homologous genes at different stages of leaf development at 25 °C and 35 °C. The relative expression levels shown here are the averages of three independent experiments.

Additional file 6. Gene expression profiles of the other 27 V14-homologous genes at different stages of leaf development at 25 °C and 35 °C. The relative expression levels shown here are the averages of three independent experiments.

Additional file 7. Gene expression profiles of the other 27 V14-homologous genes at different stages of leaf development at 25 °C and 35 °C. The relative expression levels shown here are the averages of three independent experiments.

Additional file 8. v14 seedlings on various phytohormone treatments at 25 °C. Bar = 0.5 cm; L1, the first true leaf; L2, the second true leaf.

Additional file 9. Primer sequences for complementation, RNAi, and the assessment of the processing intermediates.

Additional file 10. Primer sequences for the mRNA expression profiling of the chloroplastic gene transcripts.

Additional file 11. The un-cropped blot images of Figs. 1A, 2B, and D.

Additional file 12. The original real-time PCR data for Figs. 2A, 3B, and 4A.

Acknowledgments

Not applicable.

Authors' contributions

M. W., F. Z., H. W. and D. X.: Performing experiments and data analyses; Q. Z. and Y. L.: Conceiving the project and Writing the manuscript. All authors reviewed the manuscript. The author(s) read and approved the final manuscript.

Funding

This study was supported by the National Key Program on Transgenic Research from the Ministry of Agriculture of China (2016ZX08009002-003), the Guangdong Natural Science Foundation (2015A030313414) and the Science and Technology Program of Guangzhou, China (201607010196).

Availability of data and materials

The sequences of V14 and the mutant v14 have been deposited in NCBI under the submission IDs MZ299153 and MZ299154, respectively.

Ethics approval and consent to participate

Not applicable.

Consent for publication

Not applicable.

Competing interests

Not applicable.

Author details

¹State Key Laboratory for Conservation and Utilization of Subtropical Agro-bioresources, College of Life Sciences, South China Agricultural University, Guangzhou 510642, China. ²Guangdong Laboratory for Lingnan Modern Agriculture, Guangzhou 510642, China. ³SCAU Main Campus Teaching & Research Base, Guangzhou, China.

Received: 26 January 2021 Accepted: 28 August 2021

Published online: 06 September 2021

References

- Jimenez-Mendez N, Fernandez-Millan P, Rubio-Cosials A, Arnan C, Montoya J, Jacobs HT, et al. Human mitochondrial mTERF wraps around DNA through a left-handed superhelical tandem repeat. *Nat Struct Mol Biol*. 2010;17(7):891–3.
- Yakubovskaya E, Mejia E, Byrnes J, Hambardjiev E, Garcia-Diaz M. Helix unwinding and base flipping enable human MTERF1 to terminate mitochondrial transcription. *Cell*. 2010;141(6):982–93.
- Linder T, Park CB, Asin-Cayuela J, Pellegrini M, Larsson NG, Falkenberg M, et al. A family of putative transcription termination factors shared amongst metazoans and plants. *Curr Genet*. 2005;48(4):265–9.
- Roberti M, Polosa PL, Bruni F, Manzari C, Deceglie S, Gadaleta MN, et al. The MTERF family proteins: mitochondrial transcription regulators and beyond. *Biochim Biophys Acta*. 2009;1787(5):303–11.
- Kleine T. Arabidopsis thaliana mTERF proteins: evolution and functional classification. *Front Plant Sci*. 2012;3:233.
- Kruse B, Narasimhan N, Attardi G. Termination of transcription in human mitochondria: identification and purification of a DNA binding protein factor that promotes termination. *Cell*. 1989;58(2):391–7.
- Asin-Cayuela J, Helm M, Attardi G. A monomer-to-trimer transition of the human mitochondrial transcription termination factor (mTERF) is associated with a loss of *in vitro* activity. *J Biol Chem*. 2004;279(15):15670–7.
- Martin M, Cho J, Cesare AJ, Griffith JD, Attardi G. Termination factor-mediated DNA loop between termination and initiation sites drives mitochondrial rRNA synthesis. *Cell*. 2005;123(7):1227–40.
- Hyvarinen AK, Pohjoismaki JL, Reyes A, Wanrooij S, Yasukawa T, Karhunen PJ, et al. The mitochondrial transcription termination factor mTERF modulates replication pausing in human mitochondrial DNA. *Nucleic Acids Res*. 2007;35(19):6458–74.
- Kleine T, Leister D. Emerging functions of mammalian and plant mTERFs. *Biochim Biophys Acta*. 2015;1847(9):786–97.
- Park CB, Asin-Cayuela J, Camara Y, Shi Y, Pellegrini M, Gaspari M, et al. MTERF3 is a negative regulator of mammalian mtDNA transcription. *Cell*. 2007;130(2):273–85.
- Wredenberg A, Lagouge M, Bratic A, Metodiev MD, Spahr H, Mourier A, et al. MTERF3 regulates mitochondrial ribosome biogenesis in invertebrates and mammals. *PLoS Genet*. 2013;9(1):e1003178.
- Camara Y, Asin-Cayuela J, Park CB, Metodiev MD, Shi Y, Ruzzenente B, et al. MTERF4 regulates translation by targeting the methyltransferase NSUN4 to the mammalian mitochondrial ribosome. *Cell Metab*. 2011;13(5):527–39.
- Spahr H, Habermann B, Gustafsson CM, Larsson NG, Hallberg BM. Structure of the human MTERF4-NSUN4 protein complex that regulates mitochondrial ribosome biogenesis. *Proc Natl Acad Sci U S A*. 2012;109(38):15253–8.
- Babychuk E, Vandepoel K, Wissing J, Garcia-Diaz M, De Rycke R, Albari H, et al. Plastid gene expression and plant development require a plastidic protein of the mitochondrial transcription termination factor family. *Proc Natl Acad Sci U S A*. 2011;108(16):6674–9.
- Meskauskienė R, Wursch M, Laloi C, Vidi PA, Coll NS, Kessler F, et al. A mutation in the Arabidopsis mTERF-related plastid protein SOLDAT10 activates retrograde signaling and suppresses (1) O (2)-induced cell death. *Plant J*. 2009;60(3):399–410.
- Quesada V, Sarmiento-Manus R, Gonzalez-Bayon R, Hricova A, Perez-Marcos R, Gracia-Martinez E, et al. Arabidopsis RUGOSA2 encodes an mTERF family member required for mitochondrion, chloroplast and leaf development. *Plant J*. 2011;68(4):738–53.
- Robles P, Micol JL, Quesada V. Mutations in the plant-conserved MTERF9 alter chloroplast gene expression, development and tolerance to abiotic stress in Arabidopsis thaliana. *Physiol Plant*. 2015;154(2):297–313.
- Nunez-Delegido E, Robles P, Fernandez-Ayala A, Quesada V. Functional analysis of mTERF5 and mTERF9 contribution to salt tolerance, plastid gene expression and retrograde signalling in Arabidopsis thaliana. *Plant Biol (Stuttg)*. 2020;22(3):459–71.
- Ding S, Zhang Y, Hu Z, Huang X, Zhang B, Lu Q, et al. mTERF5 acts as a transcriptional pausing factor to positively regulate transcription of chloroplast *psbEFLJ*. *Mol Plant*. 2019;12(9):1259–77.
- Méteignier LV, Ghandour R, Meierhoff K, Zimmerman A, Chicher J, Baumberger N, et al. The Arabidopsis mTERF-repeat MDA1 protein plays a dual function in transcription and stabilization of specific chloroplast transcripts within the *psbE* and *ndhH* operons. *New Phytol*. 2020;227(5):1376–91.
- Xiong HB, Wang J, Huang C, Rochaix JD, Lin FM, Zhang JX, et al. mTERF8, a member of the mitochondrial transcription termination factor family, is involved in the transcription termination of chloroplast gene *psbJ*. *Plant Physiol*. 2020;182(1):408–23.
- Kim M, Lee U, Small I, des francs-small CC, Verling E. mutations in an Arabidopsis mitochondrial transcription termination factor-related protein enhance thermotolerance in the absence of the major molecular chaperone HSP101. *Plant Cell*. 2012;24:3349–65.
- Hsu YW, Wang HJ, Hsieh MH, Hsieh HL, Jauh GY. Arabidopsis mTERF15 is required for mitochondrial nad2 intron 3 splicing and functional complex I activity. *PLoS One*. 2014;9(11):e112360.
- Hammani K, Barkan A. An mTERF domain protein functions in group II intron splicing in maize chloroplasts. *Nucleic Acids Res*. 2014;42(8):5033–42.
- Romani I, Manavski N, Morosetti A, Tadini L, Maier S, Kuhn K, et al. A member of the Arabidopsis mitochondrial transcription termination factor family is required for maturation of chloroplast transfer RNA^{leu} (GAU). *Plant Physiol*. 2015;169(1):627–46.
- Zhang Y, Cui YL, Zhang XL, Yu QB, Wang X, Yuan XB, et al. A nuclear-encoded protein, mTERF6, mediates transcription termination of *rpoA* polycistron for plastid-encoded RNA polymerase-dependent chloroplast gene expression and chloroplast development. *Sci Rep*. 2018;8(1):11929.
- Pan Z, Ren X, Zhao H, Liu L, Tan Z, Qiu F. A Mitochondrial Transcription Termination Factor, ZmSmk3, Is Required for nad1 Intron4 and nad4 Intron1 Splicing and Kernel Development in Maize. *G3 (Bethesda)*. 2019;9(8):2677–86.
- Méteignier LV, Ghandour R, Zimmerman A, Kuhn L, Meurer J, Zoschke R, et al. Arabidopsis mTERF9 protein promotes chloroplast ribosomal assembly and translation by establishing ribonucleoprotein interactions *in vivo*. *Nucleic Acids Res*. 2021;49(2):1114–32.
- Stern DB, Goldschmidt-Clermont M, Hanson MR. Chloroplast RNA metabolism. *Annu Rev Plant Biol*. 2010;61:125–55.
- Börner T, Aleynikova AY, Zubo YQ, Kusnetsov VV. Chloroplast RNA polymerases: role in chloroplast biogenesis. *Biochim Biophys Acta*. 2015;1847(9):761–9.
- Zhelyazkova P, Sharma CM, Forstner KU, Liere K, Vogel J, Börner T. The primary transcriptome of barley chloroplasts: numerous noncoding RNAs and the dominating role of the plastid-encoded RNA polymerase. *Plant Cell*. 2012;24(1):123–36.
- Williams-Carrier R, Zoschke R, Belcher S, Pfalz J, Barkan A. A major role for the plastid-encoded RNA polymerase complex in the expression of plastid transfer RNAs. *Plant Physiol*. 2014;164(1):239–48.
- Finster S, Eggert E, Zoschke R, Weihe A, Schmitz-Linneweber C. Light-dependent, plastome-wide association of the plastid-encoded RNA polymerase with chloroplast DNA. *Plant J*. 2013;76(5):849–60.
- Chen SG, Lu JH, Cheng MC, Chen LF, Lo PK. Four promoters in the rice plastid *psbK-psbI-psbD-psbC* operon. *Plant Sci*. 1994;99(2):171–82.
- Zhang Q, Xue D, Li X, Long Y, Zeng X, Liu Y. Characterization and molecular mapping of a new virescent mutant in rice. *J Genet Genomics*. 2014;41(6):353–6.
- Hiratsuka J, Shimada H, Whittier R, Ishibashi T, Sakamoto M, Mori M, et al. The complete sequence of the rice (*Oryza sativa*) chloroplast genome: intermolecular recombination between distinct tRNA genes accounts for a major plastid DNA inversion during the evolution of the cereals. *Mol Gen Genet*. 1989;217(2–3):185–94.
- Shimada H, Sugiyama M. Fine structural features of the chloroplast genome: comparison of the sequenced chloroplast genomes. *Nucleic Acids Res*. 1991;19(5):983–95.
- Kanno A, Hirai A. A transcription map of the chloroplast genome from rice (*Oryza sativa*). *Curr Genet*. 1993;23(2):166–74.
- Mullet JE. Dynamic regulation of chloroplast transcription. *Plant Physiol*. 1993;103(2):309–13.

41. Gamble PE, Mullet JE. Translation and stability of proteins encoded by the plastid *psbA* and *psbB* genes are regulated by a nuclear gene during light-induced chloroplast development in barley. *J Biol Chem*. 1989;264(13):7236–43.
42. Chen SG, Cheng M, Chung K, Yu N, Chen M. Expression of the rice chloroplast *psaA-psaB-rps14* gene cluster. *Plant Sci*. 1992;81(1):93–102.
43. Satoh J, Baba K, Nakahira Y, Tsunoyama Y, Shiina T, Toyoshima Y. Developmental stage-specific multi-subunit plastid RNA polymerases (PEP) in wheat. *Plant J*. 1999;18(4):407–15.
44. Hernández-Verdeja T, Strand Å. Retrograde signals navigate the path to chloroplast development. *Plant Physiol*. 2018;176(2):967–76.
45. Iba K, Takamiya KI, Toh Y, Satoh H, Nishimura M. Formation of functionally active chloroplasts is determined at a limited stage of leaf development in virescent mutants of rice. *Dev Genet*. 1991;12:342–8.
46. Schrubar H, Wanner G, Westhoff P. Transcriptional control of plastid gene expression in greening Sorghum seedlings. *Planta*. 1991;183(1):101–11.
47. Dubreuil C, Jin X, Barajas-Lopez JD, Hewitt TC, Tanz SK, Dobrenel T, et al. Establishment of photosynthesis through chloroplast development is controlled by two distinct regulatory phases. *Plant Physiol*. 2018;176(2):1199–214.
48. Li N, Euring D, Cha JY, Lin Z, Lu MZ, Huang LJ, et al. Plant hormone-mediated regulation of heat tolerance in response to global climate change. *Front Plant Sci*. 2021;11:627969.
49. Kaur H, Sirihindi G, Bhardwaj R, Alyemeni MN, Siddique KHM, Ahmad P. 28-homobrassinolide regulates antioxidant enzyme activities and gene expression in response to salt- and temperature-induced oxidative stress in *Brassica juncea*. *Sci Rep*. 2018;8(1):8735.
50. Zhang Y, Su J, Duan S, Ao Y, Dai J, Liu J, et al. A highly efficient rice green tissue protoplast system for transient gene expression and studying light/chloroplast-related processes. *Plant Methods*. 2011;7(1):30.
51. van Wijk KJ, Peltier JB, Giacomelli L. Isolation of chloroplast proteins from *Arabidopsis thaliana* for proteome analysis. *Methods Mol Biol*. 2007;355:43–8.
52. Kazama T, Nakamura T, Watanabe M, Sugita M, Toriyama K. Suppression mechanism of mitochondrial ORF79 accumulation by Rf1 protein in BT-type cytoplasmic male sterile rice. *Plant J*. 2008;55(4):619–28.
53. Tsai YC, Chen KC, Cheng TS, Lee C, Lin SH, Tung CW. Chlorophyll fluorescence analysis in diverse rice varieties reveals the positive correlation between the seedlings salt tolerance and photosynthetic efficiency. *BMC Plant Biol*. 2019;19(1):403.

Publisher's Note

Springer Nature remains neutral with regard to jurisdictional claims in published maps and institutional affiliations.

Ready to submit your research? Choose BMC and benefit from:

- fast, convenient online submission
- thorough peer review by experienced researchers in your field
- rapid publication on acceptance
- support for research data, including large and complex data types
- gold Open Access which fosters wider collaboration and increased citations
- maximum visibility for your research: over 100M website views per year

At BMC, research is always in progress.

Learn more biomedcentral.com/submissions



The ties of brotherhood between *japonica* and *indica* rice for regional adaptation

Man Wang^{1,2†}, Jiehu Chen^{3†}, Feng Zhou^{1,2†}, Jianming Yuan^{1,2}, Libin Chen^{1,2}, Rongling Wu^{4*},
Yaoguang Liu^{1,2,5*} & Qunyu Zhang^{1,2,5*}

¹State Key Laboratory for Conservation and Utilization of Subtropical Agro-bioresources, College of Life Sciences, South China Agricultural University, Guangzhou 510642, China;

²Guangdong Laboratory for Lingnan Modern Agriculture, Guangzhou 510642, China;

³Science Corporation of Gene, Guangzhou 510000, China;

⁴Center for Statistical Genetics, The Pennsylvania State University, Hershey PA 17033, USA;

⁵SCAU Main Campus Teaching & Research Base, Guangzhou 510642, China

Received May 23, 2021; accepted October 20, 2021; published online December 9, 2021

Selection of beneficial genomic variants was crucial for regional adaptation of crops during domestication, but the underlying genomic basis remains largely unexplored. Here we report a genome-wide selective-sweep analysis of 655 *japonica* and 1,205 *indica* accessions selected from 2,673 landraces through principal component analysis to identify 5,636 non-synonymous single nucleotide polymorphisms (SNPs) fixed in at least one subspecies. We classified these SNPs into three groups, *jiS* (*japonica*- and *indica*-selected), *iS* (*japonica*-selected only), and *iS* (*indica*-selected only), and documented evidence for selection acting on these groups, their relation to yield-related traits, such as heading date, and their practical value in cropping area prediction. We also demonstrated the role of a *jiS*-SNP-containing gene in temperature adaptability. Our study informs genes underpinning adaptation that may shape Green Super Rice and proposes a time-saving, cost-reducing selection strategy of genomic breeding, sweep-SNP-guided selection, for developing regionally-adapted heterosis.

selective sweeps, *indica-japonica* differentiation, geographic adaptation

Citation: Wang, M., Chen, J., Zhou, F., Yuan, J., Chen, L., Wu, R., Liu, Y., and Zhang, Q. (2022). The ties of brotherhood between *japonica* and *indica* rice for regional adaptation. *Sci China Life Sci* 65, 1369–1379. <https://doi.org/10.1007/s11427-021-2019-x>

INTRODUCTION

The two subspecies of Asian cultivated rice (*Oryza sativa* L.), *japonica* and *indica*, domesticated from wild rice (*O. rufipogon* Griff. and *O. nivara* Sharma et Shastri) (Fuller et al., 2010), have distinct morphological and physiological traits and regional distributions. *Indica* varieties are adapted to lower-latitude tropical/subtropical regions with shorter days; *japonica* varieties are adapted to higher-latitude tem-

perate regions with longer days. During rice domestication, humans selected for genomic variants that improved agronomic traits and adapted to the local environment. These genomic variants form the molecular foundation of *indica-japonica* differentiation, and thus are fundamental for understanding inter-subspecific heterosis and characterizing germplasm. Studies have aimed to elucidate these genomic variants since the release of whole-genome assemblies of the first *japonica* cultivar, Nipponbare (Goff et al., 2002; Yu et al., 2005), and several *indica* cultivars, 93-11 (Yu et al., 2002; Yu et al., 2005), Zhenshan 97 (Zhang et al., 2016), Minghui 63 (Zhang et al., 2016), and Shuhui498 (Du et al.,

†Contributed equally to this work

*Corresponding authors (Rongling Wu, email: ronglingwu@phs.psu.edu; Yaoguang Liu, email: ygliu@scau.edu.cn; Qunyu Zhang, email: zqy@scau.edu.cn)

2017). Whole-genome re-sequencing of 1,083 *japonica* and *indica* varieties identified 1,120 functional variants that were fixed in *japonica* or *indica* (Huang et al., 2012). Recently, two whole-genome screens for variation in genes between *japonica* and *indica* provided additional insight (Sun et al., 2015; Yuan et al., 2017). Despite these advances, the functional significance of the identified variants/genes that differ between *japonica* and *indica* remains to be clarified.

Heterosis provides major improvements in yield and *japonica-indica* hybrids may give the highest heterosis in rice (Khush, 1995; Ouyang et al., 2009), but they face two major challenges: reproductive barriers and the identification of genetic combinations that generate hybrids that are adapted to local conditions. Studies of *japonica-indica* hybrid fertility have identified ~50 wide-compatibility loci (Xie et al., 2019) and two of them have been cloned (Chen et al., 2008; Long et al., 2008). However, the comprehensive genomic signatures of *indica-japonica* differentiation have yet to be identified and clarified. Additionally, how the interplay between human-driven selection and geographical/ecological adaptation shaped rice genetic diversity remains unclear. To develop optimum *japonica-indica* hybrids, there is an urgent need for deeper comprehension of the differences between *japonica* and *indica*.

Here we address these challenges by identifying selective sweeps in *japonica* and *indica* populations followed by functional validation. Our comparative, population genomics approach harnessed a large collection of all published data as of Jan 31 2019 for typical *japonica* and *indica* accessions, which were defined by genomic data-based principal component analysis (PCA). This comprehensive study revealed single nucleotide polymorphisms (SNPs) within protein-coding regions of adaptive significance for rice cultivars, which may represent the “genomic guide” for breeding towards regionally-adapted heterosis.

RESULTS

Genome-wide selective sweep analysis of *japonica* and *indica* populations

We used 42,189 records of whole-genome Sequence Read Archive (SRA) data from 5,166 Asian cultivated rice Biosamples (www.ncbi.nlm.nih.gov/sra/) with sequencing depth >10× and aligned coverage depth >85%. There were 6,087,038 SNPs detected between the *indica* and *japonica* panels. Subsequent SNP-assisted PCA filtered out 813 admixed accessions, after which 655 *japonica* and 1,205 *indica* accessions distributed worldwide were retained (Figure 1A and B; Tables S1–S4 in Supporting Information) for further analysis. This PCA result was also consistent with that of a tree-based selection (Figure S1 in Supporting Information). To identify the selective sweeps, we searched for genomic regions with reduced heterozygosity (H_p) (Rubin et al., 2010)

concurrent with increased genetic distance (F_{ST}) (Axelsson et al., 2013) between *japonica* and *indica*. Our analyses were performed on sliding 10-kb windows and focused on those with $H_p < 0.001$ in either of the two panels and $F_{ST} \geq 0.95$, representing the extreme ends of the distributions (Figure 1C; Figure S2 in Supporting Information). Considering that the regions reaching the H_p threshold but not the F_{ST} cut-off may be subjected to selection as well, we included them for further analysis along with those in the extreme windows. We identified 5,636 non-synonymous SNPs within 3,224 protein-coding regions (Table S2 in Supporting Information), which were categorized into three groups: *jiS* that were selected in both *japonica* (for *j* alleles) and *indica* (for *i* alleles) with $H_p < 0.001$ and $F_{ST} \geq 0.95$ in either subspecies; *jS* (only selected in *japonica* for *j* alleles) with $H_p < 0.001$ and $F_{ST} < 0.95$ only in *japonica*; *iS* (only selected in *indica* for *i* alleles) with $H_p < 0.001$ and $F_{ST} < 0.95$ only in *indica*.

We used two candidate sweeps, *SG1* for grain shape (Nakagawa et al., 2012) and *bZIP73* for cold tolerance (Liu et al., 2018), as a proof of principle for our approach to locate high-confidence sweeps, as these two traits differ between *japonica* and *indica* varieties. Indeed, we observed *japonica* H_p scores of zero over *SG1* and *bZIP73*, *indica* H_p scores of zero and 0.02943, and F_{ST} values of 1.00000 and 0.97050 for *SG1* and *bZIP73* (Figure S3 in Supporting Information), respectively, which exhibit high degrees of fixation in *japonica* and *indica* populations. Literature search and annotations in the literature-based Oryzabase (Kurata and Yamazaki, 2006) (<https://shigen.nig.ac.jp/rice/oryzabase>) indicated that some of these candidate sweep genes relate to the traits differentiated between *japonica* and *indica* varieties, including grain shape, nitrogen sensitivity, disease resistance, and cold tolerance (Table S3 in Supporting Information). Here we present evidence for selection for cold tolerance on a candidate sweep LOC_Os07g39430 (*V14*, Zhang et al., 2014) (Figure 2A). This sweep contained two non-synonymous *jiS* SNPs and demonstrated almost complete fixation not only in *japonica* and *indica* populations, but also in *O. rufipogon* and *O. nivara* genomes (Figure 2A). At 25°C the *v14* mutant (a *V14*-deficient *japonica* cultivar T65) developed albinism in its first two true leaves (Zhang et al., 2014), which may be reversed by high temperatures (30–35°C). Cold temperature (15°C), however, may bring all green-restored leaves of 25°C-grown *v14s* back to albinism (Figure 2B). We thus evaluated the effect of *V14* on temperature adaptability by genetic transformation of the *v14* mutant with the *V14-j* (derived from T65) and *V14-i* (derived from an *indica* cultivar HHZ) transgenes (denoted as *Tj* and *Ti*, respectively). We observed that *v14/Ti* showed higher tolerance to heat stress (44°C) than *v14/Tj* (Figure 2C), whereas *v14/Tj* was superior to *v14/Ti* under cold stress (4°C) (Figure 2D). The higher cold-tolerance of *Tj* was also observed in HHZ/*Tj* (Figure 2D). In contrast, all lines

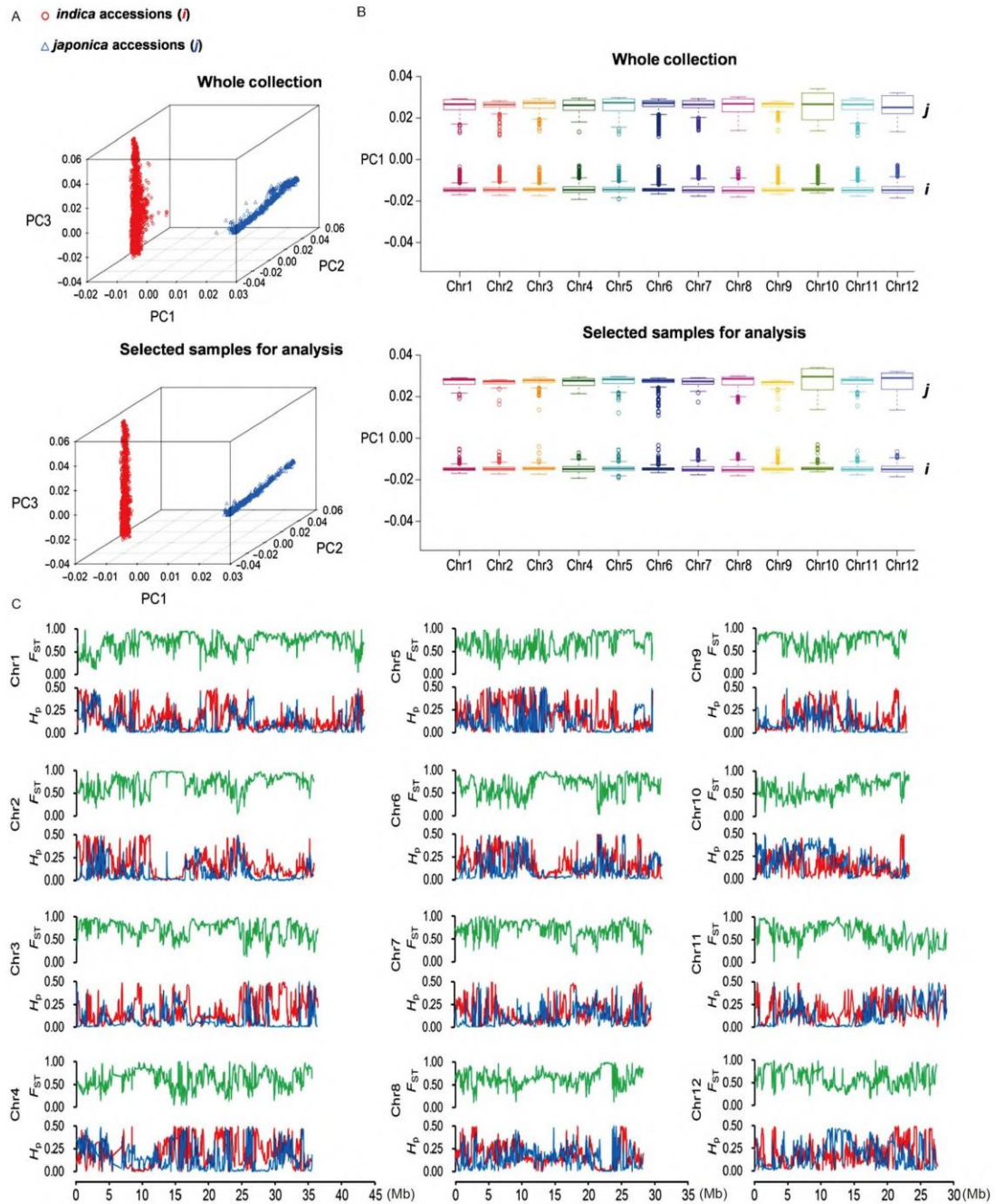


Figure 1 Selective sweep analysis of *japonica* and *indica* populations. A, PCA of the *japonica* and *indica* accessions used in this study. B, PCA plots of the first component of all *japonica* and *indica* accessions and those retained for analysis. C, The H_{vj} , H_{pi} , and F_{ST} distributions plotted along chromosomes 1–12.

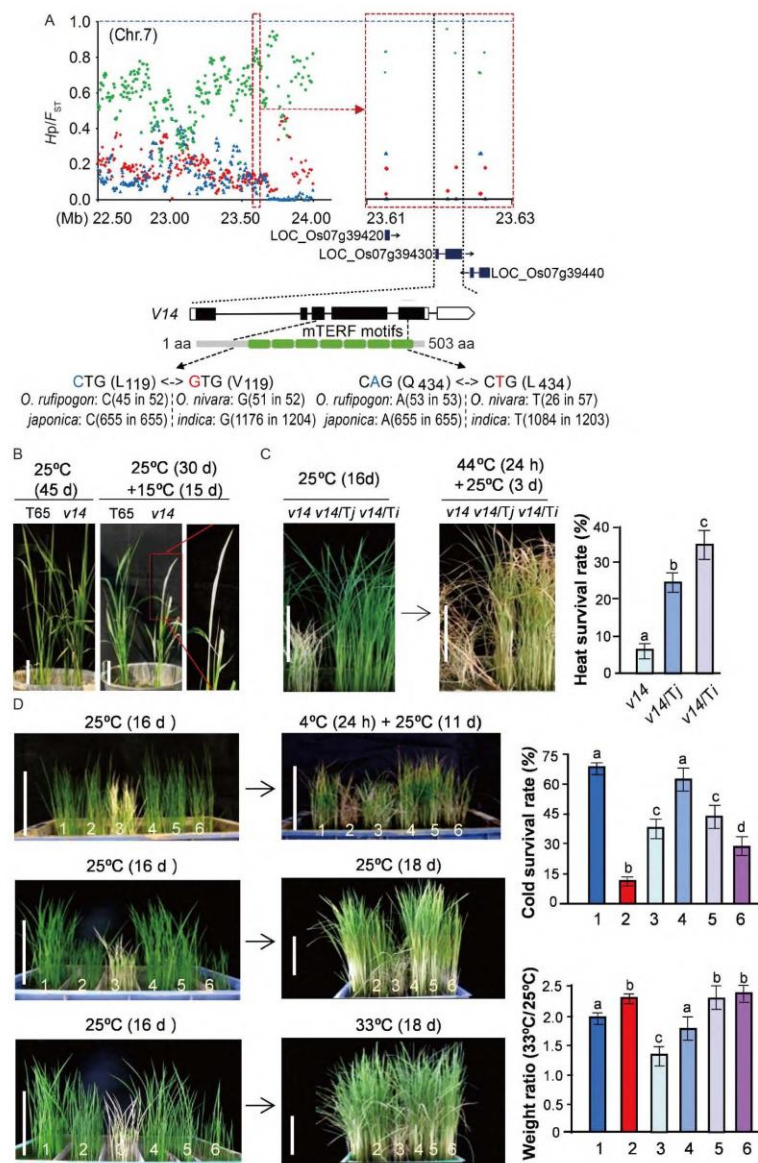


Figure 2 Temperature adaptability conferred by the *V14* (LOC_Os07g39430) sweep. **A**, H_p in *japonica* (blue) and *indica* (red) and F_{ST} (green) are plotted for 10-kb windows on chromosome 7. Below the graphs are two *jiS* SNPs in the coding region. **B**, Phenotypes of the *v14* mutant (a *japonica* cv. T65 mutant) treated by a chilling temperature. **C**, Differential heat-stress tolerance of the *v14* mutant and its transgenic complementation lines with *V14-j* (*Tj*) or *V14-i* (*Ti*), showing the heat survival rates in the right panel. **D**, Performance of T65 (1), HHZ (2, an *indica* cultivar), *v14* (3), *v14/Tj* (4), *v14/Ti* (5), and HHZ/*Tj* (6) after cold and heat treatments, showing the cold survival rates and plant weight ratios in the right panels ($n=3$). Bars with different letters represent significant differences ($P<0.01$).

bearing the endogenous or transgenic *V14-i* (HHZ, *v14/Ti*, and HHZ/*Tj*) exhibited more vigorous growth than the lines lacking *V14-i* when grown at 33°C (Figure 2D), implicating *V14-i* in adaptation to *indica*-favored conditions. These data

exemplified the adaptive value of *jiS* SNPs, which contributed to the genetic differentiation between *japonica* and *indica*, two divergent populations adapted to different agroecosystems.

Evolution of the sweep SNPs during domestication

To validate the sweeps detected, we used genomic data from wild rice and evidence of phenotypic changes associated with the candidate loci. We first used SRA data to find the candidate sweep SNPs in 58 *O. rufipogon* (*Or*-III type (Huang et al., 2012)) and 67 *O. nivara* (*Or*-I type (Huang et al., 2012)) accessions (Table S4 in Supporting Information), which mainly contributed to the *japonica* and *indica* genomes, respectively. About 94% of the SNPs (5,321/5,636) uniquely mapped to the *Or*-I and *Or*-III genomes where the major allele frequencies at 3,370 sites were at least 0.80. The evolutionary relationships among *Oryza* genomes calculated from these 3,370 sites (Figure 3A) are consistent with those based on whole-genome SNPs (Ammiraju et al., 2008; Huang et al., 2012; Stein et al., 2018). We observed that 46% of these sites (1,549/3,370) differed between the *Or*-I and *Or*-III genomes (“dimorphic sites”), whilst the rest were identical between *Or*-I and *Or*-III (“monomorphic sites”) (Figure 3B), suggesting that new mutations were introduced at the monomorphic sites during domestication. Indeed, fixed mutations were seen at 33% (606/1,821) and 1% (27/1,821) of these “monomorphic sites” in the *japonica* and *indica* genomes, respectively (“F_jm” and “F_im”, respectively) (Figure 3B). The progenitors’ genotypes, meanwhile, occupied the rest of the “monomorphic sites” but were fixed only at 31% (569/1,821) and 62% (1,126/1,821) in the *japonica* and *indica* genomes, respectively (Figure 3B). As for the 1,549 “dimorphic sites”, most of the *Or*-III type and *Or*-I type alleles became fixed in the *japonica* and *indica* genomes, respectively (Figure 3B). These findings support the hypothesis that the mapped sites represent targets of natural and artificial selection during domestication.

We further elaborated on the evolution of 3,370 mapped sites during rice domestication. Out of the 1,549 “dimorphic” sites, 886 *ji*S SNPs were inherited from the standing dimorphism between the *Or*-III and *Or*-I genomes, whereas 325 and 338 were classified to the *j*S and *i*S groups in *japonica* and *indica*, respectively (Figure 3C). Regarding those “monomorphic” sites, 95% (482/507) and 5% (25/507) of the *ji*S group were derived from F_jm and F_im, respectively (Figure 3C). For the monomorphic site-derived *j*S and *i*S SNPs, most of them (544/668 and 644/646, respectively) inherited the wild rice alleles, whilst the rest (124 and 2) were derived from F_jm and F_im, respectively (Figure 3C). These results support our speculation that the “monomorphic” sites may serve as hotspots in the recently diverged genes with adaptive potential. In agreement with this notion, the *Ka/Ks* ratios (*Ka*, the number of non-synonymous substitutions per non-synonymous site; *Ks*, the number of synonymous substitutions per synonymous site) calculated for F_jm and F_im sites were greater than 1.0 (Figure 3C), indicating positive selection at these sites during domestica-

tion. Literature search showed that many of the F_jms and F_ims fall within the genes responsible for disease resistance and stress tolerance (Tables S5 and S6 in Supporting Information). The evolution of these 3,370 sites during domestication reflects the interplay between divergent natural selection and frequent breeding activities driving the formation and maintenance of the two subspecies.

Differential allele biases at sweep SNP sites in different environments

We next validated selection acting on the candidate sweep SNPs by analyzing three recombinant inbred line (RIL) populations derived from three different *japonica-indica* crosses generated in two different regions in China with distinct climates (Figure 4A). RIL-B-GZ (F₆) was bred in subtropical China (Guangzhou, GZ) with breeding selections for optimum agronomic traits. RIL-GZ (F₇) and RIL-SY (F₁₁) (Li et al., 2018) were produced in Guangzhou and a temperate area Shenyang (SY), respectively, without artificial selection. We randomly selected five RIL-B-GZ lines and 112 RIL-GZ lines for genotyping. For RIL-SY, we used published whole-genome data for 151 lines (Li et al., 2018). Given the possible pedigree introgression between *japonica* and *indica* varieties during breeding, we filtered out any SNPs that were monomorphic between the parental lines. The analysis revealed significant differences in allele bias between the two locations. In GZ more *indica* alleles occupied the *ji*S and *i*S sites, whilst in SY more *japonica* alleles existed in the *ji*S and *j*S groups (Figure 4B). These allele biases were absent at the non-selected (NS) sites and the *j*S and *i*S sites in the RIL-GZ and RIL-SY lines, respectively (Figure 4B), reflecting differential selection biases in varied environments. Furthermore, comparison of the RIL-B-GZ and RIL-GZ lines indicated a much stronger *indica* bias in the RIL-B-GZ lines (Figure 4B; Table S7 in Supporting Information), which suggests that human-driven selection increased selection pressure on sweep regions, thus maximizing environmental effects on genomic differentiation.

Effects of selection biases on a yield-related trait, heading date

To investigate the effect of differential selection biases on agronomic traits, we revisited published genomic and phenotypic data for the 151 RIL-SY lines (Li et al., 2018) (Table S8 in Supporting Information). Pearson’s bivariate correlation analysis showed that 312 and 248 sweep SNPs (Table S9 in Supporting Information) were strongly correlated with the heading date in a subtropical area Shenzhen (SZ) and a temperate region SY, respectively (Figure 4C; Table S10 in Supporting Information): the frequency

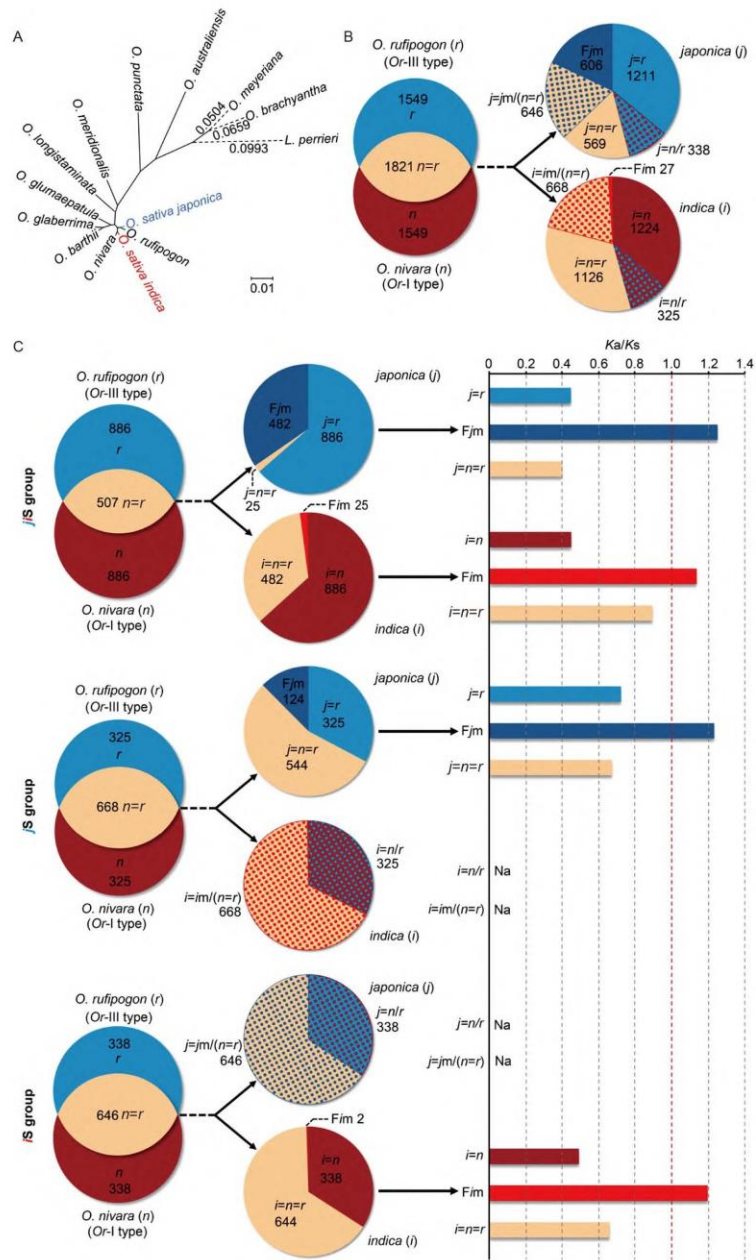


Figure 3 Evolution of the sweep SNPs during domestication. A, Phylogenetic relationships built among *Oryza* genomes using the 3,370 sweep SNPs that mapped to the genomes of the wild progenitors, *O. rufipogon* and *O. nivara*, with major allele frequencies ≥ 0.8 are shown in a maximum-likelihood tree with a bootstrap value of 1,000. B, Sweep SNPs derived from *O. rufipogon* and *O. nivara*. The figures in the pie charts represent the numbers of the SNP sites that mapped to *O. rufipogon* and *O. nivara* genomes with major allele frequencies ≥ 0.8 , of which 1,549 are "dimorphic sites" and 1,821 are "monomorphic sites". For the mutations observed at the "monomorphic sites" in *japonica* and *indica* genomes, F_{jm} and F_{im} represent fixed mutations and j_m and i_m denote random mutations in *japonica* and *indica*, respectively. C, Delineated evolution of the 3,370 mapped SNPs. Per differential selection, the sweep SNPs were categorized into three groups, *jIS* (*japonica*- and *indica*-selected), *jS* (*japonica*-selected only), and *iS* (*indica*-selected only). $Ka/Ks > 1.0$ indicate positive selection at the corresponding sites. Na, null value.

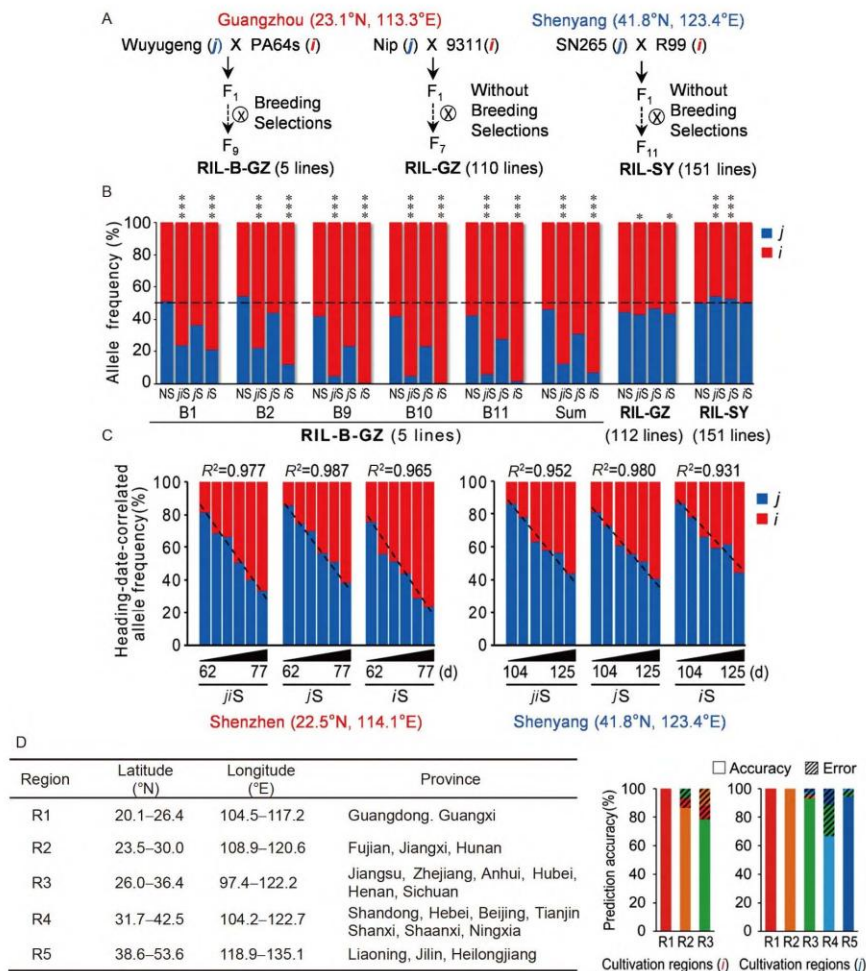


Figure 4 Selection acting on the sweep SNPs. A, Development of the *japonica-indica* RILs with or without breeding selections in two different locations. B, Frequencies of the *japonica* and *indica* alleles at sweep SNP sites and 103,988 NS sites in the RIL populations. * and ***, significant differences to NS at $P < 0.05$ and $P < 0.001$, respectively. The primary genomic and phenotypic data in B, C, and D for RIL-SY are from a previous report (Li et al., 2018). C, Correlations between the allele frequencies at the heading-date-correlated sites and heading date of RIL-SYs grown in Shenzhen and Shenyang. Trend lines were added on the bar graphs to indicate the linear correlation in Pearson correlation analysis. R^2 -squared values of the trend lines are also shown. D, A prediction model for cropping areas based on the latitudinal distribution-correlated sweep SNPs. The primary genomic and geographic datasets of 736 Chinese lowland accessions are from a previous report (Li et al., 2020). The cultivation regions are divided by latitude and displayed in the left panel, with prediction accuracy shown in the right panel.

of the *indica* alleles was positively correlated whereas the frequency of the *japonica* alleles was negatively correlated. Among these heading-date-correlated SNPs, 82 were shared by the SZ and SY groups (Table S9 in Supporting Information). To test our sweep-SNP-trait correlations, we showed the Pearson's correlation for three functionally-validated/annotated heading-date-related genes (Table S3 in Supporting Information) containing seven heading-date-correlated SNPs (Table S9 in Supporting Information):

LOC_Os03g03990, LOC_Os05g41070 (*HBF1*, Brambilla et al., 2017), and LOC_Os09g38790 (*SIP1*, Jiang et al., 2018) (Figure S4A in Supporting Information). Given that moderately late heading is preferred in subtropical regions whereas relatively early heading is desired in higher latitudes, these findings were consistent with the selection biases differentiated between subtropical and temperate areas, stressing the significance of sweep SNPs for regional breeding.

A sweep-SNP-based statistical model for cropping area prediction

We further explored the application of sweep SNPs to predicting suitable cropping areas for rice cultivars. To build our genomic prediction model, we selected by PCA 472 *japonica* and 264 *indica* Chinese lowland accessions growing in single latitudes with available genomic and geographic datasets (Li et al., 2020). Pearson's bivariate correlation analysis identified 214 and 280 sweep SNPs (Table S11 in Supporting Information) in the *japonica* and *indica* genomes, respectively, strongly correlated with the latitudinal distribution among five *japonica* (R1–R5) and three *indica* (R1–R3) cultivation regions (Figure 4D). The allele frequencies of these SNPs coupled with the PCA-based environmental covariables of R1–R5 were used for modeling (Methods). To test this model we first compared the prediction performance of latitudinal distribution-correlated sweep SNPs, non-selected SNPs, and 4dTVs (Fourfold degenerate synonymous sites of the third codons) using all 736 rice accessions (616 modeling-involved and 120 modeling-uninvolved). We observed that the sweep SNPs significantly outperformed the other two in prediction accuracy, reaching 83.7% and 93% in average in R1–R3 and R1–R5, respectively (Figure S4B, Tables S12 and S13 in Supporting Information). We next used two cross-validation (CV) schemes to assess the model prediction accuracy: predicting the locations of all (CV1) and random samples with different sizes (CV2) from 736 rice accessions. The results showed that most of the *japonica* and *indica* landraces were correctly located in CV1 (Figure 4D; Table S12 in Supporting Information), and that over 85% average prediction accuracy was achieved across nine sampling sizes for both *japonica* and *indica* in CV2 (Figure S4C and Table S14 in Supporting Information), suggesting the high predictability for rice planting areas by sweep-SNP-guided modeling.

DISCUSSION

Our study provides the genomic landscape of *indica-japonica* differentiation. While there have been a few attempts before (Huang et al., 2012; Sun et al., 2015; Yuan et al., 2017) at illuminating the genomic base of *indica-japonica* differentiation, our comparative, population genomics analysis features the application of whole-genome SNP-based PCA to sample clustering along with sample descriptions. This PCA-assisted sample filtering helped rule out the admixed accessions that may mask the real difference between *japonica* and *indica* populations, and thus lowered the signal-to-noise ratio of our selective sweep analysis where 3,224 sweep-SNP-containing protein-coding genes were identified. As these genes are selected for during domes-

tication, they are informative targets for basic research projects respecting rice development, where functional differentiation between *indica* and *japonica* should be considered. In addition, the availability of these genes permits the practical utility of them as potential targets for genomic breeding efforts and to predict agronomic potential, due to the fact that selection signatures confer many valuable agronomic traits on Green Super Rice (GSR) (Meyer et al., 2016; Olsen et al., 2006; Olsen and Purugganan, 2002; Wing et al., 2018), a new generation of sustainable crops proposed to meet future demands for yield increase, quality improvement, reduced fertilizer requirement, and resistance to disease and stress (Zhang, 2007).

Our work also introduces a sweep-SNP-guided selection strategy for breeding regionally-adapted cultivars, which stems from the adaptive value of sweep SNPs demonstrated here. In this regard, incorporation of our cropping area prediction model with allele frequencies at the sweep SNP sites may be applied to guide and accelerate selection of genetic combinations and hybrid lines that are adapted to targeted growing areas, which holds the key of genomic design and whole-genome selection, the two major phases of genomic breeding, respectively (Wing et al., 2018). This application only requires low-depth sequencing ($1\times$ minimum) of 5,636 sweep SNP sites instead of whole-genome, which may help reduce breeding costs. Furthermore, this selection platform allows breeders to locate appropriate growing areas for those hybrid lines not well adapted to local conditions but displaying good agronomic characteristics, which further makes the breeding process more cost-effective. The sweep-SNP-guided selection strategy, if adopted, may also work for other crop systems. Overall, our sweep-SNP map offers foundational resource for both basic research and crop improvement.

MATERIALS AND METHODS

Sequence sources

All the genomic data for selective sweep analysis were downloaded from the SRA at the National Center for Biotechnology Information (NCBI) (www.ncbi.nlm.nih.gov/sra/) where the filters “DNA”, “genome”, “platform illumina”, and “paired end”, were applied by Jan 31 2019. The data selected for analysis were required to have BioSample accession numbers (<https://www.ncbi.nlm.nih.gov/biosample/>) with “library_strategy=WGS”, “library_source=genomic”, “library_selection=random”, read length ≥ 75 bp, sequencing depth $>10\times$, and aligned coverage depth $>85\%$.

SNP detection and analysis

Prior to the alignment of *japonica* and *indica* data to

Nipponbare MSU v7.0 (<http://rice.plantbiology.msu.edu/>) (Kawahara et al., 2013) and Minghui 63 (MH63) (RIGW, <http://rice.hzau.edu.cn/rice/>) (Zhang et al., 2016) genomes, respectively, we first aligned the published data of these two reference genomes on blastn (<https://blast.ncbi.nlm.nih.gov/>), followed by the application of L-INS-i algorithm implemented in a multiple sequence alignment program mafft (v7.475, <https://mafft.cbrc.jp/alignment/software/>) for more accurate pairwise sequence alignment. The parameters applied in mafft were as follows: -localpair -maxiterate 1000. All the paired-end reads for *japonica* and *indica* accessions were aligned with the BWA-0.7.16a (r1181) aligner (Li and Durbin, 2009) (setting: bwa aln -n 0.04). After the BAM files were sorted and indexed by samtools-1.4 (<http://samtools.sourceforge.net/>) (Li, 2011), SNPs were called using the Genome Analysis Toolkit (GATK) following the instruction on hard filter application (<https://gatkforums.broadinstitute.org/gatk/discussion/2806/howto-apply-hard-filters-to-a-call-set>). The parameters applied were as follows: QD<2.0, FS>60.0, MQ<40.0, MQRankSum<-12.5, and ReadPosRankSum<-8.0. A minimum of three reads supporting the non-reference allele were required to call an SNP. All reported SNPs are unique sites. To calculate allele frequencies in the *japonica* and *indica* populations, we called genotypes for all SNPs by counting the sequencing reads with a minimum base quality of 20 that support either the reference or variant alleles.

Population structure analysis

Phylogenetic trees were built on the matrix of pairwise genetic distances derived from simple SNP-matching coefficients, using jModelTest (version 2.1.7) (Posada, 2008) to choose the best-fitting model according to AICc and the maximum likelihood method implemented in raxml (version 8.2.12) (Stamatakis, 2014) with 1,000 bootstrap replicates. Principal component analysis was performed using PLINK 1.9 (Chang et al., 2015; Purcell et al., 2007) and Genome-wide Complex Trait Analysis (GCTA, version 1.26.0, <http://cns.genomics.com/software/gcta/>) (Yang et al., 2011) on the filtered SNPs (MAF>0.05) at the whole-genome and chromosome levels, both of which generated two apparent clusters, *japonica* and *indica*. The rice accessions carrying two or more chromosomes scored ≤10% deviation on either side from the midpoint of the minimum pairwise distance between the *japonica* cluster and the *indica* cluster for PC1 were defined as admixed accessions, which were not included in the subsequent selective sweep analysis.

Selective-sweep analysis

Allele counts and allele frequencies at all identified SNP

sites (6,087,038 in total) were used to detect selective signals in 10-kb windows with a step size of 5 kb. We first calculated the average pooled heterozygosity (H_p) in all the windows following the methodology described in the references (Rubin et al., 2010; Axelsson et al., 2013). Briefly, at each SNP position we counted the numbers of reads corresponding to the most and least frequently observed allele (n_{MAJ} and n_{MIN} , respectively) in each population, and estimated H_p using the formula $H_p = 2 \sum n_{MAJ} \sum n_{MIN} / (\sum n_{MAJ} + \sum n_{MIN})^2$, where $\sum n_{MAJ}$ and $\sum n_{MIN}$ are sums of n_{MAJ} and n_{MIN} , respectively, in each window. The windows in the extreme tail of the distribution, of which have $H_p < 0.001$, were extracted as the putatively selected regions (Figure 1C). We then calculated F_{ST} values between *japonica* and *indica* using the method for unequal sample sizes (Weir and Cockerham, 1984). We applied an $F_{ST} \geq 0.95$ cut-off to extract the windows at the extreme higher end of the distribution (Figure 1C). Windows having $F_{ST} \geq 0.95$ with H_p scores below 0.001 in either of the populations were selected as putative selective sweeps. Considering that the windows reaching the H_p threshold but with F_{ST} values lower than 0.95 might be under selection as well, we included these windows for further validation along with those extreme windows. To preclude spurious fixation signals, we ruled out the windows containing fewer than 10 informative sites for both H_p and F_{ST} analyses. According to differential selection states, the putative sweep SNPs were classified into three groups: *jiS* (selected in both *japonica* and *indica*) with $F_{ST} \geq 0.95$ and $H_p < 0.001$ in either subspecies; *jS* (only selected in *japonica*) with $F_{ST} < 0.95$ and $H_p < 0.001$ only in *japonica*; *iS* (only selected in *indica*) with $F_{ST} < 0.95$ and $H_p < 0.001$ only in *indica*.

Estimation of the rates of synonymous and nonsynonymous substitution

Ka/Ks ratios were calculated for 3,370 sweep SNP sites that mapped to *O. rufipogon* (Or-III type) and *O. nivara* (Or-I type) (Huang et al., 2012) genomes. Only the exons within the coding regions carrying the F_{jm}, F_{im}, j=r, i=n, j=n=r, or i=n=r sites were applied to Ka/Ks calculation. The multiple sequence alignment among *O. rufipogon*, *O. nivara*, *japonica*, and *indica* populations was performed using the E-INS-i algorithm implemented in mafft (v7.475, <https://mafft.cbrc.jp/alignment/software/>) that assumes that the arrangement of the conserved motifs is shared by all sequences. The maximum iterative refinement cycles were set at 1,000. The aligned coding sequences were then subjected to Ka/Ks calculation using the kaks function provided in the seqinr package 3.6-1, which is based on an unbiased estimation of the rates of synonymous and nonsynonymous substitution (Tzeng et al., 2004).

RILs analysis

Seeds from the RIL-B-GZ lines were kindly provided by Dr. Feng Wang of Guangdong Academy of Agricultural Science. Seeds were grown in a growth chamber set at 28°C for leaf collection. For the RIL-SY lines, all the genomic sequences were obtained through the links in the reference (Li et al., 2018). The RIL-GZ lines were generated and maintained by our laboratory. Genomic DNA was extracted from leaves using a DNeasy Plant Mini Kit (QIAGEN, Germany), and genotyped on Illumina HiSeq2500 system.

Pearson correlation coefficient

The phenotypic data of the 151 RIL-SY lines were downloaded through the links in the reference (Li et al., 2018). The correlation coefficients were computed in R using the `cor.test()` function that returns both the correlation coefficient (r) and the significance level (P -value) of the correlation. The `ggpubr` R package (Ginestet, 2011) was used for data visualization. The SNPs having $|r| > 0.7$ together with $P < 0.01$ were considered strongly correlated SNPs. The summary of the r scores is in Table S12 in Supporting Information.

Sweep-SNP-guided modeling for cropping zone prediction

Published genomic and geographic datasets for 736 Chinese rice landraces were downloaded through the link in the reference (Li et al., 2020). The landraces were selected for modeling by PCA, and the cultivation areas were divided by latitude (R1–R5, Figure 4D). Pearson's bivariate correlation analysis was performed to identify latitudinal distribution-related sweep SNP sites where allele frequencies correlate with standardized latitude values. The allele frequencies (j -allele frequencies for *japonica* accessions and i -allele frequencies for *indica* accessions) at these sites were then used to build a prediction model incorporating the PCA-based environmental covariables of R1–R5. This model is available at <http://pbgarl.scgene.com>.

Genetic transformation and treatments

The fragments including the promoter and the coding and downstream regions of *V14-j* and *V14-i* were amplified from T65 and HHZ genomic DNA, respectively, using the primers V14P5 (gctttttcatatctcattgccccGAGGGTGGTTGGAGAGGAAG) and V14P3 (tctctctgagctttgcagatccGGA-GCCGCACGTTGGTCTGCA). The PCR products were then cloned into a plant expression vector pCambia 1380 with a Gibson Assembly® Master Mix (New England Biolabs, USA), followed by Agrobacterium-mediated transformation into the *v14* mutant and HHZ. Transgene expression

was confirmed by Sanger-sequencing the RT-PCR (reverse transcription-polymerase chain reaction) products of *V14*-cDNA. For the heat and cold treatments, all the plants were grown in growth chambers with the designated conditions.

Data availability

The genomic data for RIL-B-GZ and RIL-GZ lines are deposited in GenBank (<http://www.ncbi.nlm.nih.gov/genbank/>) with the accession# PRJNA623486.

Compliance and ethics The author(s) declare that they have no conflict of interest.

Acknowledgements This work was supported by the National Key Program on Transgenic Research from the Ministry of Agriculture of China (2016ZX08009002-003-003), Natural Science Foundation of Guangdong Province of China (2015A030313414), and Science and Technology Program of Guangzhou, China (201607010196). Thanks are due to Dr. Feng Wang of the Rice Research Institute of Guangdong Academy of Agricultural Sciences (China) for providing the materials of the RIL-B-GZ lines, and Prof. Shaohuan Zhou of the Rice Research Institute of Guangdong Academy of Agricultural Sciences (China) for providing the materials of the Huanhuazhan (HHZ).

References

- Ammiraju, J.S.S., Lu, F., Sanyal, A., Yu, Y., Song, X., Jiang, N., Pontaroli, A.C., Rambo, T., Currie, J., Collura, K., et al. (2008). Dynamic evolution of *Oryza* genomes is revealed by comparative genomic analysis of a genus-wide vertical data set. *Plant Cell* 20, 3191–3209.
- Axelsson, E., Ratnakumar, A., Arendt, M.L., Maqbool, K., Webster, M.T., Perloski, M., Liberg, O., Arnemo, J.M., Hedhammar, A., and Lindblad-Toh, K. (2013). The genomic signature of dog domestication reveals adaptation to a starch-rich diet. *Nature* 495, 360–364.
- Brambilla, V., Martignago, D., Goretti, D., Cerise, M., Somssich, M., de Rosa, M., Galbiati, F., Shrestha, R., Lazzaro, F., Simon, R., et al. (2017). Antagonistic transcription factor complexes modulate the floral transition in rice. *Plant Cell* 29, 2801–2816.
- Chang, C.C., Chow, C.C., Tellier, L.C., Vattikuti, S., Purcell, S.M., and Lee, J.J. (2015). Second-generation PLINK: rising to the challenge of larger and richer datasets. *Gigascience* 4, 7.
- Chen, J., Ding, J., Ouyang, Y., Du, H., Yang, J., Cheng, K., Zhao, J., Qiu, S., Zhang, X., Yao, J., et al. (2008). A triallelic system of S5 is a major regulator of the reproductive barrier and compatibility of *indica-japonica* hybrids in rice. *Proc Natl Acad Sci USA* 105, 11436–11441.
- Du, H., Yu, Y., Ma, Y., Gao, Q., Cao, Y., Chen, Z., Ma, B., Qi, M., Li, Y., Zhao, X., et al. (2017). Sequencing and *de novo* assembly of a near complete *indica* rice genome. *Nat Commun* 8, 15324.
- Fuller, D.Q., Sato, Y.I., Castillo, C., Qin, L., Weisskopf, A.R., Kingwell-Banham, E.J., Song, J., Ahn, S.M., and van Etten, J. (2010). Consilience of genetics and archaeobotany in the entangled history of rice. *Archaeol Anthropol Sci* 2, 115–131.
- Ginestet, C. (2011). ggplot2: elegant graphics for data analysis. *JR Stat Soc* 174, 245–246.
- Goff, S.A., Ricke, D., Lan, T.H., Presting, G., Wang, R., Dunn, M., Glazebrook, J., Sessions, A., Oeller, P., Varma, H., et al. (2002). A draft sequence of the rice genome (*Oryza sativa* L. ssp. *japonica*). *Science* 296, 92–100.
- Huang, X., Kurata, N., Wei, X., Wang, Z.X., Wang, A., Zhao, Q., Zhao, Y., Liu, K., Lu, H., Li, W., et al. (2012). A map of rice genome variation reveals the origin of cultivated rice. *Nature* 490, 497–501.

- Jiang, P., Wang, S., Zheng, H., Li, H., Zhang, F., Su, Y., Xu, Z., Lin, H., Qian, Q., and Ding, Y. (2018). SIP1 participates in regulation of flowering time in rice by recruiting OsTrx1 to *Ehd1*. *New Phytol* 219, 422–435.
- Kawahara, Y., de la Bastide, M., Hamilton, J.P., Kanamori, H., McCombie, W.R., Ouyang, S., Schwartz, D.C., Tanaka, T., Wu, J., Zhou, S., et al. (2013). Improvement of the *Oryza sativa* Nipponbare reference genome using next generation sequence and optical map data. *Rice* 6, 4.
- Khush, G.S. (1995). Breaking the yield frontier of rice. *GeoJournal* 35, 329–332.
- Kurata, N., and Yamazaki, Y. (2006). Oryzabase. An integrated biological and genome information database for rice. *Plant Physiol* 140, 12–17.
- Li, H. (2011). A statistical framework for SNP calling, mutation discovery, association mapping and population genetic parameter estimation from sequencing data. *Bioinformatics* 27, 2987–2993.
- Li, H., and Durbin, R. (2009). Fast and accurate short read alignment with Burrows-Wheeler transform. *Bioinformatics* 25, 1754–1760.
- Li, X., Chen, Z., Zhang, G., Lu, H., Qin, P., Qi, M., Yu, Y., Jiao, B., Zhao, X., Gao, Q., et al. (2020). Analysis of genetic architecture and favorable allele usage of agronomic traits in a large collection of Chinese rice accessions. *Sci China Life Sci* 63, 1688–1702.
- Li, X., Wu, L., Wang, J., Sun, J., Xia, X., Geng, X., Wang, X., Xu, Z., and Xu, Q. (2018). Genome sequencing of rice subspecies and genetic analysis of recombinant lines reveals regional yield- and quality-associated loci. *BMC Biol* 16, 102.
- Liu, C., Ou, S., Mao, B., Tang, J., Wang, W., Wang, H., Cao, S., Schlappi, M.R., Zhao, B., Xiao, G., et al. (2018). Early selection of bZIP73 facilitated adaptation of japonica rice to cold climates. *Nat Commun* 9, 3302.
- Long, Y., Zhao, L., Niu, B., Su, J., Wu, H., Chen, Y., Zhang, Q., Guo, J., Zhuang, C., Mei, M., et al. (2008). Hybrid male sterility in rice controlled by interaction between divergent alleles of two adjacent genes. *Proc Natl Acad Sci USA* 105, 18871–18876.
- Meyer, R.S., Choi, J.Y., Sanches, M., Plessis, A., Flowers, J.M., Amas, J., Dorph, K., Barretto, A., Gross, B., Fuller, D.Q., et al. (2016). Domestication history and geographical adaptation inferred from a SNP map of African rice. *Nat Genet* 48, 1083–1088.
- Nakagawa, H., Tanaka, A., Tanabata, T., Ohtake, M., Fujioka, S., Nakamura, H., Ichikawa, H., and Mori, M. (2012). *SHORT GRAIN1* decreases organ elongation and brassinosteroid response in rice. *Plant Physiol* 158, 1208–1219.
- Olsen, K.M., Caicedo, A.L., Polato, N., McClung, A., McCouch, S., and Purugganan, M.D. (2006). Selection under domestication: evidence for a sweep in the rice *Waxy* genomic region. *Genetics* 173, 975–983.
- Olsen, K.M., and Purugganan, M.D. (2002). Molecular evidence on the origin and evolution of glutinous rice. *Genetics* 162, 941–950.
- Ouyang, Y.D., Chen, J.J., Ding, J.H., and Zhang, Q.F. (2009). Advances in the understanding of inter-subspecific hybrid sterility and wide-compatibility in rice. *Chin Sci Bull* 54, 2332–2341.
- Posada, D. (2008). jModelTest: phylogenetic model averaging. *Mol Biol Evol* 25, 1253–1256.
- Purcell, S., Neale, B., Todd-Brown, K., Thomas, L., Ferreira, M.A.R., Bender, D., Maller, J., Sklar, P., de Bakker, P.I.W., Daly, M.J., et al. (2007). PLINK: a tool set for whole-genome association and population-based linkage analyses. *Am J Hum Genet* 81, 559–575.
- Rubin, C.J., Zody, M.C., Eriksson, J., Meadows, J.R.S., Sherwood, E., Webster, M.T., Jiang, L., Ingman, M., Sharpe, T., Ka, S., et al. (2010). Whole-genome resequencing reveals loci under selection during chicken domestication. *Nature* 464, 587–591.
- Stamatakis, A. (2014). RAXML version 8: a tool for phylogenetic analysis and post-analysis of large phylogenies. *Bioinformatics* 30, 1312–1313.
- Stein, J.C., Yu, Y., Copetti, D., Zwickl, D.J., Zhang, L., Zhang, C., Chougule, K., Gao, D., Iwata, A., Goicoechea, J.L., et al. (2018). Genomes of 13 domesticated and wild rice relatives highlight genetic conservation, turnover and innovation across the genus *Oryza*. *Nat Genet* 50, 285–296.
- Sun, X., Jia, Q., Guo, Y., Zheng, X., and Liang, K. (2015). Whole-genome analysis revealed the positively selected genes during the differentiation of indica and temperate japonica rice. *PLoS ONE* 10, e0119239.
- Tzeng, Y.H., Pan, R., and Li, W.H. (2004). Comparison of three methods for estimating rates of synonymous and nonsynonymous nucleotide substitutions. *Mol Biol Evol* 21, 2290–2298.
- Weir, B.S., and Cockerham, C.C. (1984). Estimating *F*-statistics for the analysis of population structure. *Evolution* 38, 1358–1370.
- Wing, R.A., Purugganan, M.D., and Zhang, Q. (2018). The rice genome revolution: from an ancient grain to Green Super Rice. *Nat Rev Genet* 19, 505–517.
- Xie, Y., Shen, R., Chen, L., and Liu, Y.G. (2019). Molecular mechanisms of hybrid sterility in rice. *Sci China Life Sci* 62, 737–743.
- Yang, J., Lee, S.H., Goddard, M.E., and Visscher, P.M. (2011). GCTA: a tool for genome-wide complex trait analysis. *Am J Hum Genet* 88, 76–82.
- Yu, J., Hu, S., Wang, J., Wong, G.K.S., Li, S., Liu, B., Deng, Y., Dai, L., Zhou, Y., Zhang, X., et al. (2002). A draft sequence of the rice genome (*Oryza sativa* L. ssp. *indica*). *Science* 296, 79–92.
- Yu, J., Wang, J., Lin, W., Li, S., Li, H., Zhou, J., Ni, P., Dong, W., Hu, S., Zeng, C., et al. (2005). The genomes of *Oryza sativa*: a history of duplications. *PLoS Biol* 3, e38.
- Yuan, Y., Zhang, Q., Zeng, S., Gu, L., Si, W., Zhang, X., Tian, D., Yang, S., and Wang, L. (2017). Selective sweep with significant positive selection serves as the driving force for the differentiation of *japonica* and *indica* rice cultivars. *BMC Genomics* 18, 307.
- Zhang, J., Chen, L.L., Xing, F., Kudrna, D.A., Yao, W., Copetti, D., Mu, T., Li, W., Song, J.M., Xie, W., et al. (2016). Extensive sequence divergence between the reference genomes of two elite *indica* rice varieties Zhenshan 97 and Minghui 63. *Proc Natl Acad Sci USA* 113, E5163–E5171.
- Zhang, Q. (2007). Strategies for developing Green Super Rice. *Proc Natl Acad Sci USA* 104, 16402–16409.
- Zhang, Q., Xue, D., Li, X., Long, Y., Zeng, X., and Liu, Y. (2014). Characterization and molecular mapping of a new virescent mutant in rice. *J Genet Genomics* 41, 353–356.

SUPPORTING INFORMATION

The supporting information is available online at <https://doi.org/10.1007/s11427-021-2019-x>. The supporting materials are published as submitted, without typesetting or editing. The responsibility for scientific accuracy and content remains entirely with the authors.

荣誉证书

周 峰 同志：

被评为华南农业大学“优秀共产党员”。

特发此证，以资鼓励。

中共华南农业大学委员会

二〇一七年六月

奖状

周峰同志：

在2016年度工作中表现突出，被评为
“优秀班主任”。

特发此状，以资鼓励。

华南农业大学生命科学学院

二〇一七年三月



奖状

周峰同志：

在2019年度教学工作中表现突出，被评为
“管理先进个人”。

特发此状，以资鼓励。

华南农业大学生命科学学院

二〇二〇年六月



年度考核结果通知书

周峰 同志：

你在 2011 年年度考核中，被确定为优秀等次，

特此通知。



日

年度考核结果通知书

周峰 同志：

你在 2014 年年度考核中，被确定为优秀等次，

特此通知。



2015年10月16日

年度考核结果通知书

周峰 同志：

你在 2017 年年度考核中，被确定为优秀等次，

特此通知。



2018 年 4 月 26 日